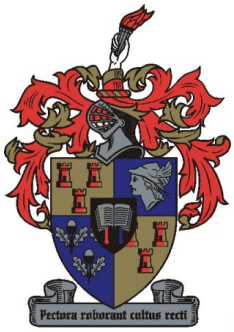

UNIVERSITEIT • STELLENBOSCH • UNIVERSITY

A Study on the Design and Material Costs of Tall Wind Turbine Towers in South Africa

by Andrew Christopher Way

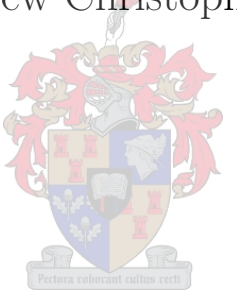

Thesis presented in fulfillment of the requirements for the degree of Master of Civil Engineering at the Faculty of Engineering at Stellenbosch University

Supervisor: Prof. G.P.A.G Van Zijl

December 2014

DECLARATION

By submitting this thesis electronically, I declare that the entirety of the work contained therein is my own, original work, that I am the authorship owner thereof (unless to the extent explicitly otherwise stated) and that I have not previously in its entirety or in part submitted it for obtaining any qualification.

Date: .....

Abstract

The aim of this project is to study the structural design and costing of various designs of tall wind turbine towers and the associated foundations in a South African context. Specific design guidelines are proposed for the design of tubular steel, concrete and concrete-steel hybrid towers and foundations for hub heights of 80, 100 and 120m. Additionally, a conclusion will be made as to whether the concrete and hybrid towers are a viable alternative to steel towers at higher hub heights.

To accomplish this, three of each type of tower (steel concrete and hybrid) and their foundations were designed according to the relevant design standards. The designs were then verified using the *Abaqus* finite element software. The costs of the designs for a South African environment were subsequently calculated according to the increases in material cost, as a function of the increase in hub height.

It was found that for the chosen design assumptions, the foundations for the concrete and hybrid towers are less material intensive, and therefore cheaper, than the steel towers. The material costs of the concrete and hybrid towers were also shown to be lower than the material costs of the steel towers, especially at hub heights of 100 to 120m. For the circumstances in this project, it was found that an increase in hub height causes an increase in energy generation of 3.52 and 6.28 percent for 80m to 100m and 80m to 120m hub heights, respectively. It is therefore deduced that, given the trends in the design and cost associated with increasing hub heights, the concrete and hybrid towers become viable alternatives to the conventional steel towers at hub heights of 100 to 120m in height.

Samevatting

Die doel van hierdie projek is om die strukturele ontwerp en koste van verskillende soorte hoë wind turbines en die toepaslike fondamente vir 'n Suid-Afrikaanse konteks te bestudeer. Spesifieke riglyne word voorgestel vir die ontwerp van silindervormige staal, beton en beton-staal hibriede torings en fondamente vir naafhoogte van 80, 100 en 120m. 'n Gevolgtrekking oor die lewensvatbaarheid van die beton en hibriede torings, in vergelyking met die gewone staal torings teen naafhoogte van 100 tot 120m sal ook gemaak word.

Met die bogenoemde as doel, is drie van elke tipe toring (staal, beton en hibried) en hul fondamente volgens die toepaslike standaarde ontwerp. Daarna is die integriteit van die ontwerpe getoets en bevestig deur gebruik van die *Abaqus* eindige-element-metode sagteware. Ten slotte, die kostes van die ontwerpe vir 'n Suid Afrikaanse omgewing is bereken en die verandering in materiaalkoste uitgedruk as 'n funksie van die verhoging in naafhoogte.

Daar is gevind dat, vir die aannames in die ontwerp, die fondamente van die beton en hybrid torings minder materiaal benodig, en dus goedkoper is as die staal torings. Verder, is die materiaalkoste van die beton en hibriede torings laer as die van die staal torings, veral vir naafhoogtes van 100 tot 120m. Verder, is daar vir die omstandighede in hierdie projek gevind dat hoër naafhoogtes stygings in energie-opwekking van 3.52 persent vir naafhoogte stygings van 80m tot 100m, en stygings van 6.28 persent vir naafhoogte stygings van 80m tot 120m lewer. Daar word dus tot die gevolgtrekking gekom dat, gegewe die tendense in die ontwerp en materiaal koste wat verband hou met die verhoging van die naafhoogte, die beton en hibriede torings 'n lewensvatbare alternatief vir die konvensionele staal torings vir naafhoogtes van 100 tot 120m word.

Acknowledgments

Firstly, I would like to thank Prof. van Zijl for his seemingly limitless patience and willingness to assist me throughout the project, it is greatly appreciated.

I would also like to express my gratitude to the Stellenbosch University Department of Civil Engineering for funding the project, it would not have happened otherwise.

To my friends, parents and Kelly, thank you for your love, patience and support. It means the world to me.

This research was presented at the Stellenbosch University Civil Engineering Departments *International Seminar on the Design of Wind Turbine Support Structures* on the 3^{rd} of September 2014, at the Stellenbosch Institute for Advanced Study (STIAS), Stellenbosch.

> *"Have you not known? Have you not heard? The LORD is the everlasting God, the Creator of the ends of the earth. He does not faint or grow weary; His understanding is unsearchable. He gives power to the faint, and to him who has no might he increases strength.*
>
> *Even youths shall faint and be weary, and young men shall fall exhausted; but they who wait for the LORD shall renew their strength; they shall mount up with wings like eagles; they shall run and not be weary; they shall walk and not faint."*
>
> Isaiah 40:28-31.

Contents

List of Figures

List of Tables

Nomenclature

Roman Upper Case

A – Area (m^2)
A_{eff} – Effective area (m^2)
A_s – Area of steel (mm^2)
$A_{s,max}$ – Maximum allowable steel area (mm^2)
$A_{s,min}$ – Minimum allowable steel area (mm^2)
B – Foundation breadth (m)
C_d – Performance power coefficient
$C_{r(z)}$ – Wind distribution scale factor
D – Foundation height (m)
D_b – Foundation wedge height (m)
D_{bot} – Diameter of tower base (m)
D_{Ed} – Fatigue damage factor
D_e – Embedded depth of foundation (m)
D_s – Depth from ground level to bottom of foundation (m)
D_{top} – Diameter of tower top (m)
D_w – Foundation wedge height (m)
E – Young's modulus (GPa)
$E_{actual,annual}$ – Actual annual energy generated (MWh)
$E_{max,annual}$ – Actual annual energy generated (MWh)
E_{annual} – Total annual energy production (MWh)
F_0 – Initial prestressing force (kN)
F_c – Compression force (kN)
$F_{d,ps}$ – Design prestressing force per tendon (kN)
F_o – Buoyancy force on foundation (kN)
F_t – Tension force (kN)
F_w – Half weight of tower and turbine (kN)
F_{wt} – Wind forces acting on tower (kN)
F_z – Tower and turbine weight (kN)
G – Shear modulus (MPa)
H – Soil depth to rock from ground level (m)
H_d – Design horizontal force $=F_{xy}$ (kN)
I – Second moment of inertia (m^4)
K – Elastic stiffness (kN/m)
L – Length (m)
L' – Effective length (m)
M – Applied moment (kNm)
M_d – Design applied moment (kNm)
M_o – Overturning moment on foundation due to wind pressure (kNm)

M_{ps} – Moment caused by prestressing force (kNm)
M_R – "Stabilizing" or "rectifying" moment of foundation (kNm)
M_x – Tower moment causing bending in the direction of the x-axis (Bending around the y axis) (kNm)
M_y – Tower moment causing bending in the direction of the y-axis (Bending around the x axis) (kNm)
M_z – Torsional tower moment causing bending around the z-axis (kNm)
N_d – Design vertical load on tower (kN)
N_{el} – Euler elastic buckling load (kN)
N – Number of load repetitions (fatigue)
$N(\Delta\sigma_i)$ – Number of resisting cycles for stress range $\Delta\sigma_i$
N_c, N_q, N_γ – Bearing capacity factors
$P_{associated}$ – Power generated for a given wind speed (kWs/m)
$P_{available}$ – Power available for generation (MW)
P_g – Power generated (MW)
P_t – Total power contained in wind resource (MW)
R – Foundation radius (m)
R_{ring} – Radius of foundation anchor ring (m)
R_{tower} – Radius of tower (m)
S_c, S_q, S_γ – Shape factors (bearing capacity design)
$S_{c,max}$ – Maximum compressive stress (fatigue design) (MPa)
$S_{c,min}$ – Minimum compressive stress (fatigue design) (MPa)
$S_{ct,max}$ – Maximum tensile stress (fatigue design) (MPa)
V – Volume (m^3)
V_d – Design vertical force at underside of foundation (kN)
V_{e50} – 3-Second gust wind speed with a 50 year return-period (m/s)
V_{ED} – Vertical design force (foundation design)(m/s)
V_f – Foundation weight (kN)
V_{ref} – Reference wind speed (m/s)

Roman Lower Case

b – Effective breadth of foundation (m)
c – Concrete cover to reinforcing (mm)
c_d – Design soil cohesion intercept (Foundation Design) (kN/m^3)
c_d – Structural factor (Wind Pressure)
c_f – Force coefficient for structural element
c_s – Structural factor
$d_{aggregate}$ – Greatest aggregate dimension (mm)
d_{eff} – Effective foundation depth (m)
d_i – Inner tower diameter (m)
d_o – Outer tower diameter (m)

d_s – Distance between tension and compression centroids (m)
e – Foundation load eccentricity (m)
e_g – Geometric imperfection of steel tower (mm)
e_q – Horizontal shear-force-induced moment lever arm $= D$ (m)
$f_{capacity}$ – Wind turbine capacity factor
f_{cd} – Design cylinder strength of concrete (MPa)
f_{ck} – Characteristic strength of concrete (MPa)
$f_{ck,cube}$ – Characteristic cube strength of concrete (MPa)
$f_{ck,fat}$ – Fatigue reference compressive strength (MPa)
$f_{ctk,min}$ – Minimum characteristic tensile strength (MPa)
f_n – Natural frequency (Hz)
f_{yd} – Steel design yield stress (MPa)
g_d – Foundation weight distributed load (kN/m)
i_c, i_q, i_γ – Inclination factors (bearing capacity design)
k – Steel tower core radius(m)
k_1, k_2 – Defines first and second slopes for S-N curves
k_H – Horizontal foundation spring stiffness (kN/m)
k_R – Rotational foundation spring stiffness (kNm/rad)
k_T – Torsional foundation spring stiffness (kNm/rad)
k_V – Vertical foundation spring stiffness (kN/m)
m – Mass (kg)
m_{tower} – Mass of wind turbine tower (kg)
m_{rotor} – Mass of rotor assembly. (Blades, nose cone, nacelle and generator) (kg)
$n(\Delta\sigma_i)$ – Number of applied cycles for stress range$\Delta\sigma_i$
n_{ri} – Number of stress load repetitions causing failure for given stress range
n_{si} – Number of stress load repetitions for given stress range
q_f – Bearing capacity (kPa)
$q_p(z_e)$ – Peak wind speed at height z_e (kPa)
r_b – Blade radius (m)
r_h – Radius of rotor cone (m)
t – Tower shell thickness (mm)
t_{bot} – Tower Bottom shell thickness (mm)
t_{mid} – Tower middle shell thickness (mm)
t_{top} – Tower top shell thickness (mm)
u_0 – Perimeter length of tower base control perimeter (m)
u_1 – Length of first control perimeter at a distance 2d from support face (m)
v_{ED} – Design shear stress (MPa)
v_{min} – Minimum shear stress resistance of concrete (MPa)
$v_{Rd,max}$ – Max allowable concrete shear stress (MPa)
$v_{b,basic}$ – Basic wind speed (m/s)
$v_{p,peak}$ – Peak wind speed (m/s)
x – Distance along foundation length (m)

x_1 – Distance to first control perimeter from tower center (m)
y – Tower radius distance (m)
z – Tensile steel reinforcing lever arm (m)
z_{hub} – Nacelle hub height (m)
v_{wind} – Wind speed (m/s)

Greek Symbols

$\Delta\sigma_{Rsk}$ – Resisting stress range at N cycles (MPa)
$\beta_{cc}(t)$ – Coefficient depending on age of concrete at fatigue loading
$\beta_{c,sus}(t, t_o)$ – Coefficient accounting for the effect of high average stresses during loading
γ – Bulk unit weight of soil (kN/m^3)
γ' – Buoyant unit weight of soil (kN/m^3)
γ_c – Partial material factor for soil cohesion intercept
γ_f – Partial load factor for variable actions
$\gamma_{f,fat}$ – Partial load factor for fatigue actions
γ_g – Partial load factor for permanent actions
$\gamma_{m,c}$ – Partial material factor for concrete
$\gamma_{m,ps}$ – Partial material factor for prestressing
$\gamma_{m,s}$ – Partial material factor for steel
$\gamma_{m,s,fat}$ – Partial material factor for steel in fatigue
γ_ϕ – Partial material factor for soil angle of shear resistance
δ – Prestressing losses
$\epsilon_a, \epsilon_b, \epsilon$ – Reduction factors (Buckling Analysis)
η_{avail} – Coefficient for availability of wind turbine
η_{elec} – Coefficient for electrical losses in generation
λ_a – Relative slenderness ratio (Buckling Analysis)
μ – Curvature coefficient (Prestressing)
ν – Poisson's ratio
ρ_{air} – Density of air (kg/m^3)
ρ_1, ρ_2 – Reinforcing ratios for steel in the x, y directions
σ_{ad} – Stress due to axial force (MPa)
σ_{bd} – Stress due to bending moment (MPa)
σ_{el} – Critical elastic shear stress (MPa)
$\sigma_{c,max}$ – Maximum compression stress in concrete section (MPa)
$\sigma_{c,min}$ – Minimum compression stress in concrete section (MPa)
σ_{cr} – Critical compressive stress (MPa)
σ_{ct} – Tensile stress in concrete section (MPa)
$\sigma_{ct,max}$ – Maximum tensile stress in concrete section (MPa)
σ_{soil} – Soil pressure (kPa)
ϕ – Design soil angle of shear resistance (deg)
ϕ_{bar} – Diameter of tensile reinforcing steel bars (mm)
ϕ_{ps} – Outer diameter of prestressing duct (mm)

Abbreviations

$ASCE$ – American Society of Civil Engineers
$BBBEE$ – Broad-Based Black Economic Empowerment
DoE – Department of Energy
$EC2;7$ – Eurocode 2;7
EQU – Limit state for equilibrium design
$EWEA$ – European Wind Energy Association
FEM – Finite Element Method
GEO – Limit state for Geotechnical design
kWh – kilo-Watt-hour
MBL – Minimum Breaking Load
MW – Mega-Watt
Pa – Pascal
PS – Pre-Stressing
$REIPPPP$ – Renewable Energy Power Producer Procurement Programme
SKA – Square-Kilometer Array
STR – Limit state for structural design
ULS – Ultimate Limit State
$WASA$ – Wind Atlas for South Africa
WTG – Wind Turbine Generator

Chapter 1

Introduction

1.1 Background

The birth of the South African wind industry was brought about by the commitment of the Department of Energy (DoE) to the reduction of South Africa's substantial carbon footprint. More than 90 percent of the power demand of the country is currently met through traditional coal-fired power stations, with most of the remainder being supplied by Koeberg Nuclear Power facility. South Africa aims to reduce its emissions by 34 and 42 percent by 2020 and 2025, respectively. To do so will require a radical diversification of the energy mix (Regency.org, 2008). As such, the Renewable Energy Independent Power Producer Procurement Program (REIPPPP) was introduced by the DoE in August of 2011.

The REIPPPP sparked the beginning of a significant South African commitment to the introduction of a wind industry. To date, 1985 Mega-Watt(MW) of wind power capacity is either in operation or has commenced construction in South Africa, with a further as-of-yet undisclosed amount of wind power still to be allocated in the next rounds of the REIPPPP. From the first, to the third round of bids, the price of wind-generated energy has dropped from 114c/kWh to 74c/kWh, a clear indication of a fast-maturing industry.

Currently, the global trend is to use taller wind turbine towers, in order to gain access to stronger, more constant and less turbulent winds. This is generally because the high wind-speed areas have already been used for wind energy generation and due to the development of improved turbine and blade technology. Due to the infancy of the South African wind industry, such optimal sites have not yet been exploited. Some of the South African wind energy projects are already using taller towers, such as the 138MW Gouda Wind Facility, currently nearing the end of its construction phase, which uses 100m concrete towers (AVENG Group and Acciona Energy South Africa, 2012).

The introduction of towers with greater hub heights give rise to designs that differ from the traditional tubular steel tower. As the height of the towers increase, so do the stiffness requirements, to the point

where the use of steel towers become increasingly expensive. As the tower heights increase, concrete and concrete-steel hybrid towers start to become economical, as alternatives to the steel towers.

1.2 Problem Statement

The current trend in the global wind industry is to use taller wind turbine towers of various designs in order to lift hub heights above the 80m mark. This allows the wind turbine access to stronger and less turbulent winds, which leads to reduced fatigue loading on the structural support system, increased energy conversion and therefore increased revenue generation. The use of precast, segmented, post-tensioned concrete and concrete-steel hybrid towers are becoming increasingly popular alternatives to the traditional tubular steel tower as a means of achieving this goal. The use of these three tower designs for hub heights ranging from 80 to 120m is to be investigated with regard to structural design, cost and increase in revenue in a South African context and to propose guidelines for the use thereof to the fast-emerging South African wind industry.

1.3 Objectives

This project aims to determine the costs of increases in tower hub height for steel, concrete and hybrid wind turbine towers, with regard to the towers and foundations. To do this, three towers of each design, at hub heights of 80, 100 and 120m are designed, with focus on the structural design of the foundation and tower. In addition, the extra revenue generated due to the turbines being exposed to stronger wind resources is calculated and presented. The cost increases are used to determine whether taller towers are likely to be feasible in a South African context. Guidelines to the local wind industry are proposed throughout the text, with regard to the choice of tower design and hub height.

1.4 Limitations

The project focuses specifically on the design and costing of the support structure of the wind turbine (tower and foundation). Additionally, the project focuses on onshore, horizontal axis wind turbines in a South African context. Other aspects of the wind turbine such as the turbine itself, the blades, nacelle and the electrical systems are not included in the design or cost analysis. The following aspects in particular, pertaining to wind turbine tower infrastructure, are excluded from this study: construction method and duration; site locality; aesthetics; variation in geotechnical conditions and the sustainability of the various technologies in a South African context.

1.5 Methodology

A literature study on the global and South African wind industries is performed in order to better understand the current status of the global and local wind energy industries and communities. An analysis is done on the wind resource and the available wind resource information in South Africa to be able to justify the use of taller wind turbine towers. The current structural design practice, with

regard to the support structure and site conditions, is studied and implemented in the design of the towers and foundations. The subsequent designs are verified using the *Abaqus 6.10* FEM software. The design costs are then obtained and compared with the increase in revenue due to the taller towers.

References

AVENG Group and Acciona Energy South Africa (Aug. 2012). *Gouda Wind Facility - NERSA Public Hearings*. AVENG Group. URL: http://www.nersa.org.za/Admin/Document/Editor/file/Consultations/Electricity/Presentations/Blue%20Falcon%20140%20Trading%20(Pty)%20Ltd.pdf.

Regency.org (2008). "Renewable Energy in South Africa". URL: http://www.regency.org/news_aug10_3.html.

Chapter 2

Literature Study

2.1 Wind Power in South Africa

The REIPPPP introduced feed-in tariffs as an incentive for the generation of renewable energy. Each renewable energy sector has its own feed-in tariff, determined by the DoE. Initially, the feed-in tariff for onshore wind generated power was R1.143/kWh, but this value later dropped to R0.897/kWh for the second round of the REIPPPP allocation process (Pickering, 2013).

The introduction of the REIPPPP saw the South African Wind industry go from being a pipe dream to becoming a reality. As stated in the REIPPPP, 1850MW of wind power is to be installed in South Africa. Round one and two of the REIPPPP saw an allocation of 1196.5MW of wind power (Forder, 2012). The conclusion of the first round of the IPPPP in late 2011 saw the allocation of 634MW of wind power through 8 projects. The second round resulted in 562.5MW being allocated through 7 projects.

The REIPPPP stresses the following points and gives preference to bidders that propose projects that, amongst others (National Energy Regulator of South Africa, 2009):

- Create local employment;
- Aim to localize technologies;
- Implement skills development strategies;
- Adhere to the principles of Broad-Based Black Economic Empowerment (BBBEE).

The third round of the REIPPPP reached closure on 29 October 2013, allocating a further 787MW of wind power in 7 projects, although the DoE has stated that it will be allocating an extra undisclosed amount of wind power due to the exceptionally competitive prices received from the third round bidders. The third round saw the price per kiloWatt-hour drop even further to an average cost of 74c. This is frowned upon by local-content enthusiasts however, as the over-competitiveness

at such low prices will mean that the constituents of wind farms that could have been made locally will more than likely be imported, as local manufacturers will not be able to match international prices.

A more gradual cost reduction would have given local manufacturers the chance to compete with their international counterparts, however, there are positives in that some parts will be able to be manufactured locally and a lower price per kWh will promote the wind energy industry. The DoE has also increased its original procurement target for renewable energy from 3725 to 6925 MW as a consequence of the highly competitive pricing it has received.

South Africa has been classified as favourable country for wind power generation due to the intensity of the wind, particularly along the west and east coast, where annual average wind speeds reach 8 meters per second (m/s) and higher, ideal for wind power generation. Due to the infancy of the wind industry in South Africa, there are only a few, if any, guidelines and no codes of practice for the wind industry. This necessitates total dependence on international companies for the near future. In order to create a locally sustainable wind industry, such guidelines need to be put into place to ensure quality control, safe structures and the cost-effectiveness of wind farms.

2.2 The Need for Higher Wind Speeds

To understand the need for taller towers and therefore stronger winds, one must understand the fundamental principles of wind power generation. The generally accepted equation used to calculate the power generated by a wind turbine is given by Equation 2.1 (Hansen, 2008):

$$P_{\text{Available}} = 0.5 \cdot \rho_{air} \cdot A \cdot v_{wind}^3 \cdot C_d \tag{2.1}$$

Where:

$$\begin{aligned} P_{Available} &= Power\ available\ for\ generation\ (MW) \\ \rho_{air} &= Air\ density\ \left(\frac{kg}{m^3}\right) \\ A &= Swept\ rotor\ area\ (m^2) \\ v_{wind} &= Wind\ speed\ \left(\frac{m}{s}\right) \\ C_d &= Performance\ power\ coefficient. \end{aligned}$$

Equation 2.1 shows that there are three variables that can be changed in order to increase the power generated by the turbine generator namely: A, v_{wind} or C_d.

Increasing A:
In order to increase the swept rotor area, A, one needs to increase the radius and thus the length of the blades. This has a quadratic effect due to the formula for the swept rotor area ($A = \pi(r_b^2 - r_h^2)$),

where r_b is the blade radius and r_h is the radius of the coned portion of the nacelle. The current trend is to use bigger turbine blades in areas of low to medium wind resources.

This approach, however, is limited by the strength of the material from which the blades are manufactured. According to the Caithness Windfarm Information Forum (2013), 1370 known (but not all-inclusive) wind turbine failures have been documented from 1996 to March of 2013, 18.8 percent of which are attributed to blade failure. It was therefore decided that this option would not be considered primarily in this study as a means of increasing the power generated by wind turbines.

Increasing C_d:
The second option to increase the productivity of wind turbines is to increase the performance power coefficient, C_d, defined as:

$$C_d = \frac{P_g}{P_t} \tag{2.2}$$

Where:

$P_g = Power\ generated\ by\ turbine\ (MW)$
$P_t = Total\ power\ contained\ in\ wind\ resource\ (MW)$

As can be seen from Equation (2.2), the value for C_d is the ratio between the energy generated by the turbine and the total energy present in the wind for the swept rotor area and hub area. The C_d value is limited to 0.59 by Betz' Limit for conventional three bladed wind turbines, although currently the value is, for high productivity turbines, generally in the range of between 0.35 and 0.45, reaching a maximum of 0.47 (Galvao, 2009; Royal Academy of Engineering, 2010).

This value range for the performance power coefficient is unlikely to rise much higher except with a noticeable change in turbine design. It was therefore decided that from a civil/structural engineering perspective this is not a viable option to pursue.

One option remains, to increase the wind speed, v_{wind}, by constructing taller turbine towers. As shown in Equation (2.1), increases in v_{wind} result in cubic increases in the $P_{\text{Available}}$ for generation. Even small increases in v_{wind} can therefore cause substantial increases in $P_{\text{Available}}$.

2.3 Cost of Tower and Foundation

The costs associated with a wind energy facility are dominated by the up-front costs of the turbine constituents, tower, foundation, construction and civil works. A study on the progressing South African wind energy industry done by Szewczuk (2012), gives a cost breakdown of a typical South African wind energy project, based on the cost-weighting of international projects. The partial breakdown is adapted from the one presented by Szewczuk and is shown in Table 2.1:

Table 2.1: Cost breakdown of a typical South African wind energy project.

Component	% of Total Cost
Grid Connection	12
Civil Works	4
Other Capital Costs	8
Tower	18.7
Electrical and Mechanical Constituents	13.56
Rotor, Blades, Rotor Accessories	17.66
Gearbox	9.2
Generator	2.4
Foundation	5*
*Assumed foundation percentage, deducted from civil works.	

The foundation costs vary considerably, from 16 percent in one source (Tegen et al., 2011), to 4 percent in another (IRENA, 2012). Relatively favourable soil and site conditions will be closer to the 4 percent mark, whereas adverse soil and site conditions can drive the cost up to the 16 percent mark. Assuming a value of 5 percent, given favourable soil and site conditions, as shown in Table 2.1, the combined cost-weight of the foundations and towers is in the order of 23.7 percent of the cost of a wind energy project.

It is therefore sensible to focus on the part of a wind turbine that contributes only a quarter of the total cost, but can have a considerable impact on the amount of energy and therefore, revenue, generated by the wind farm.

2.4 Preliminary Wind Data Calculations

Preliminary wind data calculations were performed in order to support the "taller is better" hypothesis posed by the problem statement, with regard to the tower and thus the turbine hub-height. Wind data was obtained from the Wind Atlas for South Africa (WASA) project (DoE, 2013). The most reliable and complete data set at the time was a 12 month period, corresponding to the 2011 calendar year. Two of the masts contained vast periods of no data and consequently the Butterworth mast, situated in the Eastern Cape, as well as the Noupoort mast, situated in the Northern Cape, were omitted from the preliminary calculations.

The data of the remaining 8 masts was then checked and it was found that there were only brief periods of no data in the data set and so the data was considered satisfactory for use in wind speed interpolation through the use of regression. For each mast, the yearly average wind speed for 10, 20, 40, 60 and 62m (above ground level) was obtained and curves were then plotted in order to get an extrapolated value for the mean annual wind speed at 80, 100 and 120m above ground level as a function of the wind speed at lower values.

It is understood that extrapolation serves as a mere illustrative purpose, but it is believed that the trend in wind speed increase holds true for the considered heights. The curves were all of a similar

logarithmic shape, indicating that the increase in wind speed is more evident for hub-height increments at lower heights. The extrapolated 80, 100 and 120m values were then expressed as ratios of the actual 62m values. The mean of these ratios was then used to get a mean annual value for the wind speeds at 80, 100 and 120m, as a ratio of the 62m wind speed and can be seen in Tables 2.2 and 2.3.

Table 2.2: Mean wind speed (m/s) data extrapolated to 80, 100 and 120m for 2011.

	Height above ground level (m)						
	Extrapolated			**Wind Mast Data**			
	120	100	80	60	40	20	10
Humansdorp	7.92	7.74	7.51	7.22	6.81	6.11	5.41
Napier	9.19	8.97	8.70	8.36	7.87	7.04	6.22
Beaufort West	7.42	7.24	7.02	6.75	6.35	5.68	5.01
Vredendal	7.77	7.60	7.38	7.11	6.72	6.07	5.40
Sutherland	7.75	7.56	7.34	7.04	6.63	5.92	5.21
Vredenburg	7.37	7.17	6.93	6.61	6.17	5.42	4.66
Calvinia	6.70	6.53	6.33	6.08	5.72	5.10	4.48
Alexander Bay	6.56	6.43	6.28	6.08	5.80	5.33	4.85

Table 2.3: Increase in mean wind speed (%) for 2011 WASA wind data (62m hub height reference).

	120m	**100m**	**80m**
Humansdorp	9.71	7.16	4.03
Napier	9.92	7.31	4.10
Beaufort West	9.93	7.31	4.12
Vredendal	9.27	6.84	3.85
Sutherland	10.04	7.40	4.18
Vredenburg	11.40	8.41	4.73
Calvinia	10.17	7.49	4.21
Alexander Bay	7.81	5.77	3.26
Average	9.78	7.21	4.06

It can be seen that the values for the wind speeds at 80, 100 and 120m for the eight masts, are on average 4.06, 7.21 and 9.78 percent higher than the wind speeds at 62m, respectively. The increase is better illustrated by Figure 2.1. Even though the average values are a good indication of greater wind speeds at greater heights, there is no substitute for site-specific data.

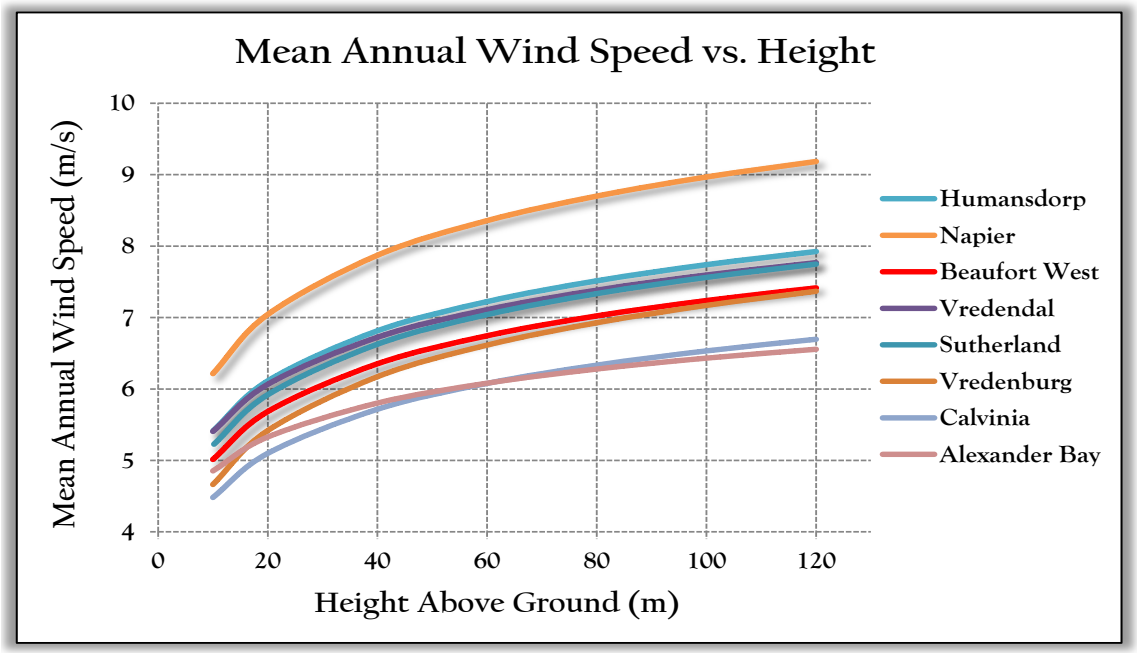

Figure 2.1: Graph of 2011 average wind speed vs. height.

2.5 High Capacity Factor vs. Higher Total Output

Greater wind speeds can result in one of two options. The first is a greatly increased capacity factor for the chosen wind turbine generator (WTG). The capacity factor is a measure of how much energy is actually generated on an annual basis, as a percentage of the total possible annual energy generation capability of the WTG, if it was running at nameplate capacity 24 hours a day, 365 days a year. This can be seen in Equation 2.3:

$$f_{\text{capacity}} = \frac{E_{\text{actual,annual}}}{E_{\text{max,annual}}} \tag{2.3}$$

Where:

$$f_{\text{capacity}} = \textit{Capacity factor}$$
$$E_{\text{actual,annual}} = \textit{Actual annual power generated by the WTG (MWh)}$$
$$E_{\text{max,annual}} = \textit{Maximum possible power able to be generated per anum (MWh)}$$

So it can be seen that greater wind speeds cause greater capacity factors.

The second option is to upgrade to a WTG with a greater nameplate capacity in order to take advantage of the higher output due to the higher average wind speeds. This will result in a lower capacity factor, but will also result in more total power generation which results in a higher revenue generated by the WTG.

2.6 Tower Construction Material

Before the introduction of multi mega-Watt wind turbines, truss type structures were sufficient to support the sub mega-Watt WTGs. The increased weight and applied moments that are common to the multi-mega-Watt WTGs of today make truss structures time consuming to erect and are generally considered unsightly by the public. As such, more than 90 percent of WTG towers today employ a tapering tubular structure made out of steel (World Steel Association, 2012).

2.6.1 Steel

Steel is considered the most cost effective material for multi mega-Watt turbines with tower heights of between 60m and 100m. This is due to the high strength-to-weight ratio of steel. Tapered tubular steel structures have disadvantages in that they become too large to transport by road when tower diameter reaches 4.5m. In addition, thicker sections are needed for steel towers with heights exceeding 80m, which often becomes too expensive to be profitable (World Steel Association, 2012). As global trends tend towards taller WTG towers, other tower designs become economical for towers taller than 80m. A steel tower during transport can be seen in Figure 2.2.

Figure 2.2: Sections of a steel turbine tower being transported. Source: North East Windmills (2013).

2.6.2 Precast Post Tensioned Concrete

The use of high strength in-situ and particularly, precast concrete has become a popular material due to its high stiffness and transportability. Precast concrete towers are manufactured off site and are transported to site as half or quarter segments. This becomes particularly applicable to the South African scene where in-situ construction can be severely delayed by bad weather conditions.

Post-tensioned concrete for use in WTG towers is well-suited, due to its high structural stiffness and ductility. The increased stiffness results in far smaller lateral deflections of the tower caused by the cyclic loading that the wind exerts on the tower. The machinery in the nacelle of the WTG will

therefore experience far less vibration-induced wear and tear.

Another issue that is addressed with a concrete tower is the reduction in noise levels during generation, due to the damping effect of the concrete (Fabcon, 2013). The maintenance of concrete towers is also believed to be simpler than for steel towers. Due to the section-by-section construction of the tower, the lifting capacity requirement of the crane for construction is greatly reduced, which may play an important role in a South African context, where the industry is in its infant stages and typical wind turbine-assembling cranes will most likely have to be shipped in from other countries.

Figure 2.3: Assembly of a precast concrete tower. Source: Inneo Torres (2008).

2.6.3 Concrete-Steel Hybrid

Another design that is rapidly gaining popularity is the concrete/steel hybrid tower. These towers typically consist of a 40-80m concrete base section, either pre-cast or cast on site, and a conventional modular tapered steel tower adding a further 40-60m to the tower height (Nordex, 2007). This design combines most of the advantages of both concepts with the ease of construction of the precast section as well as the same weight-lifting requirement as for the conventional modular steel tower approach. This approach seems to be the most popular of the newly introduced designs, due to its cost-effectiveness and simplicity.

2.6.4 In-Situ Slip-formed Concrete Construction

Another option worth considering is using slip-formed, concrete construction techniques to construct the towers. This method involves the use of sliding formwork which moves up at a rate of millimeters per hour, as the poured concrete begins to set. A notable advantage of this method is that the entire structure is cast continuously, so there are no joints.

This may or may not be a viable option for the South African wind industry, as the towers are not uniform - the thickness and diameter changes as a function of height. A slip forming industry for

uniform sections has been established in South Africa, although not extensively used. Slip-forming for conical-shaped structures like wind turbine towers, however, is a specialized field for which there are few local applications and there are therefore few local companies that have the capacity and resources available to apply this method of construction. It may be the case however, that due to the savings that are generally associated with slip forming techniques (Zayed et al., 2008), this construction method may still prove viable.

2.6.5 Other Designs

There are a small number of lesser-used designs that are new and are either just coming out of, or going into their feasibility study periods. One promising design is that of a tower made almost completely of engineered wood. German engineering firm TimberTower recently constructed their prototype 100m tall turbine tower in Hanover, Germany. The tower supports a Vensys 77 1.5MW WTG, weighing nearly 100 tons.

TimberTower claims that the towers will be able to reach heights of up to 200m while still being economically viable. The 100m tower also negates the transportation problem associated with steel towers with base diameters greater than 4.5m, as the towers are made from laminated wooden panels and wooden structural elements that are easily transported in 12m containers. There are also advantages in terms of a greatly reduced carbon footprint due to the insignificant amount of steel used in the tower, in comparison to the large quantities of steel required for the conventional steel towers (TimberTower, 2012).

This study will consider tower heights of between 80 and 120m, due to the fact that most of the windy areas in South Africa are near the coast and that even inland high-wind areas are generally not forested. Furthermore, the only towers that will be considered in this study are the conventional tapered steel tower, the precast segmented concrete tower and the steel/concrete hybrid tower. This choice is due to the fact that information will be most reliable from sources where the towers have been used fairly extensively and this therefore excludes the TimberTower from this study.

2.7 Wind Turbine Generator Choice

The choice of the WTG itself can also make a significant difference to the output of the wind farm. As discussed previously, WTG's with a higher nameplate capacity can take advantage of higher average wind speeds and thus generate considerably more power than a turbine with a lower nameplate capacity, provided that the wind resource is in fact strong enough to make the added expense worthwhile. This study will only consider one WTG, the specifics of which will be shown in a later chapter.

2.8 Foundation

Due to the differences in tower design and material, the tower foundations will differ, depending on the construction material of the tower, the weight of the nacelle and components, as well as site-specific

conditions.

2.8.1 Foundation Requirements

According to Nicholson (2011), the foundations need to satisfy requirements in terms of:

- Stiffness: The foundation needs to be stiff enough to limit the horizontal deflection, as well as the rotation of the tower to acceptable levels.
- Overturning Moment and Sliding: Due to the substantial moments about the toe of the foundation, due to the wind loading on the blades, nacelle and tower, the foundation must have a factor of safety against moment overturn of between two and three. The foundation also needs to be able to exert sufficient friction against the soil to avoid the base sliding.
- Natural Frequency Limits: Due to problems involving resonance between the natural frequency of the tower and the frequency of the rotation of the blades, the natural frequency of the tower must be sufficiently separated from the frequency of the blades. The foundation plays a role in the natural frequency of the tower and so the foundation design can be required to be adjusted in order to satisfy these requirements.

2.8.2 Site Conditions

Site conditions can play a large role in the cost of the wind turbine foundation. Weak soils create the necessity for either: large excavations in order to remove the soils and replace them with soils of more favourable properties, or piles to transfer the turbine loads from the weak soils further down to stronger soils or bedrock. The piled foundation approach is essential when the in-situ soils bearing capacity is not high enough to support the structure and loads (Hassanzadeh, 2012).

2.8.3 General Foundation Types

In general, there are three main foundation types namely: Shallow foundations, gravity foundations and piled foundations and are shown in Figures 2.4, 2.5 and 2.6.

Shallow Foundations:

Shallow foundations rely purely on the weight of the concrete in the base and the friction between the concrete and the soil in order to resist the applied forces and moments. The footprint-area of this type of foundation is therefore typically quite large and the foundation slab is thick. It has the advantage of not requiring vast amounts of excavation and back filling, but it does require large amounts of concrete and steel reinforcing.

Gravity Foundations:

This type of foundation is generally cast a few meters into the ground and covered with soil, thereby adding weight to the foundation and reducing the amount of concrete needed in terms of footprint-area

as well as thickness. It does however, require a large amount of excavation and back-filling and the buoyant forces from a potential water table can be considerable.

Piled Foundations:

In extreme cases of weak soils, piled foundations can be used, where the concrete pile cap is cast on top of a group of piles, effectively transferring the load from the weaker soil above, to the stronger soils or bedrock below, although this is only used as a last resort due to excessive cost of this option.

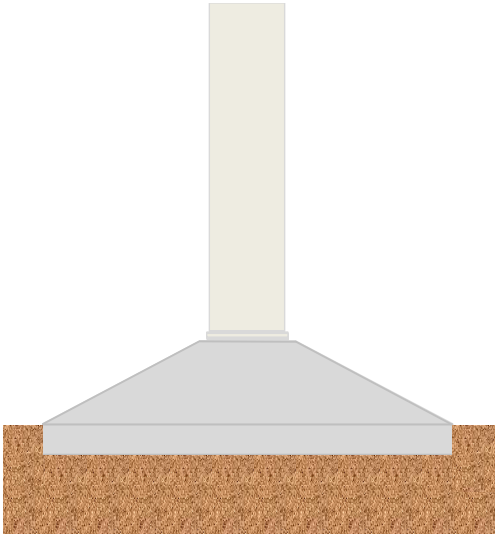

Figure 2.4: Shallow foundation.

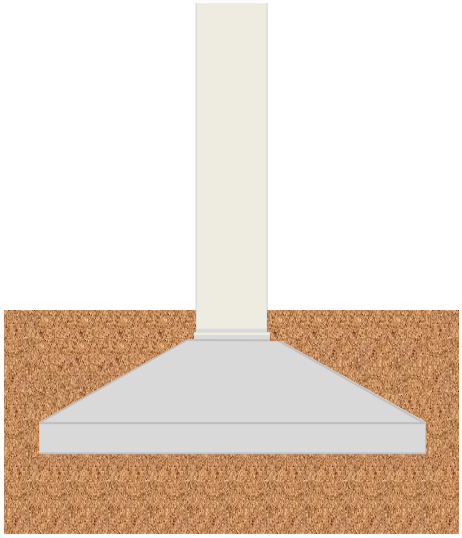

Figure 2.5: Gravity Foundation.

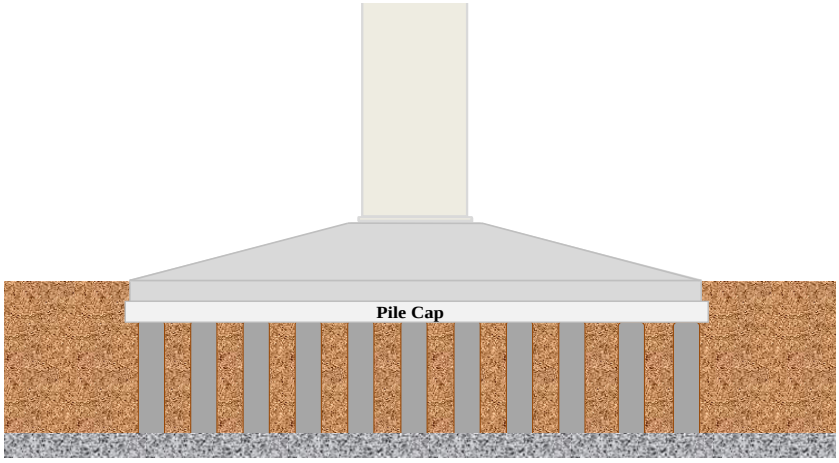

Figure 2.6: Piled Foundation.

2.9 Availability of Wind in South Africa

Although South Africa generally has more open areas to support wind energy generation than most European countries, there is a misconception that wind turbines can be placed anywhere that there is an available wind resource. This, however, is not true, due to many restricting factors that limit the available area that can be used for wind power generation.

One of the problems with wind power generation is that the turbines are fairly loud during operation.

This has led to laws being passed in most countries, enforcing a minimum distance between a turbine and any urban or residential area. This law is generally passed to enforce that the maximum ambient noise level increases are not exceeded. Also, there is much opposition to wind turbines on the premise of visual pollution. Many people perceive wind turbines as being unsightly, negatively affecting the natural landscape.

The available area is further reduced by excluding protected areas (national parks, wetlands and nature conservation areas) as well as natural heritage areas, areas with historical and cultural value and areas with former historical value (Belfiore et al., 2012). To this, one must add areas excluded by national roads, areas of high avian activity, areas of high natural ground slopes, areas around airports and telecommunication towers/beacons due to interference and many other considerations.

One particular source of area exclusion is the Square Kilometer Array (SKA) radio astronomy reserve. Due to the highly radio-reflective material and equipment used on the blade tips and the nacelle, the wind turbines are not allowed to be within the line of site of any SKA dishes (Christierson, 2013). This area excludes most of the Northern Cape and the Free-State provinces and small areas of the Western and Eastern Capes and the North-West Province.

The above mentioned factors are only the absolute restrictions, there are still the restrictions posed by local communities in the form of protest for various reasons. Thus large areas are excluded and the area available for wind power generation is far more limited than one would think. This leads to the point that there are not all that many high-wind sites available at the standard 80m hub-height, and many of those that are available have been utilized by the wind projects awarded in round one and two of the REIPPPP.

This poses an opportunity for the use of taller towers to exploit greater wind speeds at the moderate to low wind resource areas, which unlocks far larger areas that are available for wind power generation. Another option is to use taller towers at the sites that already have high wind resources and increase the nameplate capacity of the turbines in order to generate even more power.

2.10 Wind Farms as Investments

One of the big issues with wind energy facilities is that they are capital intensive, in comparison to traditional fossil-fuel power plants. According to the European Wind Energy Association (EWEA), approximately 75 percent of the total costs of a wind energy project are attributed to the main up-front costs of: the turbine; the purchase of property; the tower structure; foundations and grid connection (European Wind Energy Association (EWEA), 2010). In comparison, traditional fossil fuel power plants have relatively lower capital costs, but high running and maintenance costs that constitute between 40 and 70 percent of the total costs.

The low initial investment is attractive as the costs are spread out, which enables the revenue derived from the generation of power over time, to meet the costs. This is often why in developing countries, where capital may not be readily available, fossil fuel power plants have been favoured.

A reassuring facet of the wind industry, for investors, is the continued growth of the wind industry on a global level. Over the past two decades, the wind industry has seen exponential growth. Even throughout the economic recession of 2009 and 2010, the annual installed capacity continued to increase. This can be seen in Figure 2.7 (Global Wind Energy Council (GWEC), 2012).

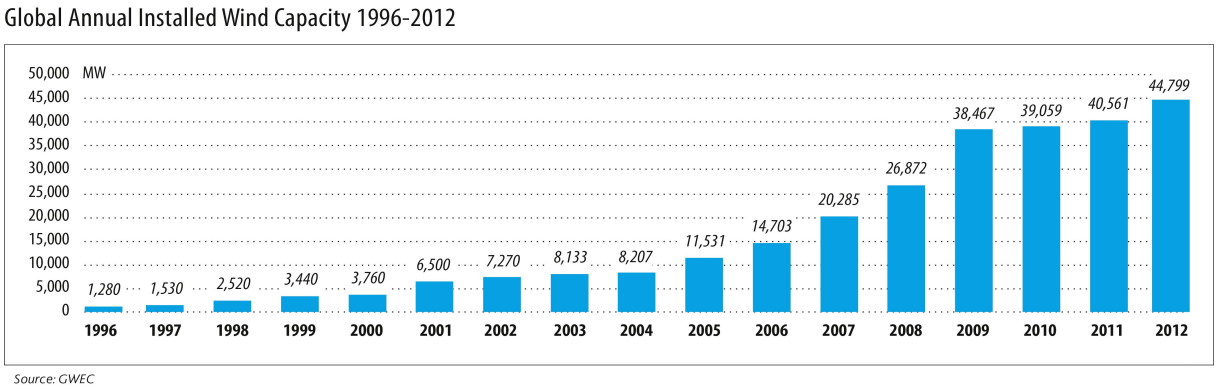

Figure 2.7: Global annual installed wind capacity between 1996 and 2012. Source: Global Wind Energy Council (GWEC).

This continued growth has turned the global wind industry into an almost-mature market that continues to grow and make strides to increase efficiency. In light of this, prices for wind-generated power drop more and more and are, in some parts of the world, at a point where they are competitive with fossil fuel-generated power. There is now healthy competition in the market that has decreased and continues to decrease the costs of production of wind turbines and their constituents.

2.11 Local Economic Effects of Wind Energy Generation

The maturity of the global market has led to widespread knowledge gain and transfer, particularly in the US, Europe and China. If the global trend is followed, South Africa stands to gain through the transfer of skills and knowledge, as enforced by the preferential treatment of project bids that adhere to the criteria, as set out in the REIPPP and stated in section 2.1. It is envisaged that, as the first country in Southern and Central Africa to embark on a wind energy "crusade", South Africa will become a hub for wind energy economies on the African continent.

The REIPPP stresses the fact that any renewable energy project bid that aims to localize technologies, amongst other factors, will gain preferred status over bids that do not. This is an essential criterion that enforces the localization of the manufacturing process so that, in time, the South African wind industry will become self-sufficient. This has and will continue to create job opportunities in the form of factory workers, wind energy specialists and technicians, to name but a few.

There is already progress towards this self-sufficiency in the form of a R300-million wind turbine tower manufacturing plant, currently under construction in the Couga Industrial Development Zone (IDZ), Eastern Cape (Nelson Mandela Bay Business Chamber, 2013) as well as the development of the

Isivunguvungu Wind Energy Converter (I-WEC), a high local-content 2.5MW wind turbine generator (Isivunguvungu Wind Energy Converter (Pty.) Ltd, 2013), amongst other developments.

2.12 Limits and Potential of Wind-Generated Power

In an economy where the wind industry is in its infancy, as is currently the case in South Africa, the limits in terms of a ceiling for wind-generated power seems premature to discuss, but it is important to note, as some European countries are reaching or have already reached this ceiling.

According to David Jones (2009), CEO of Allianz Specialized Investments, the generally-accepted limit of energy that can be generated by wind power is in the vicinity of 20 percent of the total energy production capacity of a country. This is due to the variable frequency of production of wind-generated power. At levels higher than 20 percent, variable power generation sources start to cause problems associated with managing the power grid of the nation. It is difficult to predict when the wind will blow across various areas of a nation and balancing the supply and demand of a nation's power becomes difficult when more than a fifth of generated power is derived from a variable source. This is only a future consideration for South Africa, but it will be an important factor as more wind power is added to the energy mix.

A point that links in with the above is that currently, there are no viable methods of large-scale electricity storage. This means that when the wind blows, the generated power is fed directly into the power grid and if there is no need for the power at the moment of generation, there is no way of storing the energy for use at a later stage. There are currently studies being conducted about the viability of wind farms being linked with pumped-storage systems, but this is unlikely to be viable in South Africa due to the scarcity of water, and thus suitable sites, around the country (Eskom Holdings SOC Limited., n.d.).

Wind power is considered by many to be a highly variable and unpredictable form of energy generation. This is mainly due to the variable nature of wind and the misconception that at times, wind power adds no useful energy to the national grid. This is not true, due to the geographical spread of wind turbine installments - the wind may not be blowing in certain areas, but it will be blowing in others. In addition to this, wind, like any other weather occurrence, can be forecast to a surprising degree of accuracy.

In times of low wind-generation output forecast, other forms of power generation can be utilized to balance out. Therefore, wind power will never be able to replace conventional forms of power generation on a one-to-one MW basis, but by no means does wind power need a "back-up" of conventional power generation on a one-to-one MW basis either. A study done by the American Utility Wind Interest Group concluded that (Utility Wind Interest Group, 2003):

> *"The results to date also lay to rest one of the major concerns often expressed about wind power: that a wind plant would need to be backed up with an equal amount of dispatchable generation. It is now clear that, even at moderate wind penetrations, the need for additional*

generation to compensate for wind variations is substantially less than one-for-one and is often closer to zero."

Another criticism of wind power is that it is completely inadequate to provide a predictable base-load power. This is not true either. Figure 2.8 shows the averaged hourly output of a single Siemens SWT-2.3-101 wind turbine, with a nameplate capacity of 2.3MW. This figure was complied using data from 9 of the 10 WASA wind masts for 2011, which represent more than a third of the geographic area and most of the potential wind power-areas of South Africa.

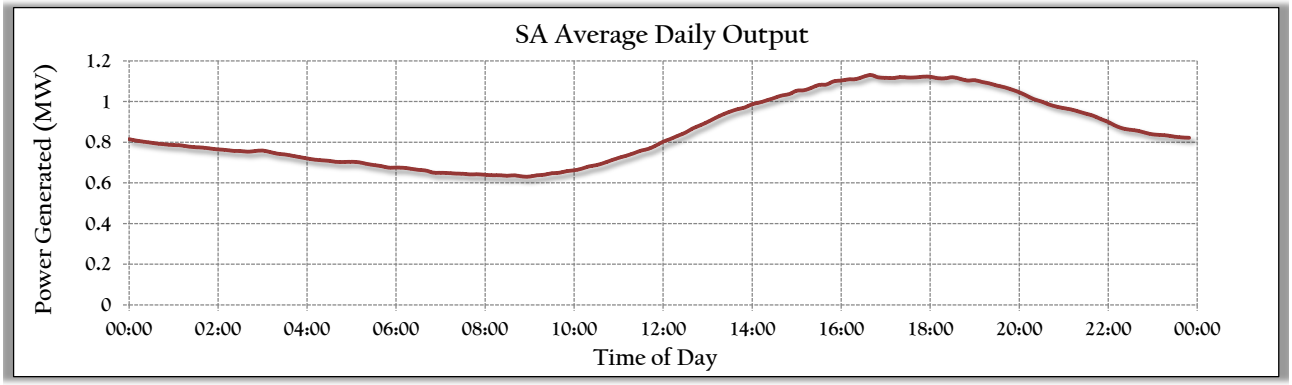

Figure 2.8: Average daily output of a single Siemens SWT-2.3-101 wind turbine in South Africa.

It can be seen from Figure 2.8 that there is a favourable rise in the average power generated after 10 a.m. and a fairly constant load until after the peak times of the evening. It is thus obvious that wind power is not an ideal form of power generation for the morning power peak, but it is useful for the base load throughout the day and the evening peak.

2.13 Similar Studies

A similar study was conducted in Sweden on 3 and 5MW turbines, with emphasis placed on how the choice of tower material and design, as well as the height of the tower, affected the cost-effectiveness of the solution. Although this study was aimed at the best solution for forested areas and thus included tower heights of up to 175m, valuable information was noted in terms of the methodology followed (Engström et al., 2010).

The results of this study, which aims to propose potential solutions to the problems of increasing tower height in South Africa, will more than likely have similar conclusions drawn in terms of cost-effectiveness linked with ease-of-construction as in Engström et al. (2010), although tower heights over 120m will not be considered in this study.

Another study conducted at the University of Iowa in 2011, used an optimization approach for the design of wind towers as well the foundations (Nicholson, 2011). Nicholson used the Solver add-in for Microsoft Excel as the optimization tool. Insight was gathered from this study, especially in terms of tower and foundation design considerations, even though it did not consider the cost element of the

analysis.

References

Belfiore, Francesco, Marco Montesi, Michele Fernetti, Charles Naidoo, and Dave Mercer (2012). "Innovative Spatial Tools for the Siting of Wind Turbines". In: *Renewable Energy World Africa Conference*.

Caithness Windfarm Information Forum (2013). "Summary of Wind Turbine Accident data to 31 March 2013". Caithness Windfarm Information Forum . URL: www.caithnesswindfarms.co.uk.

Christierson, Alice (Jan. 2013). "Potentially Astronomical Impact of the Astronomy Geographic Advantage Act". Norton Rose Fulbright. URL: http://www.nortonrosefulbright.com/knowledge/publications/74157/potentially-astronomical-impact-of-the-astronomy-geographic-advantage-act.

DoE, S.A. Department of Energy (2013). "Wind Atlas for South Africa". URL: http://wasadata.csir.co.za/wasa1/WASAData.

Engström, S., T. Lyrner, M. Hassanzadeh, T. Stalin, and J. Johansson (2010). *Tall Towers for Large Wind Turbines*. Tech. rep. Elforsk. URL: http://guidedtour.windpower.org/download/1266/Vindforsk_Project.pdf.

Eskom Holdings SOC Limited. (n.d.). "Pumped Storage". Eskom Holdings SOC Limited. URL: http://www.eskom.co.za/c/article/207/pumped-storage/.

European Wind Energy Association (EWEA) (2010). "Economics of Wind Energy". EWEA. URL: http://www.ewea.org/policy-issues/economics/.

Fabcon (2013). "Wind Turbine Towers". URL: http://www.fabcon-usa.com/products/wind-turbine-towers/.

Forder, S. (2012). "REIPPP: 2459.4MW of Preferred Bidders So Far". Energy.org. URL: http://energy.org.za/tag/REIPPP.

Galvao, F. L. (2009). ""Topics on Wind Turbine Aerodynamic Design"". In: *20th International Congress of Mechanical Engineering*. URL: http://www.aeitaonline.com.br/wiki/images/0/0e/COB09_0791_XVII_g3.pdf.

Global Wind Energy Council (GWEC) (2012). *Fig 2.7.* "Global annual installed wind capacity between 1996 and 2012.". URL: http://www.gwec.net/wp-content/uploads/2013/04/Global-Annual-Installed-Wind-Capacity-1996-2012.jpg.

Hansen, M. O. L. (2008). *Aerodynamics of Wind Turbines*. 2nd. Earthscan London, p. 3.

Hassanzadeh, M. (2012). Cracks in Onshore Wind Power Foundations. Tech. rep. Elforsk.

Inneo Torres (2008). *Fig 2.3.* "Precast concrete wind turbine tower.". URL: http://www.inneo.es/index.php/en/installation-process.html.

IRENA (2012). "Wind Power". In: *Renewable Energy Technologies: Cost Analysis Series* 1, p. 18.

Isivunguvungu Wind Energy Converter (Pty.) Ltd (2013). "The Isivunguvungu Wind Energy Converter". URL: www.i-wec.co.za.

Jones, David (Dec. 2009). "Turning Unpredictable Wind Power into a Good Investment". Allianz Specialized Investments. URL: http://knowledge.allianz.com/demography/population/?406/turning-unpredictable-wind-power-into-good-investment.

National Energy Regulator of South Africa, (NERSA) (2009). "Rules on Selection Criteria for Renewable Energy Projects Under the REFIT Programme". In: *Electricity Regulation Act No.4 of 2006: Electricity Regulations on New Generation Capacity* 1, p. 3.

Nelson Mandela Bay Business Chamber (May 2013). "DCD Establishes R300-million Wind Turbine Factory in Coega IDZ". URL: http://www.nmbbusinesschamber.co.za/blog/posts/dcd-establishes-r300-million-wind-turbine-factory-in-coega-idz.

Nicholson, J. C. (2011). "*Design of Wind Turbine Tower and Foundation Systems: Optimization Approach*". MA thesis. University of Iowa.

Nordex (2007). "Added Yields in Non-Coastal Regions". URL: http://www.nordex-online.com/fileadmin/MEDIA/Kundenzeitschrift/EN/Nordex_WPU_25_GB.pdf.

North East Windmills (May 2013). *Fig 2.2.* "Tower Sections for a Wind Turbine". URL: http://northeastwindmills.com/wp-content/uploads/2013/05/turbine-tower-sections.jpg.

Pickering, M. (2013). "Generating Power for Emerging Markets". Presented at the Stellenbosch Institute for Advanced Study (Stiαs). Globeleq. URL: http://stias.ac.za/wp-content/uploads/2013/03/WS-06-REIPPPP-Pickering-20130305b.pdf.

Royal Academy of Engineering (2010). "Wind Turbine Power Calculations". RWE Npower Renewables. URL: http://www.raeng.org.uk/education/diploma/maths/pdf/exemplars_advanced/23_wind_turbine.pdf.

Szewczuk, S. (2012). *Review of the Strategic Wind Energy Activities in South Africa*. CSIR Built Environment. URL: http://active.cput.ac.za/energy/past_papers/ICUE/2012/PDF/53.Szewczuk,%20S.pdf.

Tegen, S., E. Lantz, M. Hand, B. Maples, A. Smith, and P. Schwabe (2011). *2011 Cost of Wind Energy Review*. Tech. rep. National Energy Research Laboratory (NREL).

TimberTower (2012). "The Timber Tower: Structure and Operation". TimberTower. URL: http://www.timbertower.de/en/product/the-timbertower/.

Utility Wind Interest Group (Nov. 2003). *Wind Power Impacts on Electric-Power-System Operating Costs Summary and Perspective on Work Done to Date November 2003*. Tech. rep. 2004 Lakebreeze Way, Reston, VA: .

World Steel Association (2012). "Steel Solutions in the Green Economy - Wind Turbines". World Steel Association. URL: http://www.worldsteel.org/dms/internetDocumentList/bookshop/worldsteel-wind-turbines-web/document/Steel%20solutions%20in%20the%20green%20economy:%20Wind%20turbines.pdf.

Zayed, T., M. Reza Sharifi, S. Baciu, and M. Amer (2008). ""Slip-Form Application to Concrete Structures"". In: *Journal of Construction Engineering and Management - ASCE* 1, p. 157.

Chapter 3

Methodology

This thesis aims to:

1. Acquire and analyze South African wind data, ranging from 80-120m above ground;
2. Study the design of wind turbine support structures and foundations for steel, post-tensioned concrete and concrete-steel hybrid type towers;
3. Determine whether an increase in tower height is viable for South Africa or not, by deriving an indication of the increase in material costs;
4. Develop guidelines for the design and use of tall wind turbine towers for the South African wind industry.

3.1 Acquisition and Analysis of Wind Data

The wind data to be used is obtained from the WASA wind masts, as mentioned previously. Through the analysis of the wind data, the increase in wind speed and frequency as a function of increasing tower height will be determined.

3.2 Determining a Material Cost Comparison for Tower Designs

Once the wind data has been analysed, the respective tower designs and heights will be investigated in order to determine the material costs associated with increased hub height, to deduce whether increasing the hub height is viable or not. The investigation will consider the cost of the tower in terms of the material costs of the tower and foundation. Due to the varying costs associated with different manufacturers and materials, as well as the lack of actual South African data due to the infancy of the local wind industry, proportional cost ranges will be used to compare the different tower designs

and draw conclusions from the cost comparisons.

3.3 Development of Guidelines for the South African Wind Industry

Closely linked with the following aim, guidelines will be proposed to the South African wind industry. These guidelines will help potential investors in the South African market with respect to:

- Current status of wind power;
- The effect of increased tower height on revenue;
- Choice of tower design;
- Limited design of steel, concrete and hybrid towers;
- Limited design of the foundations;
- Choice of tower height;
- Advantages and disadvantages of each tower design.

This information will help wind farm developers in that it will be a condensed, integrated version of a large range of information that is available. This project interprets and comments on the use of existing international design guidelines for wind turbine support structures in light of South African conditions. The design of steel, post-tensioned concrete and post-tensioned concrete-steel hybrid towers is covered in selective detail. It also aims to confirm whether global trends are applicable to the South African wind industry or not.

3.4 Determining the Material Cost and Increase in Revenue of Taller Towers in South Africa

One of the main aims of this thesis is to determine whether taller wind turbine towers are in fact a viable option for South Africa by analysing the material costs associated with the tower and foundation. As stated before, South Africa has been labeled as an ideal location for wind energy and it may be that the winds are already strong enough and that taller towers are not cost-effective. Internationally, taller towers are generally used for inland sites, where the winds are, typically, not as strong as coastal sites. It remains to be seen whether this trend holds for South Africa or not.

Chapter 4

Material Cost Analysis and Revenue Generation

In order to conduct the material cost comparison of this project, different tower designs for the given site conditions will be considered. Table 4.1 illustrates the different combinations that will be used.

Table 4.1: Material cost comparison combinations for tower design and height.

Tower Design	**Tower Height (m)**	**Generator Nameplate Capacity (MW)**
Precast Post-Tensioned Concrete	80 100 120	3.0
Post-Tensioned Concrete/Steel Hybrid	80 100 120	3.0
Steel	80 100 120	3.0

The rotor diameter will be identical for all tower designs for the given nameplate capacity. The main deliverables in the material cost analysis of each combination are as follows:

- Material cost breakdown of the tower;
- Material cost breakdown of the foundation;
- Total energy generated (in MWh);
- Total and relative revenue for each tower height.

4.1 Cost Considerations

The costs involved in a project are always difficult to predict due to the effects of economies of scale, industry practice, availability of materials and labour, to name but a few. The main aim of this section is to calculate the costs involved with each tower type and height. As far as possible, the elements of a wind turbine that are common to all tower types will be left out of the analysis, so as to focus on a comparison between the different design options.

The business model aspect of a wind farm is, like most business ventures, relatively simple. Incomes must exceed expenditures to the point where an acceptable profit or return on investment is made. In this thesis, the comparative material costs will be calculated as far as possible. In addition, the increase in generated income (due to the stronger winds at increased hub heights) will also be calculated, although an entire viability analysis of the tower will not be made. Ideally, a comparison would have been made, but due to the reasons given in the following paragraph, it was omitted.

The cost comparison will mainly be in terms of the material costs associated with the towers and foundations. An entire breakdown of the tower, connection, turbine blades, nacelle and other associated costs is both difficult to carry out and introduces too many variables for the allotted time-resource available for this project. In addition to this, the wind turbine constituents and costs are the proprietary property of the respective companies and they are therefore not forthcoming with such information.

4.1.1 Foundations

It is predicted that the foundations for the concrete and concrete/steel hybrid towers will contain less reinforcing and concrete volume than the traditional steel tower, due to the increased stiffness and weight, and the lower centre of gravity of the towers. All of the foundations will be affected when a taller tower is considered and thus, a considerable increase in foundation costs is expected for the taller towers. The following aspects of the foundation costs will be considered:

- Volume of foundation reinforcing;
- Volume of concrete used in the foundation;

4.1.2 Towers

The cost of each tower will be unique to each design. As the tower manufacturers are secretive about the prices of the finished tower product particularly, the cost of the towers will also have to be calculated in terms of the material costs involved in the production of the tower, so as to give an as-accurate-as-possible comparison between the costs of the respective towers. The following cost aspects of the towers will be considered:

- Concrete tower material;
- Steel tower material;
- Prestressing costs, if applicable;

The increased productivity of the turbine, due to the increased height of the nacelle and thus higher wind speeds, leads to increased revenue generation. One of the main aims of this project is to quantify the increase in revenue generation as well as the cost incurred in doing so.

The following factors will influence the cost:

- Increased steel and concrete material costs for the extra length of tower;
- Increased material costs for the larger foundations (required to support the larger towers and provide stability for the larger overturning moment) in terms of both concrete and reinforcing steel;
- Cost of increased prestressing requirements of the concrete and hybrid towers.

4.2 Revenue Generation

The data used for the revenue calculation was obtained from the WASA wind mast for Napier, approximately 40km north of the southern most tip of Africa in the Western Cape. The data is in the form of mean wind speeds for 10 minute periods, given for heights of 10, 20, 40, 60 and 62m. As discussed in section 2.4, the data is extrapolated to the various hub heights using logarithmic equations, derived from each year's data, so as to capture as much of the variation in the wind as possible.

Only three years' worth of data were obtained from the wind masts, as the masts only started recording a few months into 2010. The years from 2011 through 2013 are thus the only full years of data. Ideally, one should obtain as many reliable years of data as possible to take into account the variation in the wind resource from year to year. The danger of taking a reference period that is too short is that the years that were studied may have been exceptionally windy years and the estimated yield might appear higher than a longer period would have produced. This will lead to shortcomings in revenue and thus reduced profits.

Figure 4.1 shows the annual variation in the mean wind speed, on a month-by-month basis. Year to year, the wind speeds vary fairly significantly over the respective months. Fortunately however, the mean annual wind speed does not fluctuate much, 8.71, 8.27 and 8.91m/s for 2011, 2012 and 2013, 80m hub height, respectively. This does not seem like a noteworthy variation, but Table 4.2 illustrates how a small change in the mean annual wind speed can make a significant difference to the revenue generated by a single turbine. The capacity factors are calculated according to Equation 2.3, using a Vestas V112 3MW wind turbine. The last column illustrates the change in revenue from year to year, using the revenue of 2011 as a reference.

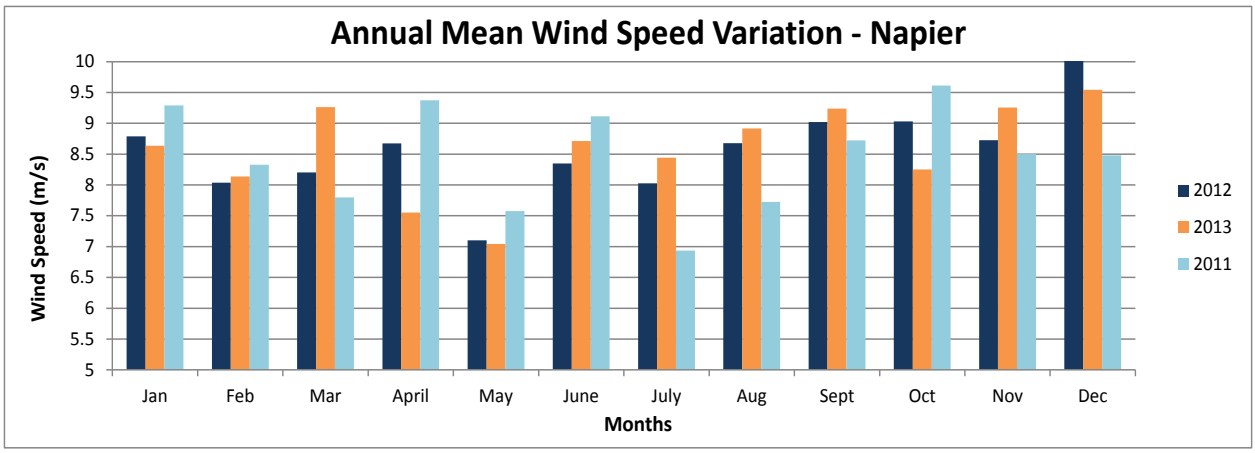

Figure 4.1: Three year mean wind speed variation for Napier (62m hub height).

Table 4.2: Effects of annual average wind speed variation (Vestas V112 3MW, 80m hub height).

Year	Annual Mean Wind Speed (m/s)	Average Instant MW Generated	MWh Generated	Capacity Factor	Revenue (R)	Normalized Revenue Change (%)
2011	8.71	1.84	14 818	0.550	10 965 209	0
2012	8.27	1.58	12 780	0.474	9 456 880	-13.76
2013	8.91	1.96	15 795	0.586	11 688 616	6.60

As can be seen from Table 4.2, a small change in the mean annual wind speed can make a considerable difference in the revenue generated over a year. In addition, wind sites can have identical mean annual wind speeds, but have different values of annual energy production.

This is due to the distribution of the wind speeds over a time period. This is the reason that obtaining reliable wind data over an extended period of time is crucial to the profitability of a wind energy project. As a consequence of the heightened risk of using short time lengths of wind data, financial institutions generally require a minimum number of years of recorded wind data before agreeing to finance a project, which varies from institution to institution.

To elaborate on the effect of annual wind speed distribution, consider the graph in Figure 4.2. The mean annual wind speeds of Vredendal and Sutherland for 2011, for an 80m hub height, are 7.33 and 7.31 m/s, respectively. The Rayleigh wind speed distributions (a specific case of a Weibull distribution) are shown in Figure 4.2 for Vredendal and Sutherland. One can see that there are more occurrences of lower wind speeds at the Sutherland mast, which translates to more periods where the wind turbine will be at a lower power output level, than at the Vredendal mast for a higher nameplate capacity turbine. This is confirmed by an analysis of the estimated power produced for 2011 at both sites, which reveals that the capacity factor for the Vredendal mast is 2.5 percent higher than at the Sutherland mast.

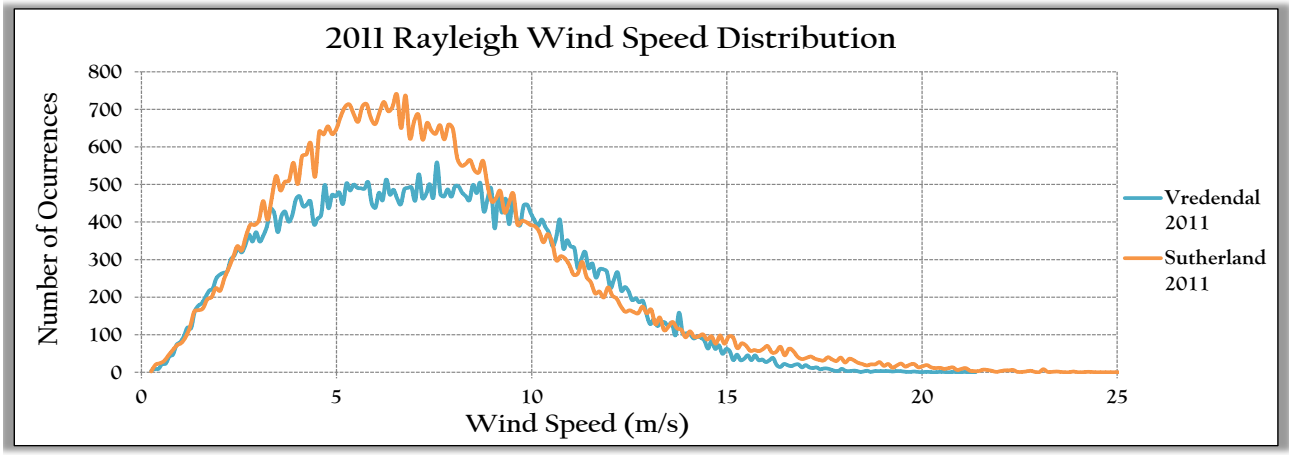

Figure 4.2: Rayleigh distribution for Vredendal and Sutherland for 2011.

Financial institutions require a certain level of confidence in the ability of a wind farm to generate revenue, to make sure that their investments are as safe as possible. The norm in South Africa is that banks require a minimum of a P90 assessment, which entails the calculation of the amount of energy a wind farm will generate with 90 percent surety. The P90 assessment is a conservative estimate of the amount of energy that will be generated and must be done with a minimum of 12 months' worth of on site (or near to the actual site) wind data, representative of the topography of the surrounding area.

Naturally, the revenue generated in a wind farm is due to the generation of power and the subsequent feeding of the power into the national grid. Thus, an increase in power generation directly translates to an increase in revenue generation. The amount of instantaneous power generated by a turbine, $P_{instant}$ in MW, is given by Equation 4.1:

$$P_{instant} = v_{wind} \cdot P_{associated} \tag{4.1}$$

Where:

$$v_{wind} = \textit{Wind velocity } \left(\frac{m}{s}\right)$$

$$P_{associated} = \textit{Power generated for given wind speed, according to Vestas V112 power curve } \left(\frac{kWs}{m}\right)$$

The data used for $P_{associated}$ was obtained from the Vestas V112 3MW wind turbine product brochure. The power curve is shown in Figure 4.3.

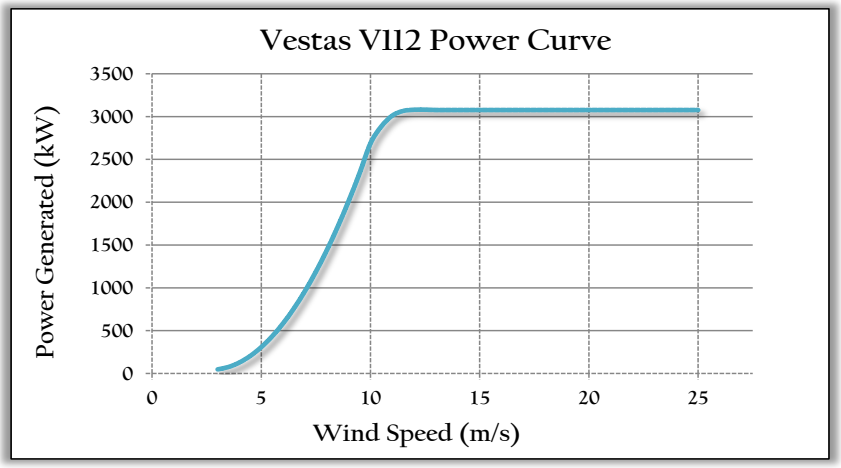

Figure 4.3: Power curve for the Vestas V112 3MW wind turbine.

In this way, the wind data from each of the 10 minute periods is converted into an instantaneous power value, which represents the energy generated in a sixth of an hour. Therefore, if the wind is blowing so that the turbine generates at maximum capacity, the turbine generates $3.075MW \cdot (1/6) = 0.5125MWh$ every 10 minute period. Naturally, if the wind blows at less than optimum, the turbine will not generate at maximum capacity and this value will be less.

The sum of the energy generated in the 10 minute intervals is then added up to get the total amount of energy generated in a year in MWh, per turbine. The data obtained from the WASA wind mast was fairly complete, with only isolated gaps in recording of the individual heights. These values were interpolated using data from just before and after the gap, so as to accurately interpolate the values. There were isolated cases where all of the height data displayed "NULL", likely indicating a malfunction with the remote-control recording of the data. In these cases, the data was disregarded completely and the capacity factor was adjusted to take cognizance of this.

Thus the total annual energy production of a wind turbine, E_{annual} in MWh, is given by the following expression:

$$E_{annual} = \Sigma \left(P_{instant} * \frac{1}{6} \right) \eta_{elec}\ \eta_{avail} \tag{4.2}$$

Where:

η_{elec} = *Coefficient for losses in generation and feeding into grid.* $\eta_{elec} = 0.97$

η_{avail} = *Coefficient for losses due to unavailability of the turbine.* $\eta_{avail} = 0.95$

This value is then the value that the power utility (ESKOM) will pay for. As mentioned in section 1.1, the average price paid for wind energy in round 1 and 2 of the REIPPP was 114 and 89.5 c/kWh, respectively. Since then however, due to strong competition in the wind industry, the average price

paid in the third round dropped further to a simple average cost of 74c/kWh (SANEA, 2014). This value, or R740/MWh, will then be used to calculate the revenue generated by each turbine.

The losses assumed for the revenue calculation are fair for the average wind farm, although, for the first few years of a South African wind farm, η_{avail} is more likely to be in the vicinity of 93 percent. This is due to the fact that generally there are initial maintenance issues with the turbines and technicians and/or parts will need to be brought in from the international community, which takes time. Therefore, the turbine may not be available for generation for a few days and the availability level drops. As the South African wind industry matures, enough turbines will be present in South Africa to warrant local technicians and parts manufacturers and so the availability percentage will rise up to the typical 95 percent plus level (Feng and Tavner, 2010).

References

Feng, Yanhui and Peter Tavner (Apr. 2010). *Introduction to Wind Turbines: Reliability & Availability.* Durham University. Course Notes, PowerPoint Slides. URL: http://www.supergen-wind.org.uk/docs/presentations/2010-04-25_1100_EWEC2010_SideEvent_Reliability_PJT.pdf.

SANEA (2014). *Wind Power Cost Drops even Further.* South African National Energy Association. URL: http://www.sanea.org.za/MediaCentre/SaneaTalkingEnergy/2013/11/Article_07.asp.

Chapter 5

Structural Design

A fictitious wind farm location will be used in order to best re-create the design and analysis of a typical wind farm in South Africa. The load applied to the structures will be in the form of a quasi-static, ultimate limit-state wind load and will follow the design and analysis guidelines as laid out in SANS 10160-3 in conjunction with the loading conditions as given in SANS 10160-1 (SANS 10160-1:2010; SANS 10160-3:2011). It should be noted that the wind speed distribution as accepted in IEC 6400-1 was used here (IEC 61400-1:2005).

5.1 Wind Regime and Distribution

Initially, it was uncertain as to whether the extreme wind conditions prescribed in IEC 6400-1 would be valid for a South African context. In particular, the requirement was questioned for the wind turbine to be able to withstand an extreme 3-second wind gust with a recurrence period of 50 years, at hub height, of 52.5 m/s irrespective of hub height.

This requirement is laid out in IEC 6400-1 for a turbine designed for IEC wind class III. A short study of SANS 10160-3 revealed that the method used to increase the wind speed as a function of height yielded lower wind speeds, even at a hub height of 120m for any of the terrain categories. Table 5.1, illustrates the wind speeds for various hub heights according to SANS 10160-3 with terrain category A - *"Flat horizontal terrain with negligible vegetation and without any obstacles"* compared to the value prescribed in IEC 6400-1.

Table 5.1: Hub height wind speed comparison of SANS 10160-3 and IEC 6400-1

SANS 10160-3				**IEC 6400-1**
Base Wind Speed (m/s)	**Hub Height (m)**	**Scale Factor**	**Reference 3-Second Gust Wind Speed (m/s)**	**Reference 3-Second Gust Wind Speed (m/s)**
vb,basic	**z_{hub}**	**cr(z)**	**Vref**	**Vref**
28	80	$1.4 \cdot 1.256$	49.24	52.5
	100	$1.4 \cdot 1.276$	50.02	
	120	$1.4 \cdot 1.292$	50.80	

The inclusion of the factor of 1.4 in the Table 5.1 is to convert from a 10-minute mean wind speed to an extreme 3-second gust wind speed and is common to both the SANS and IEC code. Further, the value stated for the IEC code already includes this factor. It should be noted that the scale factor for the 120m hub height is technically only valid up to 100m, following SANS 10160-3, though it seemed sensible to continue the extrapolation through the use of the $c_r(z)$ value.

The assumption was justified in that it did not affect the outcome, as the IEC 6400-1 value is still higher than the SANS 10160-3 values. Due to the requirements of SANS 10160-3 being met in IEC the V_{ref} value, it was decided that the IEC 6400-1 wind speed would be used in the designs of all three of the 80, 100 and 120m hub heights.

The 3-second extreme gust wind speed value is the accepted value for the design of wind turbines of class III for the Ultimate Limit State, irrespective of turbulence intensity, according to the IEC wind turbine classifications.

There are, of course, many other limit state criteria that need to be satisfied, but due to the scope of this thesis and the resources and time available, this limit state was considered as being of greater importance than the others. In particular, an analysis with regard to seismic actions will not be considered.

South Africa is not, generally, a seismically active region and particularly not along the west and east coast, where most of the current wind farms are situated. Therefore, a design case for seismic loads will not be considered in this thesis but should most definitely be included in a complete design of a wind turbine structure.

The wind speed was distributed along the height of the tower according to equation 12 (Extreme Wind Speed Model) in IEC 6400-1, clause 6.3.2.1, here referred to as Equation 5.1.

$$V_{e50} = 1.4 \cdot V_{ref} \cdot \left(\frac{z}{z_{hub}}\right)^{(0.11)} \tag{5.1}$$

Where:

$$V_{e50}(z) = \textit{3-Second extreme gust at height } z \ (m/s)$$
$$V_{ref} = \textit{10-minute mean wind speed at hub height } (m/s)$$
$$z = \textit{Height of desired wind speed}(m)$$
$$z_{hub} = \textit{Hub height } (m)$$

The use of z_{hub} as a "datum" in Equation 5.1 may be of confusion to those familiar with SANS 10160-3. This is due to the fact that, according to IEC 6400-1, class III wind turbines must be able to withstand a set extreme wind gust at hub height, irrespective of hub height. This extreme wind gust is compared to the equivalent SANS 10160-3 values in Table 5.1. The wind speed distribution along the height of the tower for a 120m tower can be seen in Table 5.2. The basic wind speeds, the peak wind speeds and the factored peak wind pressure as obtained from equation 6, in section 7.4 of SANS 10160-3 are shown. It should be noted that the values for the factored peak wind pressure include a load factor of 1.35, as prescribed in IEC 6400-1.

Table 5.2: Wind distribution along tower height for a 120m tower for the extreme wind model.

Height (z)	**Base Wind Speed ($v_{b,basic}$)**	**Peak Wind Speed ($v_{p,peak}$)**	**Factored Peak Wind Pressure ($q_p(z)$)**
(m)	**(m/s)**	**(m/s)**	**(kPa)**
120	37.5	52.5	2.29
110	37.1	52.0	2.24
100	36.8	51.5	2.20
90	36.3	50.9	2.15
80	35.9	50.2	2.09
70	35.3	49.5	2.03
60	34.7	48.6	1.96
50	34.1	47.7	1.89
40	33.2	46.5	1.80
30	32.2	45.1	1.69
20	30.8	43.1	1.54
10	28.5	39.9	1.32
0	26.4	37.0	1.14

Figure 5.1 illustrates the extreme wind speed-versus height values for all tower heights used in this project.

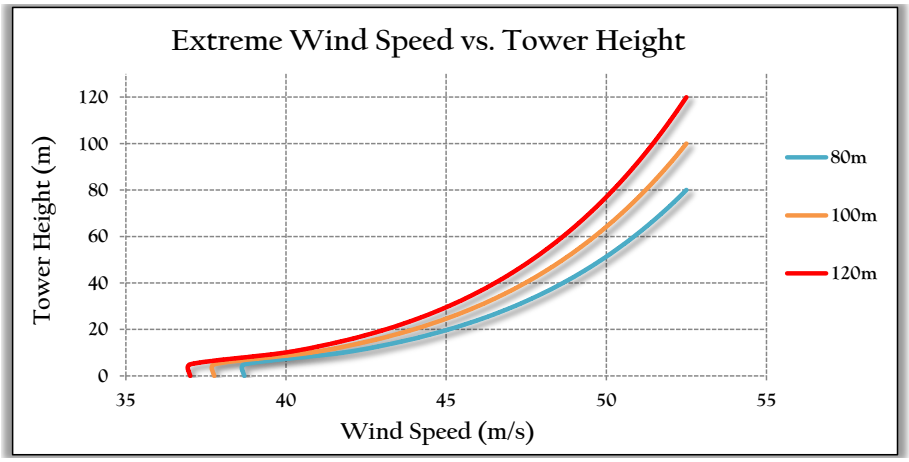

Figure 5.1: Extreme wind load as a function of tower height.

Due to the quasi-static nature of the wind load being applied to the structures, a single drag coefficient for the turbine tower would be inadequate to accurately simulate the wind loads on the tower. Section 8.10 in SANS 10160-3 outlines the analysis process to be followed when considering circular cylinders and is adopted here.

While this method is not designed to accommodate dynamic contexts, the quasi-static wind loads that are applied to the towers here are Ultimate Limit State (ULS) loads and are not dynamic-force governing. The method was therefore considered acceptable in order to calculate the ULS stresses and strains within the tower as well as in the foundations.

Section 8.10 uses external pressure coefficients as a function of the dimensionless Reynolds number, which describes the flow regime at the point under consideration, as well as the angle between the point under consideration and the point at which the load is applied. The Reynolds numbers along the towers are all in the vicinity of $1.5 - 2 \cdot 10^7$ and thus the appropriate curve in Figure 29 of SANS 10160-3, here reproduced as Figure 5.2, was used.

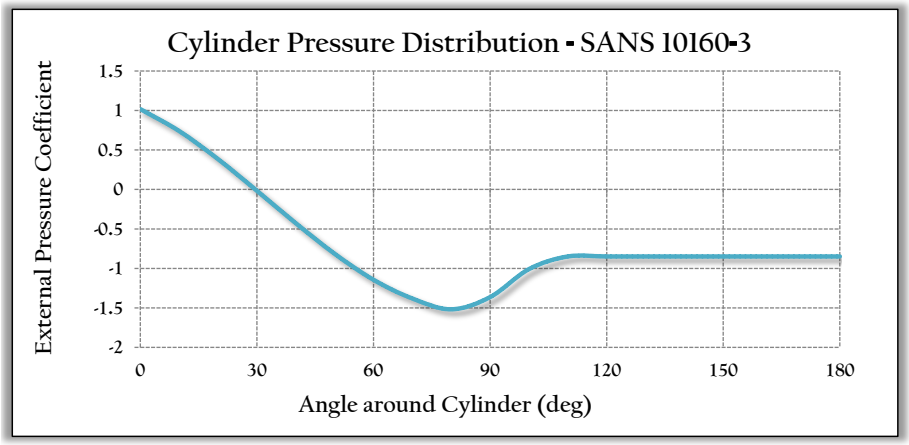

Figure 5.2: Pressure distribution for circular cylinders. SANS 10160-3, figure 29.

5.2 Loads

Figure 5.3 shows the various components of a wind turbine.

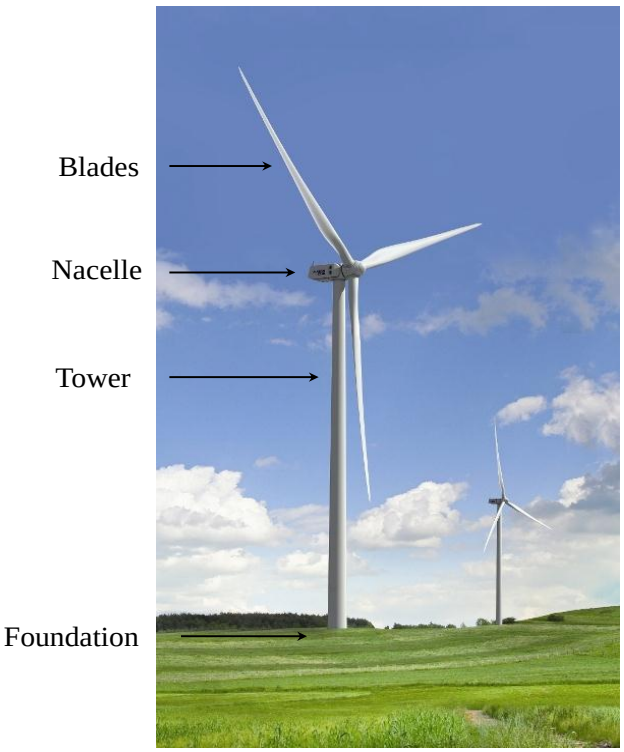

Figure 5.3: Components of a typical horizontal axis wind turbine.

5.2.1 Wind Loads on Tower

The wind loads on the towers, as mentioned earlier, were applied in the form of quasi-static pressures that act along the height of the tower. The towers were split into segments, along the height of the tower, of 5 meters in height. The wind forces that act on the tower, F_{wt}, were calculated according to Equation 9 in SANS 10160-3.

$$F_{wt} = c_s \cdot c_d \cdot c_f \cdot q_p(z_e) \cdot A_{ref} \tag{5.2}$$

Where:

$$\begin{aligned} c_s \cdot c_d &= \textit{Structural factor} = 1.0 \\ c_f &= \textit{Force coefficient for a structure or structural element} \\ q_p(z_e) &= \textit{Peak wind pressure at reference height } z_e \ (kPa) \\ A_{ref} &= \textit{Reference area of the structure or structural element } (m^2) \end{aligned}$$

In the case of a wind turbine tower, the top of the tower supports the turbine itself and thus only an external pressure coefficient is used, in comparison to a flue stack for example, where the top of

the tower is affected by the so called end effect factor, Ψ_λ, as described in clause 7.10.1.2 of SANS 10160-3. Thus the pressure coefficient reduces to the value of c_f as obtained from Figure 29 of SANS 10160-3, with a Reynolds number of 10^7.

5.2.2 Wind Loads on the Nacelle and Blades

The loads on the turbine nacelle are relatively straightforward to calculate, due to the regular, rectangular shape of the nacelle. The calculation of the loads on the blades and the rotor cone however, are more complicated due to the unusual shape of the blades and the issue of the ability of the blades to feather, depending on intensity of the wind. Due to the ultimate limit state considerations, the wind turbine will be in shut-down mode and the blades will therefore be rotated flap-wise and will be feathered out of the wind, so as to reduce the stresses and strains on the blades and nacelle.

Initially, it was assumed that the force on the blades would be relatively small and therefore negligible, due to being feathered out of the wind, but because of the considerable moment lever-arm about the base, as well as the requirement of a 15 degree yaw-misalignment in IEC 6400-1, the force on the blades, even though seemingly insignificant, does actually cause a noticeable moment about the base.

The force on the blades was thus calculated by applying the wind pressure at hub height to an equivalent reference area for the blades, having taken account of the 15 degree yaw-misalignment. The pressure was applied in conjunction with a pressure coefficient representative of the blades in their parked state.

5.2.3 Loads on Turbine Foundation

In the case of the square foundations used in this thesis, there are two main load orientations that will be considered. The first orientation considers a case where the wind blows along the x axis of the foundation and the second considers a case where the wind blows at 45 degrees to the first orientation (diagonally across the foundation), as can be seen in Figure 5.4.

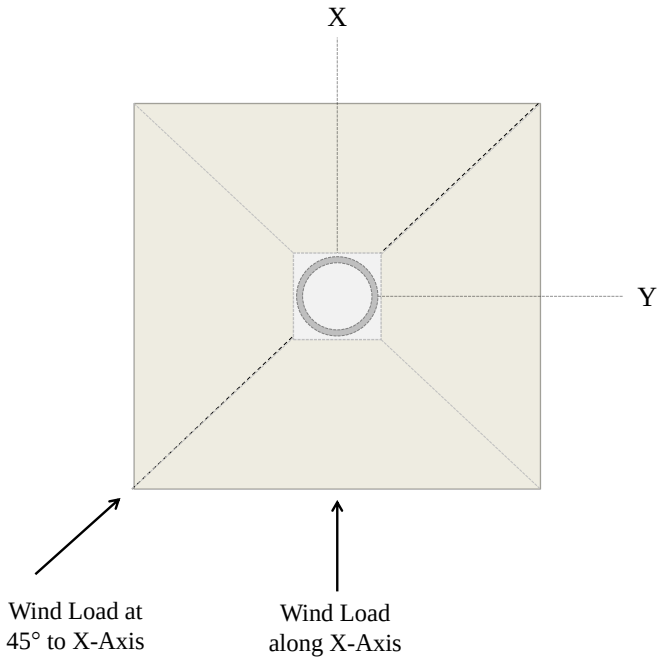

Figure 5.4: Wind Load Orientations.

Some of the calculations, especially with regard to the bearing capacity of the foundation, will thus have a value for both of the load orientations. The most conservative of the two cases will be used in the design of the foundation.

The design overturning moment used in the analysis is a combination of the moments about the x and y axes of the wind turbine, as a result of the wind pressure on the tower, blades, rotor cone and nacelle. The design moment also takes into account the so-called $P-\Delta$ effect, an eccentricity caused by the tower deflection, whereby the tower-top weight will act at an eccentricity determined by a simplified finite element model of the tower deflecting under the applied loads.

An eccentricity load acting at the center of gravity of the towers was also considered, but due to the fact that the center of gravity is close to the ground because of the thicker sections lower down, the moment lever arm would be small and thus the moment itself would be small enough to neglect. The resultant design moment was calculated as shown in Equation 5.3:

$$M_d = \sqrt{(\Sigma M_x)^2 + (\Sigma M_y)^2} \tag{5.3}$$

Where:

M_x = *Moments that cause stress in the direction of the x-axis (Bending around the y-axis)* (kNm)

M_y = *Moments that cause stress in the direction of the y-axis (Bending around the x-axis)* (kNm)

5.3 Tower Natural Frequency

One of the most important requirements for wind turbine towers is that the natural frequencies of the tower be sufficiently removed from the so called blade passing frequencies. Both the frequencies of one blade (1P) and three blades (3P) passing in front of the tower must be sufficiently separated from the natural frequency of the towers to avoid problems related to resonance (DNV/Risø, 2002).

Resonance between the tower and the blade passing frequencies causes highly increased deflections of, and vibrations in, the tower. Resonant effects generally lead to increased and premature fatigue damage or in the worst case, catastrophic failure of the tower.

The problem is compounded by the fact that the towers, particularly the steel ones, have a low level of structural damping due to the thin walled sections, typically around 1 percent, as well as that the nacelle, blades and nose cone can weigh up to as much as the tower itself. This creates a largely top-heavy system and thus it is imperative that the towers are stiff (or flexible) enough to keep the natural frequencies sufficiently separated from the 1P and 3P frequencies.

In the case of this study, the WTG used was a model V112-3MW made by the Danish company Vestas, as can be seen in Figure 5.5. The details of the turbine can be seen in Table 5.3 (Vestas Wind Systems A/S, 2011).

Figure 5.5: Vestas V112 3.0MW wind turbine (Renewable Energy World.org, 2014)

.

Table 5.3: Specifications of the Vestas V112 wind turbine.

Rated Power	3075 kW
Rotor Diameter	112 m
Cut-in Wind Speed	3 m/s
Rated Wind Speed	12 m/s
Cut-out Wind Speed	25 m/s
Survival Wind Speed	52.5 m/s
Number of Blades	3
Tower Top Weight	158 t
Wind Turbine Class	IEC III
Operational Rotor Speed	6.2 - 12.8 RPM
1P Blade Passing Frequencies	0.103 - 0.213 Hz
3P Blade Passing Frequency	0.64 Hz

As can be seen from Table 5.3, the operational rotor speed of the chosen turbine is between 6.2 and 12.8 RPM. The 1P and 3P blade passing frequencies therefore create bands within which, the towers natural frequencies cannot lie. The 1P blade passing frequency is to be avoided completely and the 3P blade passing frequency at rated power, must be avoided by at least 10 percent, above or below as mentioned previously, as recommended by Hau (2006) and DNV/Risø (2002).

A more recent publication, the ASCE/AWEA RP:2011 (2011), recommends a value of 15 percent in order to be almost certain of avoiding resonance-related problems and this value will be used in this thesis. This creates two distinct bands that limit the towers natural frequencies, as can be seen in Figure 5.6. It should be noted that Figure 5.6 applies specifically to the Vestas V112 3MW turbine. The allowable bands will change, depending on the operating frequency of the specific turbine, which can generally be found in the turbine specifications brochure.

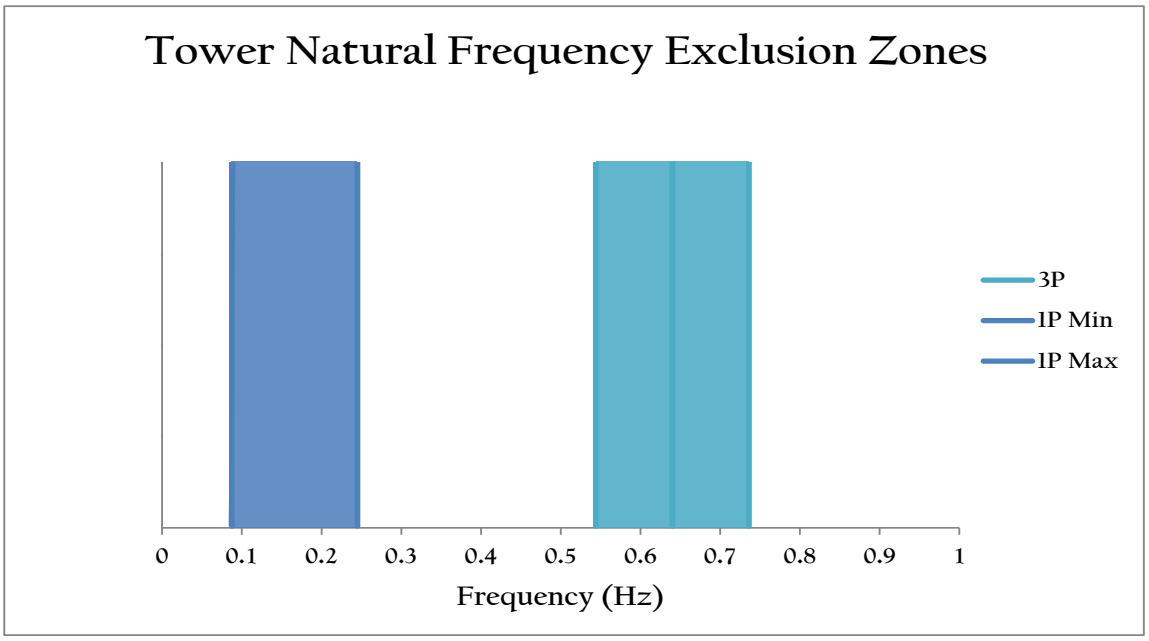

Figure 5.6: Tower frequency exclusion zones, due to rotor blade passing frequencies.

Given the above, the natural frequency of the towers, f_n, can only lie in the intervals:

$$\begin{aligned} 0 < f_n < 0.088 \quad & Hz \\ 0.245 < f_n < 0.544 \quad & Hz \\ 0.736 < f_n \quad & Hz \end{aligned}$$

Even though all of he intervals are theoretically plausible, a tower with a natural frequency between 0 and 0.088 Hz will not have enough strength or stiffness to withstand the loads applied to the tower and limit the deflections of the tower. In addition, natural frequencies higher than 0.736 Hz will require wall thicknesses that will be uneconomical, especially for the steel towers, and thus this interval is highly unlikely to be a practical option, although the concrete towers will still be checked within this interval to be sure. Thus the section between the 1P and 3P blade passing frequencies is the most likely interval within which the tower natural frequencies can lie.

The natural frequency of the towers to be designed will be obtained from a modal analysis using the Abaqus finite element analysis software, developed by SIMULIA, a subsidiary of Dassault Systems (SIMULIA, 2010). Initially, it was envisaged that hand calculations alone would be used. Due to the results obtained by modeling the tower as a cantilever beam with a lumped mass at the end of the cantilever having inadequate accuracy however, it was decided that a Finite Element Method (FEM) program would be used to obtain more accurate results. Hand calculations would thus be used and then verified through the use of the Abaqus FEM software.

Although the FEM analysis is used to verify the natural frequency of the towers, the model execution and analysis run-time take a considerable amount of time. An initial estimation was therefore required to obtain a "ballpark" figure for the natural frequency of the towers and thus a hand calculation was used. Baumeister's equation, for calculating the natural frequency of uniform cantilevers with a

concentrated mass at the end of the beam, yields results that are satisfactory for an initial estimate of the natural frequency (in Hertz) (Manwell et al., 2010). The natural frequency is calculated as shown in Equation 5.4:

$$f_n = \frac{1}{2\pi}\sqrt{\frac{3EI}{(0.23m_{tower} + m_{rotor})L^3}} \tag{5.4}$$

Where:

$$\begin{aligned} E &= Young's\ modulus\ of\ tower\ steel\ (GPa) \\ I &= Second\ moment\ of\ inertia\ of\ tower\ (m^4) \\ m_{tower} &= Mass\ of\ tower\ (kg) \\ m_{rotor} &= Mass\ of\ nacelle,\ blades\ and\ nose\text{-}cone\ (kg) \\ L &= Tower\ length(m) \end{aligned}$$

The equation is simple; the complexity is that the moment of inertia needs to be representative of the entire tower. An average of the entire tower moment of inertia is therefore often used. The equation will thus work better for the steel and concrete towers, than for the hybrid tower.

5.4 Fatigue Analysis

This section serves to communicate the need for a fatigue analysis to be performed on the towers and foundations, to make sure that the towers are adequate in their design with regard to fatigue strength. A short description of the fatigue design process will be presented, although a fatigue analysis will not be performed in this project, the reasons for which are given later in the section.

Fatigue is a phenomenon that occurs when materials are subject to cyclic loading. In wind turbines, the cyclic loading takes the form of the high repetition bending moments that the support structures are subject to. Failure can occur in the concrete, in the form of crushing or punching shear, in the steel in the form of tensile yielding or at the interaction between concrete and steel reinforcing in the form of bond-failure. This happens when the fatigue stress repetitions exceed the fatigue strength of the material under consideration.

5.4.1 General Procedure for Fatigue Design

The method used widely for reinforced concrete towers and foundations is the one presented in the FIB Model Code first draft (2010) for the concrete, in conjunction with the method in Eurocode 2 for the steel reinforcing (FIB Model Code 2010). Insightful information on the matter was also gained from Göransson and Nordenmark (2011). The method as discussed in the ASCE/AWEA RP2011, will be used for the fatigue analysis description for the steel tower sections.

5.4.2 Fatigue Check for Concrete - FIB Model Code section 5.1.11.1

In this method, the number of load repetitions until failure of the material is approximated for constant amplitude stresses. Similar to the Eurocode method, a fatigue reference compressive strength, $f_{ck,fat}$, is estimated and the concrete stresses are compared to this. The fatigue loads on the structure are given serviceability load factors. The following method is for compression of the concrete in the towers and foundations:

Pure Compression

The fatigue loading on the element under consideration causes maximum, $S_{c,max}$, and minimum, $S_{c,min}$, compressive stresses, given by:

$$S_{c,max} = \frac{|\sigma_{c,max}|}{f_{ck,fat}} \tag{5.5}$$

$$S_{c,min} = \frac{|\sigma_{c,min}|}{f_{ck,fat}} \tag{5.6}$$

$$\Delta S_c = |S_{c,max}| - |S_{c,min}| \tag{5.7}$$

The fatigue reference compressive strength may then be approximated from:

$$f_{ck,fat} = \beta_{cc}(t)\ \beta_{c,sus}(t,t_0)\ f_{ck}\left(1 - \frac{f_{ck}}{250}\right) \tag{5.8}$$

Where:

$\beta_{cc}(t)$ = *Coefficient depending on the age of concrete at the beginning of fatigue loading, from section 5.1.9.1.*

$\beta_{c,sus}(t,t_0)$ = *Coefficient to account for the effect of high average stresses during loading. Taken as* 0.85 *for fatigue loading.*

For values of $S_{c,min} > 0.8$, take $S_{c,min} = 0.8$. If $0 \leq S_{c,min} \leq 0.8$, the following Equations apply:

$$logN_1 = \left(12 + 16S_{c,min} + 8S_{c,min}^2\right)(1 - S_{c,max}) \tag{5.9}$$

$$logN_2 = 0.2logN_1\,(logN_1 - 1) \tag{5.10}$$

$$logN_3 = \frac{logN_2\,(0.3 - 0.375S_{c,min})}{\Delta S_c} \tag{5.11}$$

Depending on the values for N_1:

$$\text{If } logN_1 \leq 6 \text{ then } logN = logN_1 \tag{5.12}$$

$$\text{If } logN_1 > 6 \text{ and } \Delta S_c \geq 0.3 - 0.375S_{c,min}, \text{ then } logN = logN_2 \tag{5.13}$$

$$\text{If } logN_1 > 6 \text{ and } \Delta S_c < 0.3 - 0.375S_{c,min}, \text{ then } logN = logN_3 \tag{5.14}$$

Where:

N = *Number of load repetitions until fatigue failure occurs.*

Compression-Tension

Only valid when $\sigma_{ct,max} \leq 0.026|\sigma_{c,max}|$:

$$logN = 9(1 - S_{c,max}) \tag{5.15}$$

Where:

$\sigma_{ct,max}$ = *Maximum tensile stress* (MPa)
$\sigma_{c,max}$ = *Maximum compressive stress* (MPa)

Pure Tension and Tension-Compression

Only valid when $\sigma_{ct,max} > 0.026|\sigma_{c,max}|$:

$$logN = 12(1 - S_{ct,max}) \tag{5.16}$$

Where:

$S_{ct,max}$ = *Maximum tensile stress level* (MPa)
$= \dfrac{\sigma_{ct,max}}{f_{ctk,min}}$
$f_{ctk,min}$ = *Minimum characteristic tensile strength* (MPa)

Following this, for each of the above cases, the Palmgren-Miner rule can then be used to assess the state of the elements with regard to fatigue failure. Failure occurs if the fatigue damage, $D_{Ed} \geq 1$:

$$D_{Ed} = \Sigma \left(\frac{n_{si}}{N} \right) \tag{5.17}$$

Where:

n_{si} = *Number of stress-load repetitions at a given stress level and range*
N = *Number of stress-load repetitions causing failure at the same stress level and range, from the above Equations*

5.4.3 Fatigue Check for Steel Reinforcing and Prestressing - Eurocode 2, section 6.8

This method also uses the Palmgren-Miner rule to evaluate the adequacy of the reinforcing and prestressing steel, with regard to fatigue strength:

$$D_{Ed} = \Sigma \frac{n(\Delta\sigma_i)}{N(\Delta\sigma_i)} \leq 1 \tag{5.18}$$

Where:

$n(\Delta\sigma_i) =$ *Number of applied cycles for a stress range* $\Delta\sigma_i$
$N(\Delta\sigma_i) =$ *Number resisting cycles for a stress range* $\Delta\sigma_i$

The method uses characteristic strength curves, also known as S-N curves, in order to determine the number of stress load repetitions an element can withstand before failure. The following figure is adapted from the S-N curve out of Eurocode 2 for prestressing and reinforcing steel:

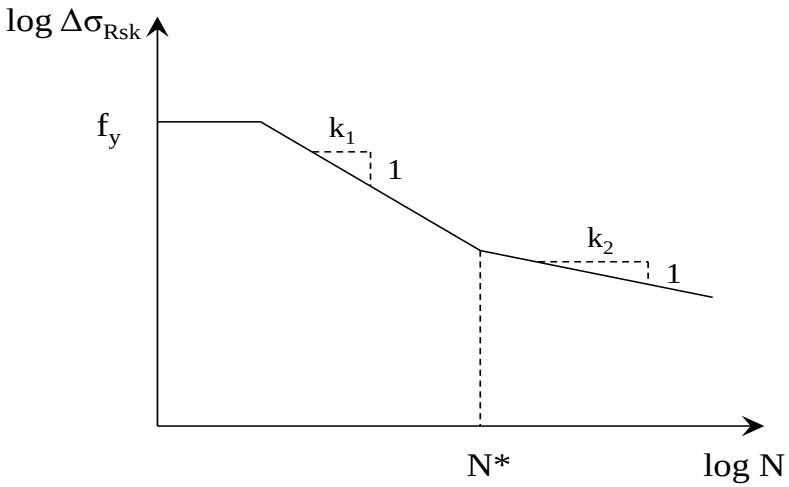

Figure 5.7: S-N curve for prestressed and reinforcing steel. Adapted from Eurocode 2, figure 6.30.

Thus there are two regions wherein the value of $\Delta\sigma_{Rsk}$ can lie, either on the first slope or the second. The table references in the following two equations refer to the respective tables in Eurocode 2. The following Equations are therefore given, from Göransson and Nordenmark (2011):

$$N(\Delta\sigma_i) = N \cdot \left(\frac{\Delta\sigma_{Rsk}/\gamma_{m,s,fat}}{\gamma_{F,fat} \cdot \Delta\sigma i} \right)^{k_1} \quad if \ \gamma_{F,fat} \cdot \Delta\sigma_i \geq \frac{\Delta\sigma_{Rsk}}{\gamma_{m,s,fat}} \tag{5.19}$$

$$N(\Delta\sigma_i) = N \cdot \left(\frac{\Delta\sigma_{Rsk}/\gamma_{m,s,fat}}{\gamma_{F,fat} \cdot \Delta\sigma i} \right)^{k_2} \quad if \ \gamma_{F,fat} \cdot \Delta\sigma_i < \frac{\Delta\sigma_{Rsk}}{\gamma_{m,s,fat}} \tag{5.20}$$

Where:

$N* =$ *Number of cycles until fatigue failure for steel type. Tables 6.3N and 6.4N*

$\Delta\sigma_{Rsk} =$ *Resisting stress range at N* cycles. Tables 6.3N and 6.4N*

$\gamma_{m,s,fat} =$ *Partial material factor for steel.* $\gamma_{m,s,fat} = 1.15$ *for fatigue verification. Table 2.1N*

$\gamma_{F,fat} =$ *Partial factor for fatigue loading.* $\gamma_{F,fat} = 1$

$k_1, k_2 =$ *Define the first and second slopes in Figure 5.7, respectively. Tables 6.3N and 6.4N*

5.4.4 Fatigue Check for Steel Tower

The most common and thorough method for the fatigue check of the steel tower is once again, the use of the Palmgren-Miner rule, as suggested in the ASCE/AWEA RP2011. The method follows the same formulation as Equation 5.18. The applicable S-N curves can be found in Figure 7-1 of the ASCE/AWEA RP2011.

The reason for the fatigue checks not being done in this project, is that the load spectra for the serviceability limit state required for the fatigue verification is highly specific to the element under consideration, whether it be the tower or the foundation. The load spectra involve complex analyses that should only be carried out in the case of a final design, as the simulations require vast amounts of time and computational resources. Each of the wind turbine models would have to have been exposed to fatigue loads with repetitions in excess of 10^6 cycles. It was thus decided that the fatigue analysis be left out of this project due to time constraints.

Many researchers faced with this problem turn to the study done by LaNier (2005), within which are load spectra for towers and foundations. These load spectra apply to those specific towers, with those specific turbines and those specific foundations. Thus any variation in geometry, wind load or turbine use for a similar project disqualifies this data for use in a fatigue analysis.

There have been many efforts made by the same organization, the National Renewable Energy Laboratory (NREL), to adjust the data for use in projects with different swept rotor areas, hub heights and turbine masses, however, it was felt that adjusting the data for so many differing elements will result in a questionable result with regard to fatigue verification.

In further defense of the decision to leave the fatigue verification out of this project, all of the steel towers were, with the exception of the 80m tower, thickened for stiffness purposes, which will increase the fatigue life of the steel due a reduction in the stress concentration levels in the sections. Also, in the buckling analyses of all the steel sections, the applied stresses are always below 60 percent of the buckling stress capacity of the sections at the ultimate limit state, which gives further confidence that fatigue will not be a governing factor in this project.

It is therefore argued that the comparison made in this project is not influenced by fatigue considerations. In a comprehensive wind turbine support structure design however, a fatigue analysis is absolutely necessary. In addition, it is recommended that fatigue verification be done with simulated

data that relates directly to the wind turbine and support structure under consideration.

5.4.5 Crack Width Limitation

Further, an aspect that is important to the design of the concrete parts of the support structure, but is not dealt with in this project, is the limiting of cracks to acceptable widths in order to prevent the ingress of water and harmful substances into the foundation and tower reinforcing/prestressing in addition to aesthetic considerations.

5.4.6 Torsion and Shear

The effects of torsion and shear stresses in the towers were not considered. This is due to the limitation of scope, in addition to the findings of Nicholson (2011), that the shear and torsion stresses in steel towers are generally insignificant in comparison to the bending and axial stresses for steel towers. According to Consolis Hormifuste (2011), horizontal and vertical reinforcing is only included in the concrete towers for the handling of segments and to resist temperature-gradient stresses and is sufficient to resist torsion and shear stresses from wind loading. In addition to this, most of the precast concrete and hybrid towers use the segment connections to resist torsion and shear stresses. Further literature on the torsional and shear effects on precast concrete and hybrid towers can be found in Grünberg and Göhlmann (2013).

References

Consolis Hormifuste (Nov. 2011). *Precast Concrete Towers and Foundations: A Huge Market Coming Ahead*. Presentation at Danish Concrete Association (DBF): Beton Til Vindmøller (Concrete for Wiind Turbines) Conference. URL: http://www.slideshare.net/slides_eoi/jaime-de-rbago-precast-concrete-wind-towers-and-offshore-foundations-a-huge-market-coming-ahead.

DNV/Risø (2002). *Guidelines for Design of Wind Turbines*. 2nd ed. Accessed 29th March 2014. Copenhagen: Det Norske Veritas (DNV) and Risø National Laboratory.

ASCE/AWEA RP:2011 (2011). American Wind Energy Association (AWEA) and the American Society of Civil Engineers (ASCE) 2011: Recommended Practice for Compliance of Large Land-based Wind Turbine Support Structures.

FIB Model Code 2010. International Federation for Structural Concrete *(fib)* 2010: Model Code 2010 First Draft.

IEC 61400-1:2005. International Electrotechnical Commission 61400-1:2005: Wind Turbines - Part 1: Design Requirements.

SANS 10160-1:2010. South African National Standards 10160: Part 1: Basis of structural design. South African Bureau of Standard (SABS). 1 Dr Lategan Road, Groenkloof, Pretoria.

SANS 10160-3:2011. South African National Standards 10160. Basis of structural design and actions for buildings and industrial structures. Part 3: Wind actions. South African Bureau of Standard (SABS). 1 Dr Lategan Road, Groenkloof, Pretoria.

Göransson, Frida and Anna Nordenmark (2011). "Fatigue Assessment of Concrete Foundations for Wind Power Plants". MA thesis. Chalmers University of Technology.

Grünberg, Jürgen and Joachim Göhlmann (2013). *Concrete Structures for Wind Turbines*. Ed. by Konrad Burgermeister. Wiley.

Hau, Erich (2006). *Wind Turbines: Fundamentals, Technologies, Application, Economics*. 2nd ed. Berlin: Springer-Verlag.

LaNier, M. W. (2005). *LWST Phase I Project Conceptual Design Study: Evaluation of Design and Construction Approaches for Economical Hybrid Steel/Concrete Wind Turbine Towers*. Tech. rep. National Renewable Energy Laboratory (NREL).

Manwell, J.F., J.G. McGowan, and A.L. Rogers (2010). *Wind Energy Explained: Theory, Design and Application*. Wiley. ISBN: 9780470686287. URL: http://books.google.co.za/books?id=roaTx_Of0vAC.

Nicholson, J. C. (2011). "*Design of Wind Turbine Tower and Foundation Systems: Optimization Approach*". MA thesis. University of Iowa.

Renewable Energy World.org (2014). *Fig 5.5.* "Vestas V112-3.0 MW wind turbine". URL: http://www.renewableenergyworld.com/rea/news/article/2010/09/vestas-secures-first-european-order-for-v112-wind-turbine.

SIMULIA (2010). *Abaqus Finite Element Analaysis Software. Version 6.10-2.* Dassault Systems.

Vestas Wind Systems A/S (2011). *General Specification V112: 3.0 MW 50/60 Hz*. Product specification brochure. Hedeager 44, 8200 Aarhus N, Denmark.

Chapter 6

Foundation Design

The foundations of a wind turbine tower are also linked to the natural frequency of the tower. The foundations are not infinitely stiff in reality, and this needs to be taken into account when calculating the natural frequency of the tower. The natural frequency of the towers can decrease by up to 20 percent when the stiffness of the foundations and the underlying geotechnical conditions are considered, under special conditions, though this figure is generally in the vicinity of 5 percent for normal geotechnical conditions (DNV/Risø, 2002).

Typically, the foundation is modeled as resting on a set of springs, to account for the stiffness of the underlying soil. More sophisticated approaches to soil spring modeling include the use of non-linear elements to represent the soil when in-depth behavior of the soil is to be investigated.

In addition to having an effect on the natural frequency of the tower, the foundations are also to fulfill the requirements in terms of the stiffness required by the turbine itself and to limit tower deflections to an acceptable level. The stiffness requirements are generally prescribed by the turbine manufacturer.

6.1 Bearing Capacity

One of the most important parts of the foundation design is making sure that the soil does not suffer general, local or punching shear failure. In the case of general shear failure of the soil, the ground surface on both sides of the footing heaves, although the final slip only occurs on one side of the foundation, along with the obvious tilting of the foundation which in this case, would be catastrophic (Craig, 2004).

Excessive settlements are characteristics of both the punching and local shear failure modes. The ultimate bearing capacity of the soil in the design will be checked and compared with the ultimate loads applied. The partial load factors according to IEC 6400-1 and EC7 need to applied, as well as

the partial safety factors with regard to the values for ϕ and c, the soil angle of shear resistance and cohesion intercept, respectively. The following table gives a summary of the partial safety factors and load factors that are applicable to the limit state verifying structural resistance (STR), geotechnical (GEO) and overall stability analysis (EQU).

Table 6.1: Partial safety and load factors for the geotechnical design and overall stability check.

Action Description	**Safety/Load Factor Description**	**Standard**	**Symbol**	**STR & GEO**	**EQU**
Permanent Actions	Dead Load - Unfavourable	EC7/IEC 6400-1	γ_{g1}	1.1	1.1
	Dead Load - Favourable	EC7/IEC 6400-1	γ_{g1}	0.9	0.9
	Foundation	EC7/IEC 6400-1	γ_{g2}	1	1.1
	Foundation	EC7/IEC 6400-1	γ_{g2}	1	0.9
Variable Actions	Static Windload	IEC 6400-1	γ_f	1.35	1.35
Geotech. Actions	Angle of Shear Resistance	EC7	γ_ϕ	1.25	-
	Soil Cohesion Intercept	EC7	γ_c	1.4	-

The ultimate bearing capacity of a soil, q_f, in a shallow foundation is given by the following, according to Craig (2004):

$$q_f = c_d N_c s_c i_c + \gamma D_e N_q s_q i_q + \frac{1}{2}\gamma b N_\gamma s_\gamma i_\gamma \tag{6.1}$$

Where:

$$\begin{aligned}
i_c, i_q \text{ and } i_\gamma &= \textit{Inclination factors} \\
s_c, s_q \text{ and } s_\gamma &= \textit{Foundation shape factors} \\
N_c, N_q \text{ and } N_\gamma &= \textit{Bearing capacity factors} \\
c_d &= \textit{Design soil cohesion intercept } (kN/m^3) \\
\gamma &= \textit{Bulk unit weight of soil } (kN/m^3) \\
D_e &= \textit{Embedded depth of foundation } (m) \\
b &= \textit{Effective breadth of foundation } (m)
\end{aligned}$$

The inclination, shape and bearing capacity factors are calculated as follows, for drained soil conditions (Craig, 2004; DNV/Risø, 2002):

$$i_c = \left(1 - \frac{H_d}{V_d + A_{eff} \cdot c_d \cdot cot(\phi_d)}\right)^2 \tag{6.2}$$

$$i_q = i_c \tag{6.3}$$

$$i_\gamma = i_q^2 \tag{6.4}$$

$$s_c = 1 + 0.2 \cdot \frac{b}{L'} \tag{6.5}$$

$$s_q = s_c \tag{6.6}$$

$$s_\gamma = 1 - 0.4 \cdot \frac{b}{L'} \tag{6.7}$$

$$N_c = (N_q - 1) \cdot cot(\phi) \tag{6.8}$$

$$N_q = e^{\pi \cdot tan(\phi)} \cdot tan\left(45 + \frac{\phi}{2}\right)^2 \tag{6.9}$$

$$N_\gamma = \frac{1}{4} \cdot (N_q - 1 \cdot cos(\phi))^{3/2} \tag{6.10}$$

Where:

H_d = *Design horizontal force at top of foundation* (kN)

V_d = *Design vertical force at underside of foundation* (kN)

A_{eff} = *Effective foundation area (b*L')* (m^2)

ϕ = *Design soil angle of shear resistance* (deg)

L' = *Effective length of foundation* (m)

The following factors are specifically for undrained soil conditions ($\phi = 0$), where the u denotes undrained soil conditions:

$$N_{cu} = \pi + 2 \tag{6.11}$$

$$s_{cu} = s_c \tag{6.12}$$

$$i_{cu} = 0.5 + 0.5 * \sqrt{1 - \frac{H_d}{A_{eff} \cdot c}} \tag{6.13}$$

In addition to checking the bearing capacity, another mode of soil failure must be checked. This failure mode is specifically for foundations with large load eccentricities, where the load eccentricity is greater than 0.3 times the width of the foundation, i.e. $e > 0.3 \cdot B$. In this mode of failure, the soil under the unloaded part (heel) of the foundation fails and thus the following Equation is used to work out the bearing capacity (DNV/Risø, 2002):

$$q_f = c_d N_c s_c i_c (1.05 + (tan\phi)^3) + \gamma' b N_\gamma s_\gamma i_\gamma \tag{6.14}$$

Where:

γ' = *Buoyant unit weight of the soil* (kN/m^3)

The inclination factors are now of the form:

$$i_q = i_c = 1 + \frac{H_d}{V_d + A_{eff} * c_d * cot(\phi_d)} \tag{6.15}$$

$$i_\gamma = i_q^2 \tag{6.16}$$

$$i_{cu} = \sqrt{0.5 + 0.5 * \sqrt{1 - \frac{H_d}{A_{eff} * c}}} \tag{6.17}$$

The final design bearing capacity, q_d, is the smallest of the two failure modes calculated bearing capacity. A fairly large factor of safety accompanies the bearing capacity check, usually between 2 and 3, to account for the difficulty in accurately predicting soil properties (Craig, 2004).

6.2 Sliding Resistance

The foundation also needs to be checked to see if it has sufficient resistance against sliding, i.e. the entire base displaces perpendicular to the tower height. This is not typically a problem for wind turbine foundations, due to the large weight of the turbine atop the tower, but it will be checked for completeness sake. The following condition is used to make sure that the foundation satisfies the sliding resistance requirement, with a relatively low factor of safety of between 1.5 and 2, for drained and undrained soil conditions, respectively:

$$H_d < A_{eff} \cdot c + V_d \cdot tan\phi \tag{6.18}$$

$$H_d < A_{eff} \cdot c \tag{6.19}$$

In addition, it must be verified that the design horizontal force does not exceed 0.4 times the applied vertical load, i.e:

$$\frac{H_d}{V_d} < 0.4 \tag{6.20}$$

6.3 Resistance Against Overturning

Perhaps the most obvious check against the failure of a wind turbine is that of the resistance the support system has against the overturning moment that it is subjected to, as a result of the wind loading on the tower, nacelle, blades and nose cone. The sum of the stabilizing and overturning moments are taken about the toe of the foundation to evaluate whether the support system satisfies the design criteria. The resistance of the wind turbines against overturning is adequate when the stabilizing moments, ΣM_R, outweigh the overturning moments, ΣM_O, by an acceptable factor of safety of between 2 and 3 (Das, 2004), as shown in Equation 6.21:

$$\begin{aligned} \Sigma M_O &< \Sigma M_R \\ M_d + e_q H_d &< (F_z + V_f - F_o) \cdot \frac{B}{2} \end{aligned} \tag{6.21}$$

Where:

F_z = *Design vertical force, due to tower and turbine weight* (kN)

V_f = *Design vertical force, due to foundation weight* (kN)

F_o = *Buoyancy force exerted on foundation due to ground water* (kN)

e_q = *Height from bottom of foundation to tower base* (m)

6.4 Foundation Stiffness

Following on from section 2.8, the foundations are required to have certain stiffness in order to satisfy the requirements of the wind turbine manufacturer. In this project, the stiffness of the foundations will also be used as input values in the Abaqus models. The foundations will be placed on top of springs with vertical, horizontal and rotational degrees of freedom in order to incorporate the effect the ground has on the wind turbine.

Ideally, the foundations should be placed on sets of non-linear springs however, this involves highly complex simulations, due to the uncertainty of the soil properties. Each soil type has its own nuances and so each different site condition will require specialist geotechnical expertise. It was thus felt that the complex modeling of the soil was not worth the time it would require and would not have a noticeable effect on the outcome of the project. In addition to this, the stiffness of the foundations in this model far exceed the requirements of the turbines and thus it was deemed acceptable to use linear springs instead.

The stiffness of the foundations were calculated according to the guidelines given in DNV/Risø (2002), which are based on work done by Gazetas (1983) and Elsabee (1973), for circular footings embedded in stratum over bedrock. Figure 6.1 illustrates the ground and foundation orientation.

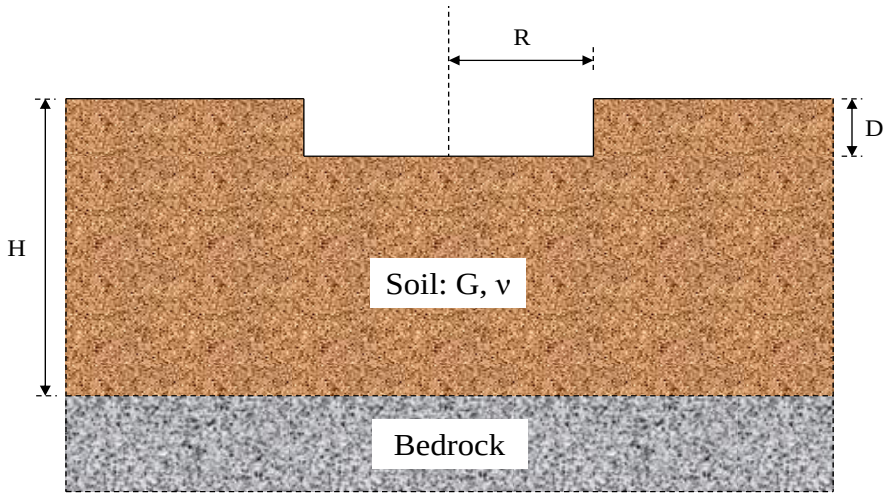

Figure 6.1: Illustration of foundation and soil orientation. Adapted from DNV/Risø (2002).

The foundation stiffness in terms of the vertical, horizontal, rocking and torsional stiffness are given

as, respectively:

$$K_V = \frac{4GR}{1-\nu}\left(1+0.28\frac{R}{H}\right)\left(1+\frac{D}{2R}\right)\left(1+\left(0.85-0.28\frac{D}{R}\right)\frac{D/H}{1-D/H}\right) \tag{6.22}$$

$$K_H = \frac{8GR}{2-\nu}\left(1+\frac{R}{2H}\right)\left(1+\frac{2D}{3R}\right)\left(1+\frac{5D}{4H}\right) \tag{6.23}$$

$$K_R = \frac{8GR^3}{3(1-\nu)}\left(1+\frac{R}{6H}\right)\left(1+\frac{2D}{R}\right)\left(1+\frac{0.7D}{H}\right) \tag{6.24}$$

$$K_T = \frac{16GR^3}{3}\left(1+\frac{8D}{3R}\right) \tag{6.25}$$

Where:

$G = Soil\ shear\ modulus\ of\ soil\ (MPa)$

$R = Foundation\ radius\ (m)$

$\nu = Poisson's\ ratio\ of\ soil$

$H = Soil\ depth\ to\ bedrock\ from\ ground\ level\ (m)$

$D = Depth\ from\ ground\ level\ to\ bottom\ of\ foundation\ (m)$

Although Equations 6.22 through 6.25 were originally intended for circular footings, they represent a conservative formulation for square foundations. It should be noted that the formulas are only valid for the following ranges:

$$D/R \leq 2 \tag{6.26}$$

$$D/H \leq 0.5 \tag{6.27}$$

All 9 of the foundations designed in this project fall well within the required ranges.

6.5 Tensile Steel Reinforcement

Due to the high tensile stresses caused by the overturning moment of the tower, the foundations require substantial amounts of tensile reinforcing. Unlike most beams, the foundation slabs require reinforcing just above the bottom surface, as well as just below the top surface. The reinforcing was done according to Eurocode 2, with a beam-design approach.

In order to design the reinforcing, the shear and bending moment diagrams first need to be obtained. The complex forces and stresses present within the foundations were simplified into bite-sized 2D forces and stresses. The overturning moment from the tower is split into a compression-tension force couple (F_c and F_t) that account for a quarter of the tower and turbine weight as well. The rest of the tower and turbine weight, F_w, is then applied at the center of the tower. The other forces and stresses present are the soil-reaction stress, σ_{soil}, and the own weight, g_d, portrayed by line-loads, and

the horizontal shear-force, F_{xy}, acting at the tower base in the form of a point-load. The layout is shown in Figure 6.2, for the case of wind blowing right to left.

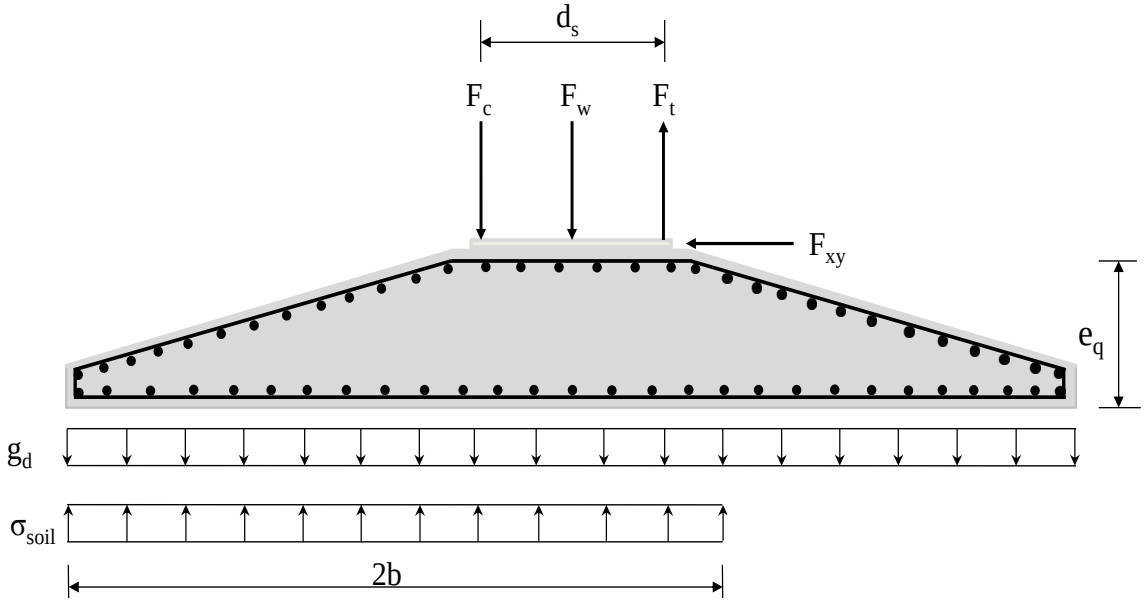

Figure 6.2: Illustration of foundation reinforcing scenario.

In order to approximate the bending moment as a force couple, as shown, the assumption is made that a quarter of the anchor ring on which the tower rests is in compression and the opposite quarter is in tension. From this, the distance between centroids, d_s, of the approximated 2D forces must be calculated, according to Landén and Lilljegren (2012), with reference to Figure 6.3:

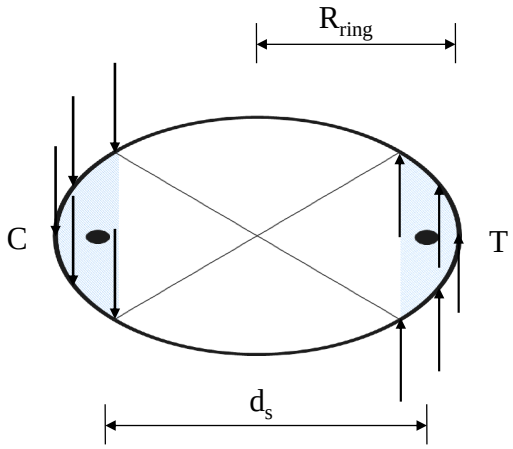

Figure 6.3: Illustration of anchor ring compression-tension force couple.

$$d_s = \frac{4R_{ring}}{\pi} \int_{-\frac{\pi}{4}}^{\frac{\pi}{4}} cos\phi \; d\phi$$

$$d_s = \frac{4R_{ring}}{\pi} \cdot \sqrt{2} \tag{6.28}$$

Where:

$R_{ring} = Radius\ of\ anchor\ ring\ (m)$

$\phi = Angle\ of\ incline\ of\ quarter\ section\ (deg)$

It should be noted that here, a uniform soil pressure is assumed, where in reality the distribution is partly uniform and then triangular. In addition, the bending moment and shear force diagrams should be considered for both the perpendicular and 45° wind directions, although they are only shown for the perpendicular wind direction here.

It was noted however, by Landén and Lilljegren (2012), that the differences in bending moments and shear forces between a uniform and triangular soil pressure distribution are negligible, for ultimate limit state calculations. Also, they noted that the difference between the bending moment and shear force diagrams obtained from a perpendicular and 45° wind direction were small enough to be ignored.

The distribution of the foundation weight should also have a distribution according to the shape of the foundation, but for the purpose of obtaining the maximum positive and negative bending moments, it is assumed to be constant. This assumption is however, slightly conservative. The rest of the equations relating to the foundation reinforcing design are shown in Equations 6.29 through 6.32.

$$F_c = \frac{M_d + F_{xy}D}{d_s} + \frac{F_z}{4} \tag{6.29}$$

$$F_t = \frac{M_d + F_{xy}D}{d_s} - \frac{F_z}{4} \tag{6.30}$$

$$F_w = \frac{F_z}{2} \tag{6.31}$$

$$g_d = \frac{V_f}{L} \tag{6.32}$$

Where:

$F_c = Equivalent\ compression\ force\ and\ a\ quarter\ of\ F_z\ (kN)$

$F_t = Equivalent\ tension\ force\ and\ a\ quarter\ of\ F_z\ (kN)$

$F_w = Half\ of\ F_z\ (kN)$

$g_d = Distributed\ load\ of\ foundation\ weight\ (kN/m)$

$M_d = Design\ overturning\ moment\ (kNm)$

$D = Foundation\ height\ (m)$

$F_z = Design\ vertical\ force\ of\ tower\ and\ turbine\ (kN)$

$V_f = Foundation\ weight\ (kN)$

The effective breadth, b, and the upwards soil pressure, σ_{soil}, of the foundations are found by taking vertical and moment equilibrium of the structure and solving the resulting equations simultaneously. The shear force diagrams are then drawn according to the following inequalities, for a distance x from the left hand side of the foundation:

$$\text{When } x < \frac{L-d_s}{2}: \qquad V(x) = \sigma_{soil} \cdot x - g_d \cdot x$$

$$\text{When } \frac{L-d_s}{2} \leq x < \frac{L}{2}: \qquad V(x) = \sigma_{soil} \cdot x - g_d \cdot x - F_c$$

$$\text{When } \frac{L}{2} \leq x < \frac{L+d_s}{2}: \qquad V(x) = \sigma_{soil} \cdot x - g_d \cdot x - F_c - F_w$$

$$\text{When } \frac{L+d_s}{2} \leq x < 2b: \qquad V(x) = \sigma_{soil} \cdot x - g_d \cdot x - F_c - F_w + F_t$$

$$\text{When } 2b \leq x < L: \qquad V(x) = \sigma_{soil} \cdot b - g_d \cdot x - F_c - F_w + F_t$$

The bending moment diagrams are then drawn similarly. Note that the vertical forces are inverted, for easier moment visualization:

When $x < \frac{L-d_s}{2}$:

$$M(x) = g_d \cdot \frac{x^2}{2} - \sigma_{soil} \cdot \frac{x^2}{2}$$

When $\frac{L-d_s}{2} \leq x < \frac{L}{2}$:

$$M(x) = g_d \cdot \frac{x^2}{2} - \sigma_{soil} \cdot \frac{x^2}{2} + F_c \cdot \left(x - \frac{L-d_s}{2}\right)$$

When $\frac{L}{2} \leq x < \frac{L+d_s}{2}$:

$$M(x) = g_d \cdot \frac{x^2}{2} - \sigma_{soil} \cdot \frac{x^2}{2} + F_c \cdot \left(x - \frac{L-d_s}{2}\right) + F_w \cdot \left(x - \frac{L}{2}\right)$$

When $\frac{L+d_s}{2} \leq x < 2b$:

$$M(x) = g_d \cdot \frac{x^2}{2} - \sigma_{soil} \cdot \frac{x^2}{2} + F_c \cdot \left(x - \frac{L-d_s}{2}\right) + F_w \cdot \left(x - \frac{L}{2}\right) - F_t \cdot \left(x - \frac{L+d_s}{2}\right) - F_{xy} \cdot D$$

When $2b \leq x < L$:

$$M(x) = g_d \cdot \frac{x^2}{2} - \sigma_{soil} \cdot 2b \cdot (x-b) + F_c \cdot (x - \frac{L-d_s}{2}) + F_w \cdot (x - \frac{L}{2}) - F_t \cdot (x - \frac{L+d_s}{2}) - F_{xy} \cdot D$$

The foundations will be designed according to the ultimate limit state with tension reinforcing being provided for the tension stresses in the top, as well as the bottom of the foundation. For ease of calculation, the maximum required reinforcing steel will be provided throughout the foundation, in both directions. In practice, the reinforcing would be able to have been reduced at a certain point, according to code requirements, which would result in reduced steel use. An example of a typical bending moment diagram and sign convention for wind turbine foundations is shown below, in Figure 6.4. Bending causing a tension force in the bottom left, and top right halves of the foundation is defined as positive.

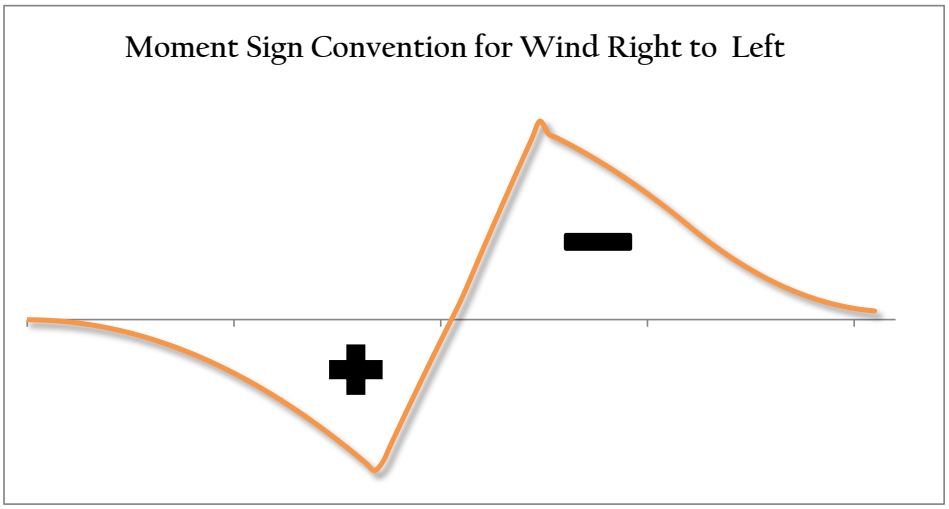

Figure 6.4: Typical bending moment diagram and associated sign convention.

Once the shear force and bending moment diagrams have been determined, the reinforcing design process can begin. The amount of steel required, A_s to resist the overturning moment transferred from the tower, for the bottom of the foundation, with guidance from The Concrete Center (2012) is given by:

$$A_s = \frac{M}{\gamma_{m,s} \cdot f_{yd} \cdot z} \tag{6.33}$$

Where:

$$\begin{aligned}
M &= Maximum\ applied\ moment\ (kNm) \\
f_{yd} &= Design\ yield\ stress\ of\ reinforcing\ steel\ (MPa) \\
z &= Lever\ arm\ for\ reinforcing\ (m) \\
&= \frac{d}{2}(1 + \sqrt{1 - 3.53 \cdot K}) \leq 0.95d \\
K &= \frac{M}{(f_{ck} \cdot bd^2)} \\
f_{ck} &= Characteristic\ concrete\ strength\ (MPa) \\
b &= Breadth\ of\ concrete\ section\ (m) \\
d &= Effective\ depth\ of\ concrete\ section\ (m) \\
\gamma_{m,s} &= Partial\ material\ factor\ for\ steel.\ \gamma_{m,s} = 0.87
\end{aligned}$$

The only problem with the Equation 6.33 is that it is dependent on the effective depth of the section. This is a problem as the foundation tapers, as a cut-off pyramid shape, above the rectangular block and thus the effective depth of the foundation is not constant. Thus, an average effective depth of the foundation is accepted. This is a conservative approach, as the deeper sections will contain more steel than is actually required, as most of the bending moment is present at the thicker sections towards

the middle. It does however, greatly reduce the time spent in design, as one does not have to check every point for adequacy of reinforcing.

There are further procedures to be followed, when the K value exceeds 0.168, for which compression reinforcement is required at the top of the section, but this is not the case for any of the foundations and so the matter will not be pursued any further. The reinforcing will all be in the form of high tensile steel bars, locally referred to as "Y-bars", the properties of which are shown in Appendix A and are summarized in Table 6.2:

Table 6.2: Tensile reinforcement information.

Bar Type	**Bar Diameter (mm)**	**Bar Area (mm^2)**	**Characteristic Yield Strength (MPa)**	**Mass (kg/m)**
Deformed	32	804.25	450	6.313

There are also other clauses that need to be heeded from Eurocode 2. Particularly those to do with the minimum and maximum allowable reinforcing ratios in clause 9.2.1.1 and the minimum and maximum bar spacing.

$$A_{s,min} \geq \frac{0.26 f_{ctm} \cdot b_t \cdot d}{f_y} \geq 0.0013 b_t \cdot d$$
$$A_{s,max} \leq 0.04 A_c$$
$$s_{min} > \phi_{bar} > 20 > d_{aggregate} + 5$$
$$s_{max} \leq 400mm$$

Where:

A_c = *Cross-sectional area of concrete section* (mm^2)

ϕ_{bar} = *Diameter of one bar of reinforcing* (mm)

$d_{aggregate}$ = *Size of aggregate used in concrete* (mm)

s_{min}, s_{max} = *Minimum and maximum allowable spacing of longitudinal reinforcement* (mm)

The reinforcing calculation will be done for both the bottom and top tensile reinforcing. It should be noted that the length of the reinforcing bars for the top of the foundation will be slightly longer than those for the bottom, due to the inclination of the taper in the foundation. Also, some of the spacing distances chosen may be rather irregular.

This is due to the substantial saving in steel costs associated with using these irregular spacings, in comparison with using spacings that are more regular but are 15mm narrower, for example. There is also a requirement for reinforcing steel to pass through the anchor ring, so as to properly bond the ring to the concrete that is not covered in this project. The total amount of foundation reinforcing

required for each tower height and design will then be calculated and compared to the others.

6.6 Designing for Punching Shear

Due to the considerable weight of the wind turbine and tower, in conjunction with the large overturning moment, spread over the relatively small area of the tower base, a punching shear calculation needs to be carried out in order to ensure that there is no punching shear failure in the foundation. Figure 6.5 illustrates the angle at which the punching shear plane in the foundation forms, adapted from EN 1992-1-1:2004*:*

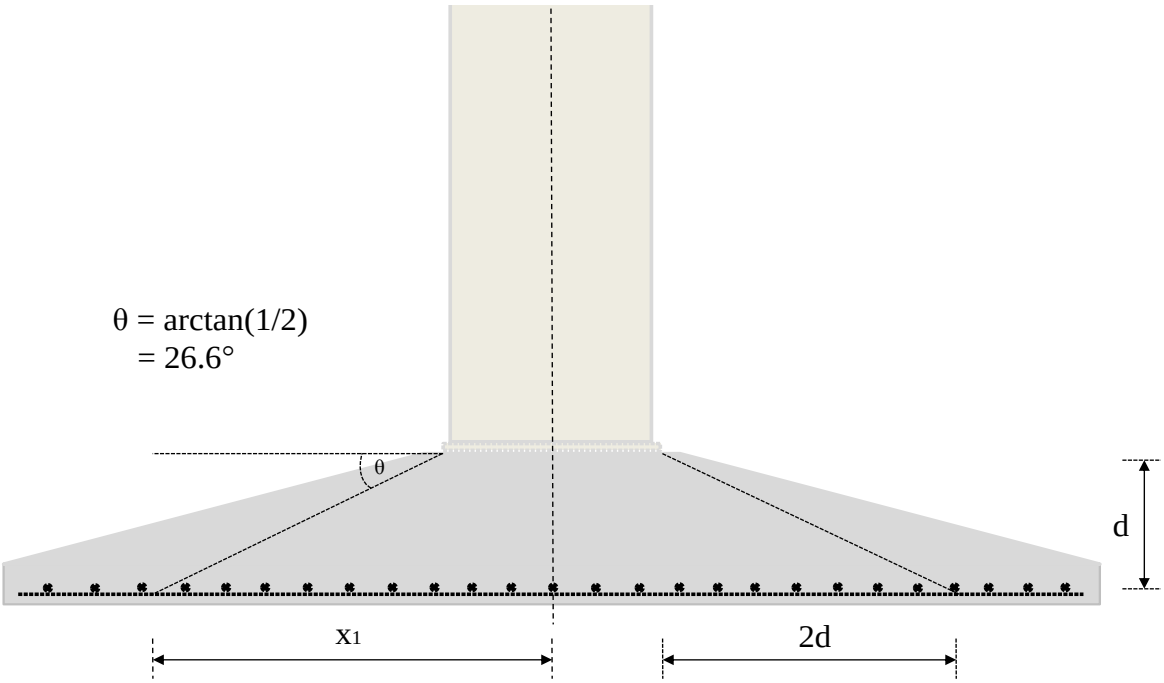

Figure 6.5: Illustration of shear plane orientation. Adapted from EN 1992-1-1 (2004) fig. 6.12.

The design check is done according to the punching shear procedure laid out in section 6.4.3 of EN 1992-1-1. The check requires that the shear be checked at the face of the column or in this case, tower, as well as at a basic control perimeter, u_1, at a distance of $2d_{eff}$ away from the face of the tower:

$$u_1 = 2\pi x_1 \tag{6.34}$$

Where:

$$x_1 = R_{tower} + 2d_{eff}\ (m)$$
$$R_{tower} = Tower\ radius\ (m)$$
$$d_{eff} = Average\ effective\ depth\ of\ the\ slab\ d_{eff} = d_y + d_z (m)$$

$$
\begin{aligned}
d_y &= \textit{Effective depth to the reinforcement in the one orthogonal direction } (m) \\
&= \frac{D - c - \phi_{tb}}{2} \\
d_z &= \textit{Effective depth to the reinforcement in the other orthogonal direction } (m) \\
&= \frac{D - c - 3\phi_{tb}}{2} \\
D &= \textit{Full depth of slab } (m) \\
c &= \textit{Concrete cover distance to reinforcing } (m) \\
\phi_{tb} &= \textit{Diameter of bottom reinforcing bars } (m)
\end{aligned}
$$

It should be noted that the values for d_{eff}, d_y and d_z vary along the length of the foundation. If shear reinforcing is required at the basic control perimeter, then a further perimeter, $u_{out,eff}$, should be found where there is no longer a need for shear reinforcing. In this project however, the foundations will be designed such that punching shear reinforcement is not required, as a means of fairly comparing the different tower designs.

6.6.1 Shear Check at Tower Face

The shear stress at the face of the tower, v_{ED} in MPa, is calculated as follows:

$$v_{ED} = \frac{\beta \; V_{ED}}{u_0 \; d_{eff}} \tag{6.35}$$

Where:

$$
\begin{aligned}
\beta &= 1 + 0.6\pi \frac{e}{D_{tower} + 4d_{eff}} \\
e &= \textit{Loading eccentricity } e = \frac{M_{ED}}{V_{ED}} \; (m) \\
V_{ED} &= \textit{Vertical design force } (kN) \\
u_0 &= \textit{Perimeter at the face of the tower } u_0 = 2\pi R_{tower} \; (m) \\
c &= \textit{Concrete cover distance to reinforcing } (m) \\
D_{tower} &= \textit{Diameter of the tower } (m)
\end{aligned}
$$

The value of v_{ED} must be less than the maximum allowable stress at the perimeter at the tower face, $v_{Rd,max}$ in MPa, calculated as follows:

$$v_{Rd,max} = 0.4 v f_{cd} \tag{6.36}$$

Where:

$$v = 0.6\left(\frac{1 - f_{ck}}{250}\right)$$

$f_{ck} = Characteristic\ cylinder\ strength\ of\ concrete\ (MPa)$

$f_{cd} = Design\ cylinder\ strength\ of\ concrete\ f_{cd} = \frac{f_{ck}}{\gamma_{m,c}}\ (MPa)$

$\gamma_{m,c} = Partial\ material\ factor\ for\ concrete\ \gamma_{m,c} = 1.5$

6.6.2 Shear Check at Control Perimeter

Along with the check at the tower perimeter, a similar check must be done at the control perimeter, u_1, in order to make sure that shear reinforcing is not required to resist punching shear. The perimeter, u_1, corresponds to the perimeter shown in Figure 6.5. The shear force acting at u_1, as a result of the tower, nacelle, blade and nose cone weights in addition to the applied moment and eccentricity, reflected in the value for β, is given as:

$$v_{ED} = \frac{\beta\ V_{ED,reduced}}{u_1\ d_{eff}} \tag{6.37}$$

Where:

$V_{ED,reduced} = V_{ED} - \Delta V_{ED}$

$\Delta V_{ED} = Net\ upward\ force\ on\ foundation\ within\ control\ perimeter\ (kN)$

v_{ED} must be less than the allowable shear stress at u_1, $v_{Rd,c}$. For sections without shear reinforcing, this is given as:

$$v_{Rd,c} = C_{Rd,c} \cdot k \cdot (100\rho_I f_{ck})^{(1/3)} \geq v_{min} \tag{6.38}$$

Where:

$$C_{Rd,c} = \frac{0.18}{\gamma_{m,c}}$$

$$k = 1 + \sqrt{\frac{200}{d_{eff}}} \leq 2.0 \quad (d\ in\ mm)$$

$$\rho_I = \sqrt{\rho_{iy} * \rho_{iz}} \leq 0.02$$

$\rho_{iy}, \rho_{iz} = Reinforcing\ ratios\ for\ the\ orthogonal\ directions$

$$v_{min} = 0.035 \cdot k^{(3/2)} f_{ck}^{(1/2)} \qquad (MPa)$$

It follows that if these criteria are satisfied, then shear reinforcing is not required to resist the punching shear force in the foundation.

References

Craig, R. F. (2004). *Craig's Soil Mechanics*. 7th ed. New York: Spon Press.

Das, B.M. (2004). *Principles of Foundation Engineering*. 5th. New Delhi: Cengage Learning.

DNV/Risø (2002). *Guidelines for Design of Wind Turbines*. 2nd ed. Accessed 29th March 2014. Copenhagen: Det Norske Veritas (DNV) and Risø National Laboratory.

Elsabee, F. (1973). "*Static Stiffness Coefficients for Circular Foundations Embedded in an Elastic Medium*". MA thesis. Massachusets Institute of Technology.

EN 1992-1-1:2004*:* European Committee for Standardization. EN 1992-1-1:2004 (Eurocode 2): Design of concrete structures - Part 1-1: General Rules and Rules for Buildings.

Gazetas, G. (1983). "*Analysis of Machine Foundation Vibrations: State of the art*". In: *Soil Dynamics and Earthquake Engineering* 2, p. 32.

Landén, Nicklas and Jacob Lilljegren (2012). "Three-Dimensional Strut-and-Tie Modelling of Wind Power Plant Foundations". MA thesis. Chalmers University of Technology.

The Concrete Center (2012). *Practical Design to Eurocode 2 - Beams.* MS PowerPoint Slides. URL: http://www.concretecentre.com/pdf/lecture%202%20beams%20-%20oct%2012%20-%20end.pdf.

Chapter 7

Tower Design

This section describes the design of the towers. Due to the fact that there are three different tower designs: the steel shell, concrete and concrete-steel hybrid towers, there are a number of design criteria that need to be satisfied, as the design check of one tower design may not be applicable to the rest.

The steel shell tower and the top section of the hybrid tower are designed with highly-optimized shell thicknesses in order to save on material costs, while still satisfying the strength and stiffness requirements of the system. The strength requirements of the steel towers are in terms of the resistance of the tower against buckling and ability to withstand the loads applied to the structure.

Typically, concrete and concrete-steel hybrid towers do not suffer from the low natural frequency problems that the steel towers do. Conversely, they can often be too stiff, and run into the 3P frequency range of the turbine. The considerable thickness of the tower shells (400mm+) required to resist the tension stresses developed in the tower exacerbate this. The towers therefore often incorporate prestressing strands, which allow the tower walls to be thinner, yet still able to resist the tension stresses.

In addition to reducing the tower wall thickness, and thus the weight of the concrete towers, the prestressing force exerted on the structure ensures that the concrete does not go into the post-cracked range. Once the concrete has cracked, the concrete material enters into a highly non-linear region that is complicated to model. In addition to this, the Young's modulus of the concrete drops considerably, which results in reduced stiffness, increased tower tip deflections and poorer fatigue-life performance.

7.1 Buckling Strength

Figures 7.1 and 7.2 illustrate the general buckling shape for steel cylinders under unit axial load and bending moment. The tower buckling shape will be slightly different to this, due to the difference in magnitude between the axial force and applied moments.

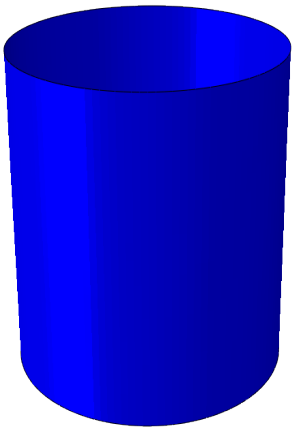

Figure 7.1: Undeformed general buckling shape illustration.

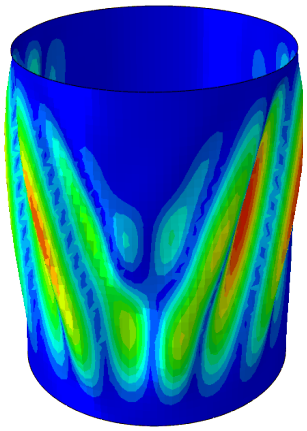

Figure 7.2: Deformed general buckling shape illustration.

The buckling resistance was checked in accordance with the method prescribed in DNV/Risø (2002), which is based on the Danish codes DS449:1983 and DS412:1998. The method is summarized below:

The stress due to the axial force, σ_{ad}, and applied bending moment, σ_{bd} in MPa, are calculated by:

$$\sigma_{ad} = \frac{N_d}{2\pi Rt} \tag{7.1}$$

$$\sigma_{bd} = \frac{M_d}{\pi R^2 t} \tag{7.2}$$

A dimensionless reduction factor, ϵ_a, is determined by:

$$\epsilon_a = \frac{0.83}{\sqrt{1 + 0.01\frac{R}{T}}} \tag{7.3}$$

$$\epsilon_b = 0.1887 + 0.8113\epsilon_a \tag{7.4}$$

$$\epsilon = \frac{\epsilon_a \sigma_{ad} + \epsilon_b \sigma_{bd}}{\sigma_{ad} + \sigma_{bd}} \tag{7.5}$$

The critical elastic buckling stress of a tubular, cylindrical steel section, σ_{el} in MPa, and relative slenderness ratio with regard to local buckling buckling, λ_a, are given as:

$$\sigma_{el} = \frac{E_d}{\left(\frac{R}{t}\sqrt{3(1-v^2)}\right)} \tag{7.6}$$

$$\lambda_a = \sqrt{\frac{f_{yd}}{\epsilon \sigma_{el}}} \tag{7.7}$$

For slenderness ratios in the interval $0.3 < \lambda_a < 1$, within which all the towers lie, the critical compressive stress, σ_{cr}, is given by:

$$\sigma_{cr} = (1.5 - 0.913\sqrt{\lambda_a}) f_{yd} \tag{7.8}$$

The Euler elastic buckling load for a cantilever beam of hollow cylindrical cylindrical shape, N_{el} in kN, with relative slenderness ratio, λ_r, is calculated as:

$$N_{el} = \frac{\frac{1}{4}\pi^3 E_d R^3 t}{H^2} \tag{7.9}$$

$$\lambda_r = \sqrt{\frac{\sigma_{cr}}{\frac{N_{el}}{2\pi Rt}}} \tag{7.10}$$

The core radius of a hollow cylindrical tube, k, and equivalent geometric imperfection, e_{gi} are given by:

$$k = R/2 \tag{7.11}$$

$$e_{gi} = 0.49(\lambda_r - 0.2)k \tag{7.12}$$

If the geometric imperfection is greater than $0.002H$, then an additional imperfection increment, Δe, must be added to get the final e_g in m:

$$\Delta e = e - \frac{2H}{1000} \tag{7.13}$$

$$e_g = e_{gi} + \Delta e \tag{7.14}$$

In the following inequality, the stresses due to the axial force and applied bending moment are combined in order to determine whether the combined effect is greater than the critical buckling resistance of the tower section:

$$\frac{N_d}{2\pi Rt} + \frac{N_{el}}{N_{el} - N_d} * \frac{M_d}{\pi R^2 t} \quad \leq \sigma_{cr} \tag{7.15}$$

Where:

N_d = *Design axial force from tower own weight and turbine weight* (kN)
M_d = *Design moment* (kNm)
R = *Centerline tower radius*(m)
t = *Tower shell thickness*(m)
E_d = *Young's modulus of steel* (GPa)
v = *Poisson's ratio of steel*
f_{yd} = *Steel design yield stress* (MPa)
σ_{cr} = *Critical compressive stress* (MPa)

This check was performed at the tower top, middle and base. It was deemed sufficient as the tower thicknesses and diameters taper linearly from top to bottom, with the exception of the 120m steel tower and therefore, the stresses between these points will also satisfy the criteria. In addition to this, it was found that the stresses in the steel towers were always far below the critical buckling stress, with the stiffness requirements of the towers governing the thickness of the shell sections. It should be noted that the critical buckling stress of the tower sections are noticeably lower than the design

yield stress of the steel.

As stated before, the thickness of the steel shell is generally determined by stiffness requirements and not by buckling capacity, with the exception of the top of the steel towers. The minimum top thickness of the towers was set to 15mm as used in a similar study, which corresponds to a diameter/wall thickness ratio of 200.

This is more than likely due to the pronounced effect of initial imperfections on thinner-walled sections and that thinner sections are more likely to be damaged in the transportation and construction process, or that initial geometrical imperfections may occur during the manufacture of the tower top, which is more intricate than the rest of the tower as a result of the interface between the tower and the turbine.

7.2 Stiffness Requirements

For any steel tower height above 90-100 meters, the towers suffer from a low natural frequency that often lies in the upper range of the $1P$ frequency of the turbine. Thus, the tower thicknesses are almost always increased above the required thicknesses for resistance against buckling. The shell thickness is therefore crucial in determining whether the natural frequency of the tower lies within the acceptable range, as discussed in section 5.3. An illustration of the first two natural frequencies of a concrete tower is shown in Figure 7.3

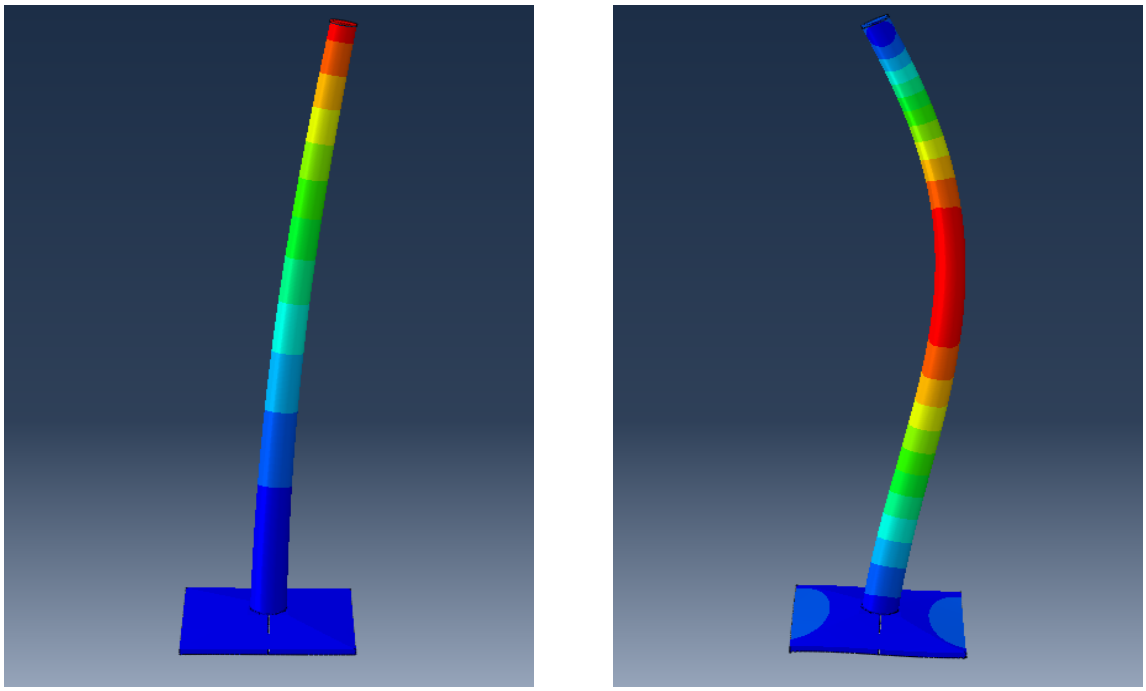

Figure 7.3: Two typical natural frequencies of a steel tower.

The classic Equation for the determination of natural frequency, f_n, is shown in Equation 7.16:

$$f_n = \frac{1}{2\pi}\sqrt{\frac{K}{m}} \tag{7.16}$$

Where:

$K = System\ stiffness\ (N/m)$

$m = System\ mass\ (kg)$

The hand calculation shown in Equation 5.4 is repeated here as a simple illustrative tool to help to describe the stiffness requirements involved in the determination of the natural frequency.

$$f_n = \frac{1}{2\pi}\sqrt{\frac{3EI}{(0.23m_{tower} + m_{rotor})L^3}}$$

The similarities between the two equations are clear: the approximated flexural stiffness of the tower is given by $\frac{3EI}{L^3}$, which is the typical stiffness of a cantilever beam and takes the place of the K term in the first equation. Similarly, the mass of the system is represented by a small portion of the tower mass, due to the center of gravity of the tower being much lower than the top of the tower, as well as that the weight is distributed along the considerable length of the tower. A much greater proportion of the mass is attributed to the tower top mass due to the distance it lies away from the foundation, as well as that the mass is concentrated over a small area.

From Equation 5.4, repeated above, it can be seen that there are certain variables that notably affect the natural frequency of a wind turbine tower. The natural frequency of the tower decreases rapidly with an increase in the length of the tower. Increasing the mass of the tower and more so, the mass of the turbine itself, also decrease the natural frequency of the tower, although not to such an extent as the length. The only things that increase the natural frequency of the tower are the Young's modulus of the steel and the (second) moment of inertia of the tower sections.

It is apparent that the only elements that can be changed in order to increase the natural frequency for the higher steel towers, without changing the turbine model or tower height, are: the mass of the tower, the tower material (and thus, E) and the tower cross-section. The E value is constant for steel material and so only the tower cross section and weight are variable. The moment of inertia, I, of a hollow cylinder is calculated as follows:

$$I = \frac{\pi}{64} \cdot (d_o^4 - d_i^4)$$

Where:

$d_o = Outer\ tower\ diameter\ (m)$

$d_i = Inner\ tower\ diameter\ (m)$

Unfortunately, simply increasing the tower cross section, and thus the value of I is not as clear-cut a solution as one might think. As mentioned previously, there are limitations to the outer diameter of the steel towers. The base diameter is limited to 4.5m due to transport laws and the tower top diameter is limited to 3m, as required by the turbine manufacturers. Ultimately therefore, the only

variable that can change the natural frequency of the tower is the shell thickness.

There are other factors that are not included in the hand calculation, such as the weight and stiffness of the foundation, that also play a role in the determination of the natural frequency. The influence of these factors will not be discussed in detail here, as they will be reflected in the Abaqus model.

Increasing the thickness of the tower sections near the base has the greatest effect in increasing the natural frequency of the tower, as it increases the stiffness, while at the same time, increasing the mass lower down as shown in Figure 7.4, which lessens the effect of the enormous"point mass" at the top of the tower. It is true that increasing the thickness at the top of the tower will increase the stiffness, but it also increases the mass near the top, which dampens the positive effect of the increased stiffness. The thickness at the base of the tower is therefore always increased to the maximum thickness, limited by plate manufacturing capability to 75mm for steel towers, before the top tower thickness is increased.

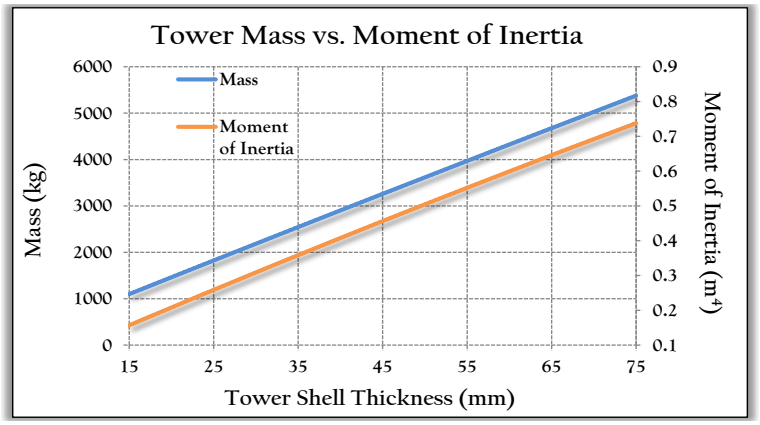

Figure 7.4: Tower mass vs. moment of inertia for various shell thicknesses.

In extreme cases, where the natural frequency cannot be increased enough by increasing the tower shell thickness, the lower sections of the tower can be kept at a greater diameter, often the same as the base diameter, and then taper more steeply to the top. Although, one must take cognizance of the fact that blades deflect towards the tower and so the due checks must be done to ensure that the blades will not impact against the tower in the case of an extreme operating gust.

7.3 Concrete Tower Prestressing

The prestressing in the strands is designed on the basis of limiting the stresses in the concrete to below the mean flexural tensile strength of the concrete so that the section remains in an uncracked state (EN 1992-1-1:2004:).

$$\sigma_{ct} \leq f_{ctm} \tag{7.17}$$

Where:

$\sigma_{ct} = Tensile\ stress\ in\ concrete\ section\ (MPa)$

$f_{ctm} = Mean\ flexural\ tensile\ strength\ of\ concrete\ (MPa)$

In addition, it is important to take note of the increased compressive stress in the section, as a result of the prestressing. In extreme cases, when high levels of prestressing are required, the compressive strength of the concrete may be exceeded under particular load combinations and the section may fail due to crushing. The resultant stress in the section must thus lie in the acceptable interval, while being careful to take note of the sign of the stress:

$$\frac{f_{ctm}}{\gamma_{m,c}} < \frac{N_d}{A} \pm \frac{M_d y}{I} \pm \frac{M_{ps} y}{I} < \frac{f_{ck,cube}}{\gamma_{m,c}} \tag{7.18}$$

$$f_{ctmd} < \frac{N_d}{A} \pm \frac{M_d y}{I} \pm \frac{M_{ps} y}{I} < f_{cd,cube} \tag{7.19}$$

Where:

$f_{ctmd} = Design\ mean\ flexural\ concrete\ stength\ (Pa)$

$f_{ck,cube} = Characteristic\ concrete\ cube\ strength\ (Pa)$

$A = Cross\ sectional\ area\ (m^2)$

$M_{ps} = Moment\ caused\ by\ prestressing\ (Nm)$

$y = Distance\ from\ neutral\ axis\ to\ extreme\ fiber\ of\ section\ (m)$

The orientation of the prestressing, self weight and bending moment stress distributions on a tower section are illustrated in Figures 7.5 through 7.7:

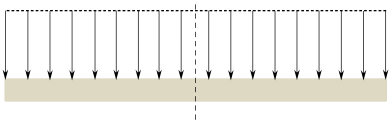

Figure 7.5: Illustration of prestressing stress.

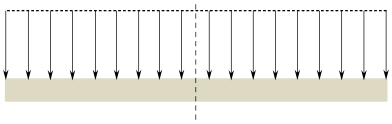

Figure 7.6: Illustration of self weight stress.

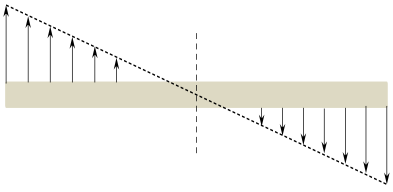

Figure 7.7: Illustration of stress due to bending moment.

The prestressing forces were applied through the use of 16 tendons, equally spaced around the circumference at 22.5° intervals. The tendons all require a concrete cover, c, of 70mm from the outer face of the tower to the outer sheath of the tendon. The prestressing tendons used were based on the BBR CONA multistrand prestressing system (Structural Systems - Prestressing Technology, 2012).

In order to be effective from any wind direction, only 7 of the tendons can be effective to resist tension at any given time, as the two down the center line of the section will not have any effect in resisting the tension force, as shown in Figure 7.8.

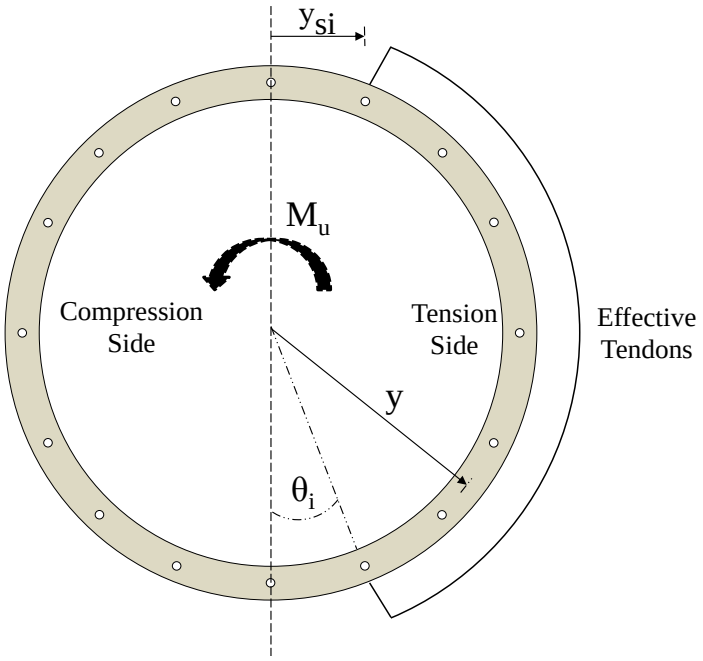

Figure 7.8: Illustration of prestressing orientation and effective tendons for resisting tension stresses.

The bending moment caused by the application of the prestressing forces at a tower cross section is calculated as follows:

$$M_{ps} = \Sigma(F_{d,ps} * y_{si}) \tag{7.20}$$

Where:

$F_{ps} = Design\ prestressing\ force\ per\ tendon\ (N)$

$y_{si} = Lever\ arm\ distance\ away\ from\ center\ line\ of\ section\ (m)$

The calculation of each individual lever arm, to be multiplied with the prestressing force, each time is tedious and so a more efficient way is shown in Equation 7.21:

$$M_{ps} = F_{ps} * y * (\Sigma Sin\theta_i) \tag{7.21}$$

Where:

$y = R_{tower} - c - \frac{\phi_{ps}}{2}\ (m)$

$\phi_{ps} = Outer\ diameter\ of\ prestressing\ duct\ (m)$

$\theta = Angle\ from\ center\ line\ of\ section\ for\ each\ active\ tendon\ (deg)$

The moment is then calculated and used in Equation 7.19 at each 5m interval to check against crushing and tensile failure. The available prestressing tendon information as obtained from Structural Systems *"Prestressing Technology"* catalogue as shown in Tables 7.1 and 7.2:

Table 7.1: Prestressing strand properties - Minimum breaking load (MBL).

Nominal Strand Diameter (mm)	**Steel Area (m^2)**	**Characteristic Tensile Strength (MPa)**	**Strand MBL (kN)**
12.7	100.1	1860	184
15.2	143.3	1745	250
15.2 EHT	143.3	1820	261

Table 7.2: Prestressing tendon information (cont.).

Tendon Unit Designation	**Number of Strands**	**I/O Duct Diameter (mm)**	**MBL 15.2mm/15.2 EHT strand (kN)**
406	4	50/57	1000/1044
706	7	65/72	1750/1827
1206	12	80/87	3000/3132
1906	19	100/107	4750/4959
2206	22	110/117	5500/5742
3106	31	120/127	7750/8091
4206	42	135/142	10500/10962
5506	55	150/157	13750/14355

Depending on the prestressing force required for each tower, a selection will be made from Tables 7.1 and 7.2. The values given on the right hand side represent the minimum breaking load of the number of strands present in the tendon. The booklet also mentions that combinations of numbers of wire strands are permissible. All the strands are stressed to 80 percent of their MBL, as recommended by Structural Systems. The prestressing force is also subject to a partial safety factor, $\gamma_{m,ps}$ =1.15, as prescribed in Eurocode 2.

The prestressing tendons are subject to various losses associated with the relaxation of the steel strands, jacking and friction losses, elastic shortening, creep and shrinkage of the concrete. The concrete-related losses will not be covered in this project. The jacking losses arise when the jacking stress is released and the strands retract towards the (typically) conical wedges, which are then pulled back into the anchorage device, locking the tendon in place (Kelley, 2000). When this happens, a small distance of around 6mm of the strands retract into the tendon, effectively losing a portion of the prestressing.

The friction losses are attributed to the sheath or duct resisting the jacking force being applied to the strands. Two friction forces arise from this, a force that increases with increasing strand length and a force as a result of directional changes in the duct length. Steel relaxation losses are, as the name

implies, due to the steel relaxing over time, thus also reducing the effective prestressing force over time. The losses in the prestressing system are calculated as follows, according to Eurocode 2:

$$F_{d,ps} = \frac{F_0}{\gamma_{m,ps}} * (e^{-(\mu\alpha+\kappa x)} - \delta_{anchor} - \delta_{relax})) \tag{7.22}$$

Where:

$F_{d,ps}$ = *Design prestress force per tendon* (kN)

F_0 = *Initial prestress force (0.8MBL)* (kN)

μ = *Curvature coefficient*

α = *Inclined angle of tower* (rad)

κ = *Wobble friction coefficient* $\left(\frac{rad}{m}\right)$

x = *Strand (tower) length* (m)

δ_{anchor} = *Anchorage loss fraction*

δ_{relax} = *Steel relaxation loss fraction*

$\gamma_{m,ps}$ = *Material factor for prestressing materials*

The data relating to the above-mentioned prestressing characteristics was obtained from the Structural Systems brochure. The value stated for κ in the documentation of 0.008 $\frac{rad}{m}$ caused exceptionally high friction losses due to the length of the tower and so the ducts would have to be flushed with water soluble oil so as to reduce the value to the design value of 0.0016 $\frac{rad}{m}$.

The losses associated with the 120m concrete tower will thus be particularly high in comparison to normal losses encountered when prestressing. In comparison, the losses associated with directional changes will be much smaller, also due to the fact that there is little directional change in the turbine towers.

The values chosen to represent the data in Equation 7.22 are shown in Table 7.3:

Table 7.3: Data used in the calculation of the prestressing losses of the towers.

Tower	$\gamma_{\mathbf{m,ps}}$	μ	κ	**x**	α	$\delta_{\mathbf{anchor}}$	$\delta_{\mathbf{relax}}$
Concrete 80	1.15	0.1	0.0016	80	0.028	3%	2.5%
Hybrid 80	1.15	0.1	0.0016	80	0.036	3%	2.5%
Concrete 100	1.15	0.1	0.0016	100	0.023	3%	2.5%
Hybrid 100	1.15	0.1	0.0016	100	0.024	3%	2.5%
Concrete 120	1.15	0.1	0.0016	120	0.019	3%	2.5%
Hybrid 120	1.15	0.1	0.0016	120	0.018	3%	2.5%

In practice, a designer should consider the use of post-tensioning shorter sections of the tower. Thereby

consecutive sections of the tower can be post-tensioned together, which gives the tower rigidity during erection. In addition, the shorter lengths will result in reduced prestressing losses.

References

DNV/Risø (2002). *Guidelines for Design of Wind Turbines*. 2nd ed. Accessed 29th March 2014. Copenhagen: Det Norske Veritas (DNV) and Risø National Laboratory.

DS412:1998. Dansk Ingeniørforening. Danish Standards Association DS412:1998: The Danish Code of Practice for Loads for the structural use of steel.

DS449:1983. Dansk Ingeniørforening. Danish Standards Association DS449:1983: The Danish Code of Practice for the Design and Construction of Pile Supported Offshore Steel Structures.

EN 1992-1-1:2004*:* European Committee for Standardization. EN 1992-1-1:2004 (Eurocode 2): Design of concrete structures - Part 1-1: General Rules and Rules for Buildings.

Kelley, G., ed. (Sept. 2000). *Prestress Losses in Post-Tensioned Structures.* PTI Technical Notes. Issue 10. September 2000. URL: http://www.post-tensioning.org/Uploads/technote10.pdf.

Structural Systems - Prestressing Technology (2012). Structural Systems. www.structuralsystemsuk.com/downloads/PreStressing.pdf. 20 Hilly Street. Mortlake. New South Wales. Australia.

Chapter 8

FEM Analyses

Various analyses were performed using a finite element method (FEM) analysis program, Abaqus, in order to validate results and accurately determine the natural frequencies of the wind turbine towers. This chapter discusses the modeling of the wind turbine towers, the analyses performed and the results obtained from the analyses.

8.1 Modeling Wind Turbine Towers

8.1.1 Model Type

The tower modeling was done using the Abaqus Standard/CAE interface. Initially, shell elements were envisaged to be the ideal element to use in the models, due to their inexpensive computational requirements. The use of shell elements would greatly reduce the time needed to run analyses. On the other hand, the foundations would be complex to model with shell elements and the interface between shell (tower) and solid elements (foundation) is difficult to incorporate into the model and can lead to stress concentrations that are not representative of reality.

An alternative is to use full 3D elements. The use of full 3D elements allow for simpler construction of the geometry and a better interface between the various parts of the models, which is particularly useful for the interface between the tower, base plate and foundation. The disadvantage of using 3D elements is that, due to the high slenderness ratio of the towers, only one element would span the thickness of the tower shell, which may cause computational errors in the models, particularly with the steel towers.

Generally, this is a problem when shear stresses are in question, as the stresses only have one element through which to represent a vast multitude of stresses. In this case, the shear stresses are not of particular interest. In addition to this, the use of shell elements is encouraged when the model can essentially be simplified to a “semi-2D” model, that is, when the change of the analysed feature across

the third direction can be neglected. Due to the inability of the shell elements to represent stresses across this third direction anyway, it was decided to use 3D elements, due to their modeling simplicity.

The objectivity study below does not include stress verification, but only primary variables such as displacement, velocity and acceleration. The study was done on the effect of mesh size on the wind turbine. A concrete tower, without foundation, with a height of 80m was analysed with various mesh sizes in order to determine the effect of mesh sizes on the natural frequency analysis. The mesh size was varied from an inaccurate 2m hexagonal element, to a 0.08m hexagonal element, which corresponds to one highly truncated element over the tower thickness, to four equally dimensioned elements over the thickness respectively. The results are shown in Table 8.1.

Table 8.1: Mesh element size comparison.

Maximum Mesh Element Size (mm)	Elements Over Thickness	Analysis Time (s)	Natural Frequency (Hz)
2000	1	2	0.88
1000	1	2	0.91
600	1	3	0.918
500	1	3	0.92
250	1	13	0.924
125	2	117	0.925
80	4	20935	0.926

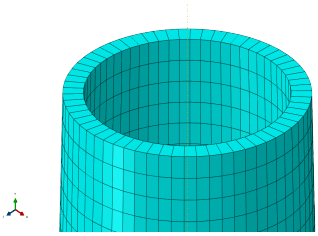

Figure 8.1: One element over thickness.

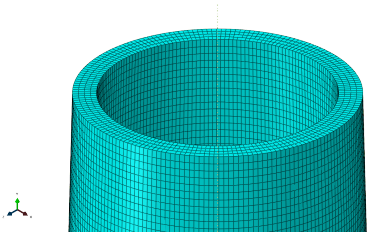

Figure 8.2: Four elements over thickness.

As can be seen from Table 8.1, the error in the use of mesh sizes equal to 2-3 times the shell thickness is in the order of 0.86 percent, which is acceptable. As the stress distribution through the thickness of the shell is not of importance, the use of 3D elements with mesh sizes that allow only one element across the tower shell thickness are acceptable for use in the analyses.

8.1.2 Model Element Types

8-Node Linear Hexagonal "Brick" Element

The second decision to be made was the choice of element type for the various 3D models. The first option is an 8-node linear hexagonal brick element with 3 degrees of freedom (DOF) per node, the preferred element to be used in 3D FEM models. The 8-node brick is the simplest and most efficient element to use, due to its rectangular shape and well-ordered mesh configuration. It is preferred over tetrahedral elements, due to the reduced number of elements required for the same mesh size and thus,

reduced computational requirements.

The drawback of this element is that it can only be used in cases of relatively simple geometry. Complex geometry introduces warped and distorted elements, which lead to inaccuracies in results. Figures 8.3 and 8.4 illustrate the 8-node brick and the use thereof in a mesh.

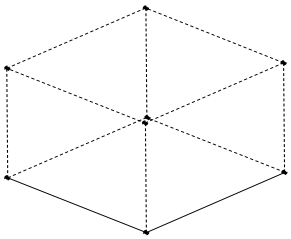

Figure 8.3: 8-Node hexagonal brick element.

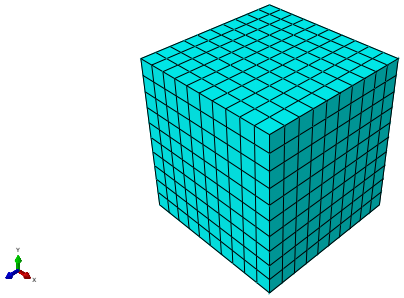

Figure 8.4: Mesh with hexagonal brick elements.

4-Node Linear Tetrahedral Element

The other element that was considered is the 4-Node linear tetrahedral element, with 3 DOF per node. This element is more complex than the brick element because of the equations in the element formulation, as well as that meshes that use tetrahedral elements have far more elements than a brick mesh (5 tetrahedral elements are needed for every 1 brick element).

Another known problem with linear tetrahedral elements is that they tend to be too stiff in bending-related analyses, which is not ideal for the case of wind turbine towers, with high levels of bending (Wang et al., 2004). This is due to a phenomenon commonly known as shear-locking, whereby the elements are unable to accurately assume the correct deformation shape, even with a fine mesh. The solution to this problem is to use a quadratic formulation, which adds an additional node to each side of the element. This enables the element to assume the correct deformed shape, although it does notably increase computation time.

Tetrahedral elements do have a distinct advantage over brick elements in that they can be used to model more complex shapes, where brick elements become distorted. Figures 8.5 and 8.6 illustrate the 4-node tetrahedral element and the use thereof in a mesh.

Due to the above-mentioned advantages and disadvantages, it was decided that the 8-node brick element would be used wherever possible and that the tetrahedron element would only be used when the mesh quality using brick elements is poor. As the geometry of the towers is relatively simple, brick elements were used to model the entire tower. The foundations however, could not be completely modeled using brick elements, as the slope on the top side of the foundation created largely warped elements. It was then decided to model the bottom block of the foundation with brick elements and the sloped part of the foundation with tetrahedron elements, as shown below in Figure 8.7.

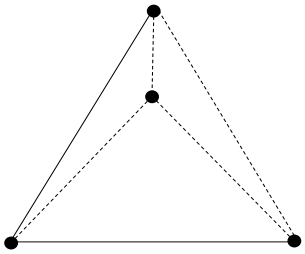

Figure 8.5: 4-Node tetrahedral element.

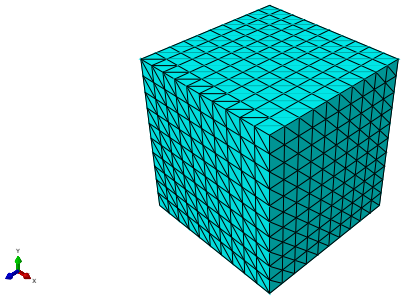

Figure 8.6: Mesh with tetrahedron elements.

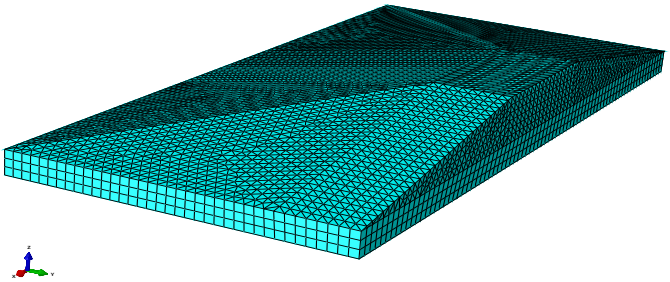

Figure 8.7: Foundation mesh using brick and tetrahedron elements.

8.2 Analyses Performed

Using Abaqus, each tower was subjected to three analyses. First, a modal frequency analysis was performed to accurately determine the natural frequency of the tower and see whether it lay in the acceptable frequency range.

The second analysis involved the calculation of the buckling stress of each tower. In this analysis, the ultimate loads are applied to the structure and the analysis determines a factor relative to the buckling load to describe how safe, or under designed the model is. A factor of 1 indicates that the model is exactly on the brink of failure due to buckling. Values less than 1 indicate failure and anything over 1 indicates safety against buckling failure.

The final analysis was a static load analysis with the ultimate limit state loads applied to the wind turbine structure, with the intent of checking the hand-calculated stresses and tower-tip deflections, to include the so-called $P - \Delta$ effect for the tower top weight.

8.3 Loads

The loads included (also applicable to the buckling analysis):

- Wind loads acting directly on tower;

- Wind loads acting on the nacelle, blades and nose-cone;
- Own weight of tower, and turbine;
- Torsional moment on tower;
- Tower top weight eccentricity and
- Prestressing on tower, where applicable.

The wind loads acting on the tower were modeled as surface tractions, following a user-defined analytical field that described the wind pressure as a function of tower height. The surface tractions follow the curvature of the cylinder. The loads are based on figure 29 of SANS 10160-3, using averaged pressure coefficients on the front and one side of the cylinder.

This approach is somewhat conservative, but it was considered in case of vortex-shedding and dynamic effects which have thus far been neglected. The wind loads acting on the nacelle, blades and nose-cone were applied in the form of concentrated forces, acting at the center of the nacelle, 2m above the tower top. This approach was later modified for the buckling analysis, as the approximation of the load orientation did not accurately assimilate the true wind action on the structure for the purpose of a buckling analysis. The loading was therefore modified to more accurately approximate the capacity of the towers against buckling failure.

The torsional moment due to the blades was applied in the form of an applied moment, acting on the top face of the tower. The own weight of the assembly was modeled by gravity loads acting on the respective sections of the assembly. The prestressing force was applied to the top face of the towers as a pressure load. Figure 8.8 illustrates the applied loads for the static load and buckling analysis.

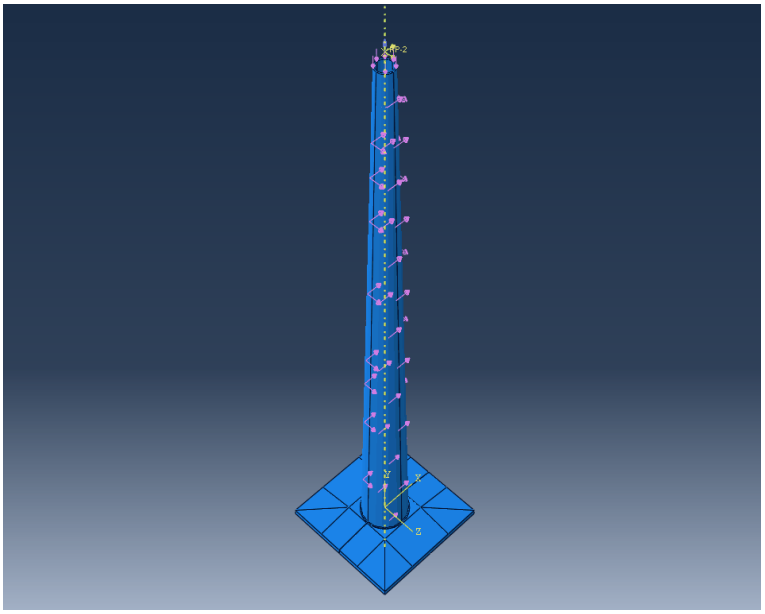

Figure 8.8: Ultimate loads applied to the tower and foundation structure.

8.4 Foundation Support Modeling

As previously discussed in section 6.4, the effect of the underlying soil is taken into account by using springs. The foundation is then modeled as being supported with regard to vertical, horizontal, rocking and torsional stiffness by these springs. The spring stiffness values are calculated using Equations 6.22 through 6.25. These stiffness values are then distributed to the springs on the underside of the foundation at 9 equidistant points, as shown in Figure 8.9. The particulars of the springs can be seen in Appendix H.

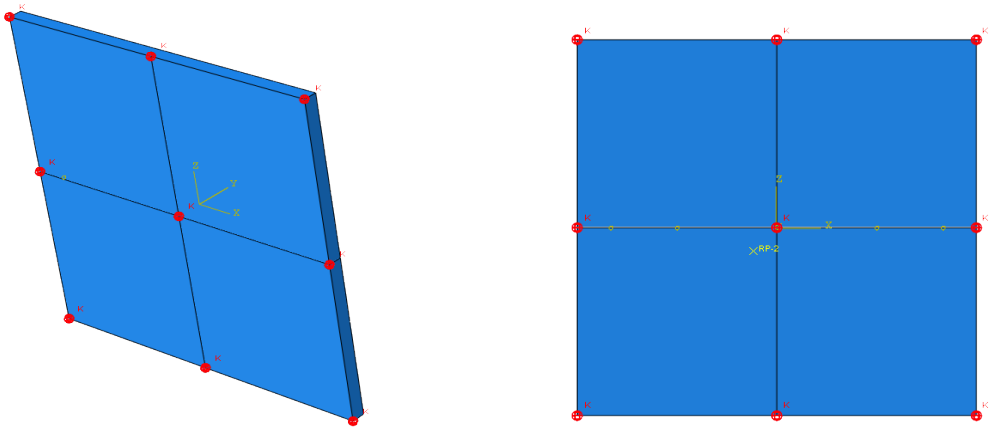

Figure 8.9: Foundation spring orientations.

References

Wang, E., T. Nelson, and R. Rauch (2004). *Back to Elements - Tetrahedra vs. Hexahedra*. CAD-FEM GmbH.

Chapter 9

Results

9.1 Final Wind Turbine Design Dimensions

The final designs here are highly dependent on the choice of safety factors associated with the foundation design and wind loading. In addition, the choice of soil type has a considerable effect on the size of the foundations. With that taken into consideration, the final design of the wind turbine support structures is shown below.

9.1.1 Final Tower Dimensions

After the verification of the design criteria of the towers, the dimensions of the wind turbine support structures were finalized. The complete dimensional details can be seen in Appendices B and C. Tables 9.1 through 9.5 and Figures 9.1 through 9.5 give a summary of the dimensional details of the wind turbine towers:

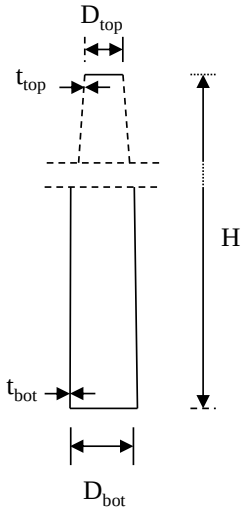

Figure 9.1: Illustration of tower dimension parameters.

Table 9.1: Steel tower dimensions. The * indicates that the properties do not taper linearly from top to bottom.

		80m	**100m**	**120m**
Top Outer Diameter (m)	D_{top}	3	3	3
Bottom Outer Diameter (m)	D_{bot}	4.5	4.5	4.5*
Top Shell Thickness (mm)	t_{top}	15	15	15
Bottom Shell Thickness (mm)	t_{top}	34	55	75*

It can be seen from Table 9.1 that the steel shell thickness appears to increase almost linearly across the various tower heights. However, this is not the case for all the towers, particularly the 120m steel tower as mentioned in Section 7.2. The 120m steel tower diameter is kept at a constant diameter of 4.5m for the first 45m of the tower height, in addition to the shell thickness being kept at a maximum of 75mm also for the first 45m of the tower.

Table 9.2: Concrete tower dimensions.

		80m	**100m**	**120m**
Top Outer Diameter (m)	D_{top}	3	3	3
Bottom Outer Diameter (m)	D_{bot}	7.5	7.5	7.5
Top Shell Thickness (mm)	t_{top}	200	250	250
Bottom Shell Thickness (mm)	t_{bot}	275	325	350

It was decided to keep all of the bottom diameters of the concrete towers at 7.5m. Greater diameters are possible and are used, although less frequently. A wider base can reduce the tower thickness requirements, but at the same time, increase the weight and material requirements of the tower. It can also drive the stiffness of the tower too high and increase the prestressing requirements. The sections of the tower will also become more cumbersome and difficult to transport.

The top sections of the towers could also have been slightly thinner, but a sacrifice would have to be made in terms of reducing the concrete cover below recommended levels. As it stands, the concrete cover is just adequate to comply with the requirements of the prestressing tendons. Using a higher grade of concrete would allow for a reduction in the tower wall thickness, but would necessitate an innovative change in the design of the prestressing system. Such a system is used by Acciona Wind Systems in their concrete towers, which incorporates a cross between internal and external prestressing. In this project however, it was decided to keep the sections slightly thicker.

Table 9.3: Hybrid tower dimensions.

			80m	100m	120m
Steel	Top Outer Diameter (m)	D_{top}	3	3	3
	Bottom Outer Diameter (m)	D_{bot}	4.3	4.3	4.3
	Top Shell Thickness (mm)	t_{top}	15	15	15
	Bottom Shell Thickness (mm)	t_{bot}	25	25	25
	Steel Section Height (m)		40	40	40
Concrete	Top Outer Diameter (m)	D_{top}	4.6	4.6	4.6
	Bottom Outer Diameter (m)	D_{bot}	7.5	7.5	7.5
	Top Shell Thickness (mm)	t_{top}	200	200	300
	Bottom Shell Thickness (mm)	t_{bot}	200	200	300
	Concrete Section Height (m)		40	60	80

It can be seen in Table 9.3 that both the 80m and the 100m tower have the same overall dimensions and wall thicknesses. There is however, an increase in the prestressing force in order to make up for the increased loads in the case of the 100m tower. It should also be noted that there is an increase in the tower diameter from the steel section to the concrete section. This allowance is to make sure that there is enough space for the connection between the two sections, as well as for sufficient concrete cover for the connection. The connection between the tower sections is not covered in this study.

As can be seen in Tables 9.1 through 9.3, the concrete sections are substantially thicker than their steel counterparts, due to the limited capacity for tension and compression strength as well as material stiffness. This can be seen as both a positive and a negative aspect. The positives are that the larger sections provide extra mass, which increases the stabilizing moment of the tower, as will be discussed in the following chapter. One of the negatives are that a lot more material is required per tower. Craning the sections into place will also take longer than for the steel towers, that typically have 3-5 sections per tower. Figure 9.2 illustrates the considerable difference in tower weights

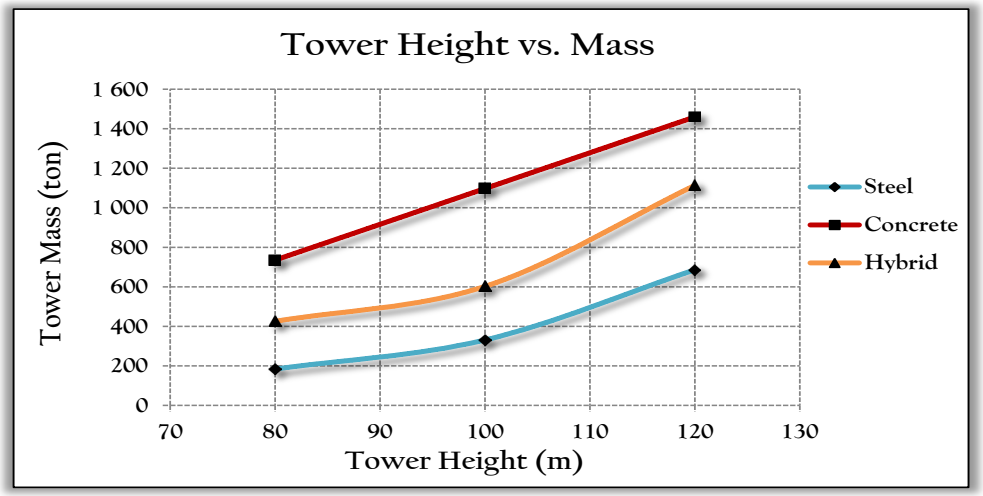

Figure 9.2: Comparison of tower masses for various heights.

9.1.2 Final Foundation Dimensions

The foundations are all designed in a square shape with a block portion on the bottom, tapering to a raised square platform on the top upon which the turbine tower lies. The platform width and length, L_p, is 5m for the steel towers and 8m for the concrete and hybrid towers, respectively. The dimensions of the foundations for the wind turbine towers are shown in Tables 9.4 and 9.5, with reference to the foundation illustration shown in Figure 9.3. Tables 9.4 and 9.5 and Figures 9.3 and 9.4 are summaries of the information contained in Appendices D and E.

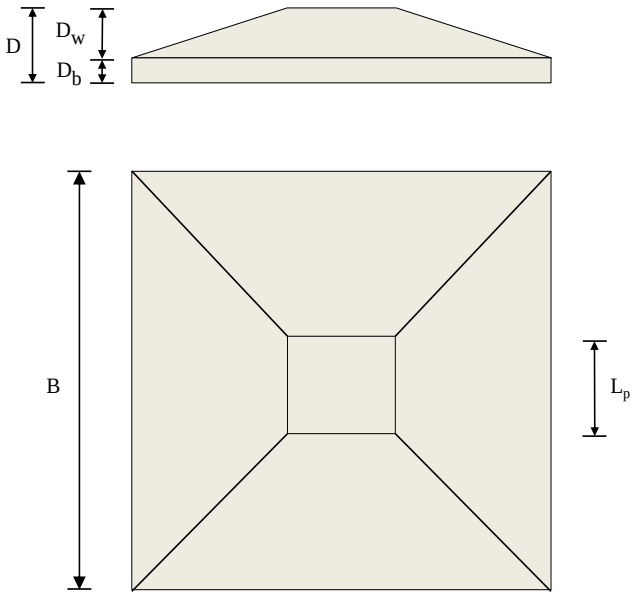

Figure 9.3: Illustration of foundation dimension parameters.

Table 9.4: Final dimensions of the designed wind turbine foundations.

Height	**Tower**	**Breadth**	**Block Height**	**Wedge Height**	**Total Height**	**Volume**
(m)		**B (m)**	**D_b** (m)	**D_w** (m)	**D (m)**	**V (m^3)**
80	Steel	21.00	0.75	1.45	2.2	606
	Concrete	20.00	0.8	0.7	1.5	459
	Hybrid	20.50	0.7	1.05	1.75	598
100	Steel	21.75	0.75	1.75	2.5	707
	Concrete	20.25	0.95	1.1	2.05	622
	Hybrid	21.75	0.7	1.65	2.35	721
120	Steel	23.25	0.95	1.8	2.75	921
	Concrete	22.75	0.65	1.8	2.45	774
	Hybrid	22.75	0.8	1.65	2.45	832

Table 9.5: Foundation concrete and steel reinforcing requirements.

Height (m)	Tower	Foundation Concrete Volume (m^3)	Foundation Steel Reinforcing (kg)
80	Steel	606	53 106
	Concrete	459	38 266
	Hybrid	598	43 975
100	Steel	707	62 846
	Concrete	622	47 040
	Hybrid	721	62 887
120	Steel	921	82 464
	Concrete	774	72 813
	Hybrid	832	71 647

As can be seen in Table 9.4, the foundation volume is proportional to the tower height. An increase in tower height requires an increase in foundation concrete volume for one of the following reasons:

- To provide extra weight to counter the tower overturning moment;
- To provide extra foundation height negating the need for punching shear reinforcing;
- To increase the spread area of the foundation to prevent bearing capacity failure, or
- To provide more weight at the base in order to raise the natural frequency of the system.

The tensile reinforcement requirements of the towers shown in Appendix E are summarized in Table 9.5. The reinforcing follows a trend similar to that of the concrete volume requirements. As the tower height increases, the tensile reinforcement requirement increases. Notably, the tensile reinforcement requirement for the foundations is governed by the clause that defines the minimum amount of reinforcing steel required, according to Eurocode 2. This was the case for all 9 of the foundations, with the minimum allowable reinforcement being between 1.5 and 2.5 times the amount required to resist the bending moment in the slabs for the 80m and 120m towers, respectively.

Therefore, as can be seen from Figure 9.4, the amount of steel reinforcement required is almost directly proportional to the volume of concrete in the foundation. This will not likely be the case when considering wind turbines in IEC wind class II and I, as the highly increased bending moment will play a significantly greater role in the reinforcing requirements.

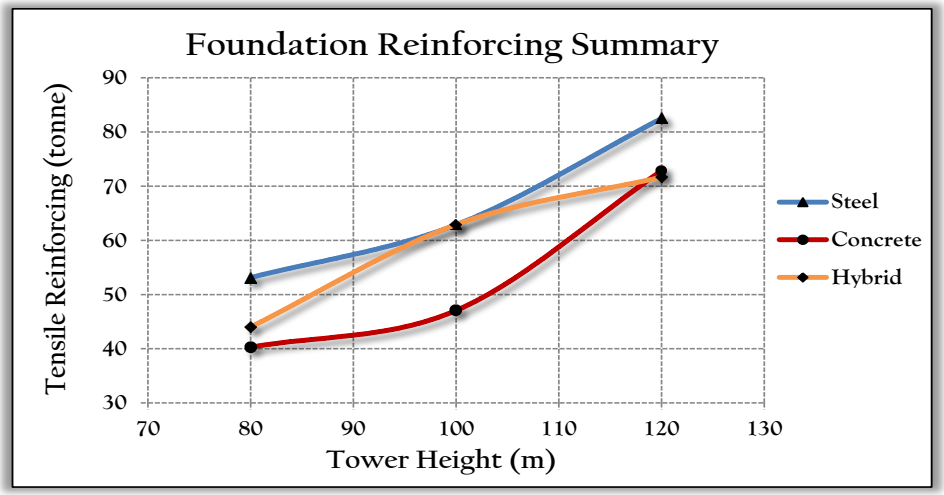

Figure 9.4: Comparison of tensile reinforcement requirements for various tower heights.

In the case of all the steel towers, the increase in foundation volume was due to the need for extra weight to counter the overturning moment from the wind loading, so as to achieve a "safety factor" against overturning of at least 2.5, according to Equation 6.21. This condition is prevalent when the water table is at ground level, which causes a buoyancy force that acts against the own weight of the foundation, tower and nacelle assembly.

It was found in this study that bearing capacity (Equation 6.1) failure was not a problem for the steel towers with the chosen soil conditions. None of the steel tower foundations had any problems with punching shear (Section 6.6) and did not need to be adjusted in order to avoid the use of shear reinforcing, however any tower taller than 120m is likely to need an increase to the foundation height to deal with this, as the 120m was near the limit.

Initially, it was assumed that the foundations of the concrete towers would fail in bearing, due to the sheer weight of the structure. This was partly the case, but for the 80m tower, the foundation design was governed by overturn of the structure, when the water table is at ground-surface level. As the weight of the towers increase with height, the 100m tower foundation was governed by simultaneous overturn and bearing failure with a ground-surface water level (undrained soil conditions). The 120m tower foundation has adequate weight to prevent overturn, but is governed by the bearing capacity, also in an undrained soil condition (water level at ground surface).

Just as the hybrid towers are a combination of the steel and concrete towers, so are their foundation designs. Similar to the steel towers, the main problem is due to the need for a stabilizing moment that exceeded the overturning moment by a factor of 2.5 with the water table at ground level. Due to the contribution of weight from the lower concrete section of the tower, less of an increase in foundation volume was required than for the steel towers.

Figure 9.5 graphically shows the foundation volume versus tower height for all nine of the designed towers. It can be seen that the volume of the hybrid and concrete tower foundations increase more logarithmically, whereas the foundation volume of the steel towers increase exponentially. From this

study, the trend with the hybrid and concrete tower foundations is that they will tend to be more sparing with regard to the amount of concrete needed for greater hub heights. The concrete tower foundations are shown to be the most cost-effective for all towers.

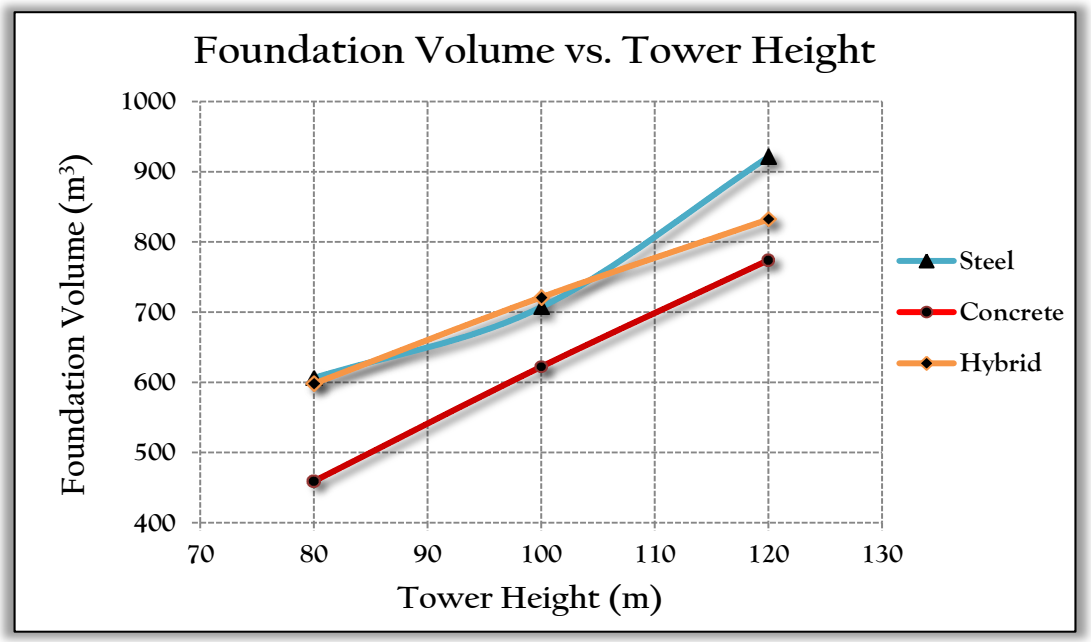

Figure 9.5: Comparison of foundation volumes for various heights.

9.2 FEM Analysis Results

9.2.1 Natural Frequency

The first natural frequency of each of the towers was determined using Abaqus. For the 80m steel and concrete towers, the first four modes were checked to ensure that the analyses were running correctly, as shown in Figures 9.6 and 9.7.

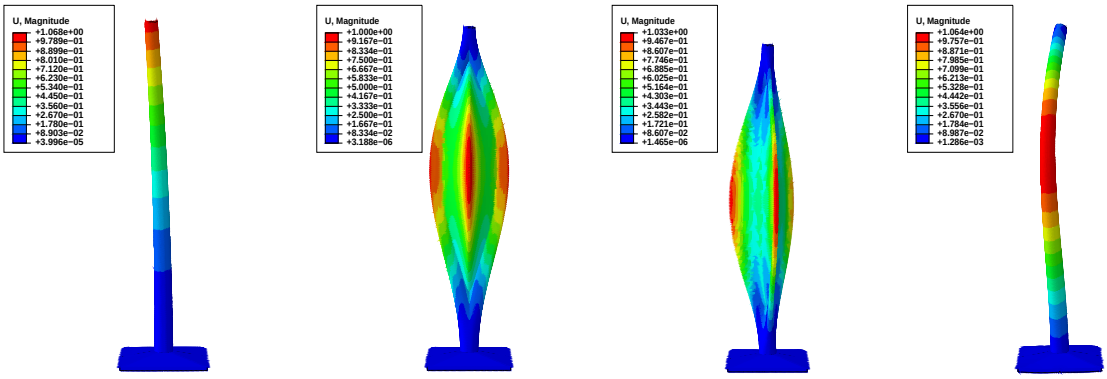

Figure 9.6: First four natural frequencies for the 80m steel tower.

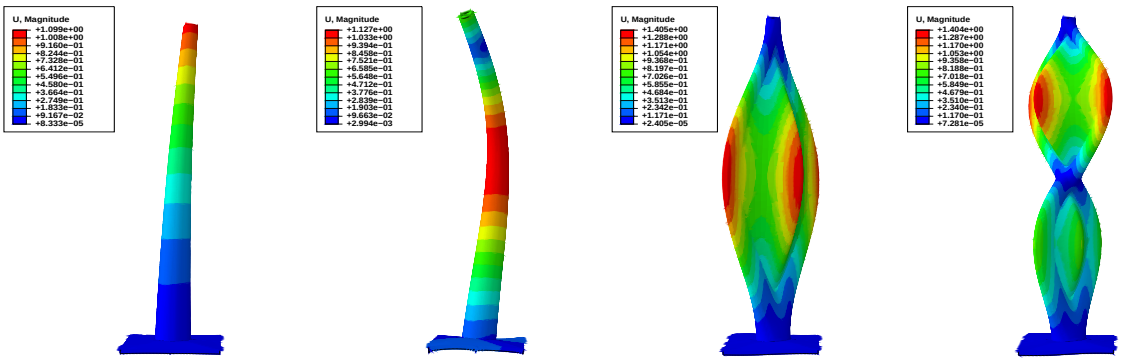

Figure 9.7: First four natural frequencies for the 80m concrete tower.

The first natural frequencies of all of the towers correspond to vibration in the windward-leeward direction and are always the lowest natural frequencies. The higher mode frequencies can either be multiple-waves of the first natural frequency, as seen in the second figure for the concrete tower, or ovalisation of the tower, as can be seen in the second figure of the steel tower. It is thus the first frequencies that are of interest to compare to the allowable frequency bands. All the towers were within the allowable range with little or no change to design, with the exception of the 120m steel tower.

The 120m steel tower was particularly problematic to design because of the interaction between the natural frequency of the tower and the operating frequency of the turbine. As shown in section 5.3, the lower limit of the wind turbine tower-foundation system is 0.245 Hz. The 100m steel tower was just above the lower limit with a little adjustment to the shell thickness or tower cross section. The 120m tower as designed for buckling violated the 15 percent separation from the 1P blade passing frequency criteria. The shell thickness at the bottom of the tower was increased to the maximum plate thickness, 75mm, and then tapered to 15mm at the top. This however, was not adequate to raise the natural frequency sufficiently and so the tower shell thickness was kept at a maximum of 75mm for the first 45m of the tower height.

This also proved to be insufficient, as the natural frequency of the system was still below the limit. In a final attempt to make the design satisfy the stiffness criterion, the tower diameter was kept at a constant 4.5m for the first 45m of the tower height, and then tapered to 3m at the top. This lifted the natural frequency to 0.238Hz, which is still below the 15% separation limit from the 1P frequency. The value of 0.238 is approximately 12 percent separated from the 1P frequency, which is acceptable according to both Hau and DNV/Risø (Section 5.3) and so it was left at this value, although the design of the tower is unlikely to be economically feasible.

This is the inherent problem with traditional steel towers. As the tower gets taller than 90-100m, the stiffness requirements of the tower become too strict for the tower to bear and so economically unfeasible designs result. Due to this, the concrete and concrete-steel hybrid designs become more favourable for tower heights over 100m. This problem with steel towers is exacerbated by the use of larger turbines, that cause even more top-heaviness of the system, due to the increased head weight of the turbine, blades and nose-cone.

The use of larger wind turbines generally reduces the natural frequency requirements by lowering the natural frequency bands of the tower-foundation system, due to the slower rotation speed of the blades. The effect of using turbines with greater nameplate capacity and blade length on the natural frequency exclusion zones is shown in Figure 9.8. Unfortunately, the gains in the lowered natural frequency requirements are outweighed by the negatives associated with increased mass-concentration, due to the heavier turbine at the top of the tower.

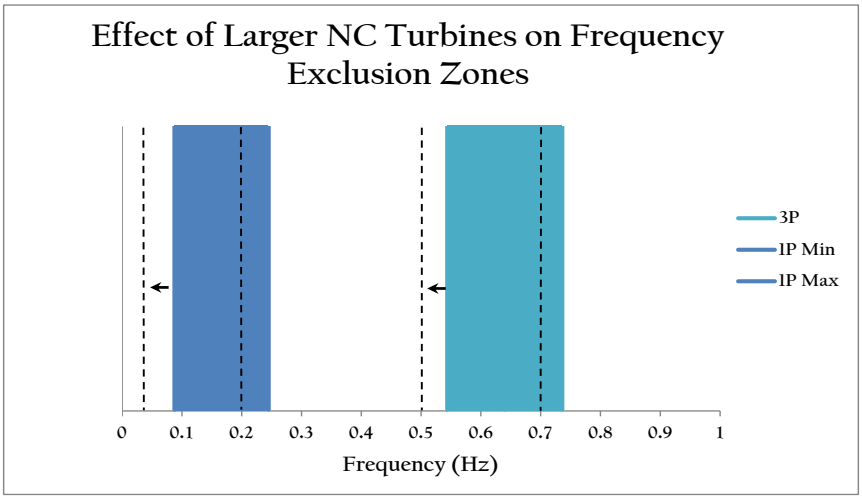

Figure 9.8: Effect of lower rotation speed of larger nameplate capacity turbines on tower natural frequency exclusion zones.

All the natural frequencies of the towers were within the specified limit with the exception of the 120m steel tower, as mentioned previously. The results of the Abaqus natural frequency analyses are shown in Table 9.6. It should be noted that the effect of the prestressing was neglected in the natural frequency analyses.

This is a debated topic, but according to Breccolotti and Venanzi, 2009:

> *"For the cases where the hypothesis of linear materials and bonded tendons can be assumed, the effect of prestressing can be neglected, since the variation in the deformed equilibrium configuration do not signicantly modify the dynamic properties of the structure".*

The matter of post-tensioning-dependent frequency is to be studied further by the research group at Stellenbosch University. The hand calculation is calculated according to Equation 5.4. As can be seen, it is relatively accurate for most of the towers, the largest error being 12.3 percent.

Table 9.6: Tower natural frequencies.

Height (m)	Tower Type	Hand Calc. Natural Frequency (Hz)	Natural Frequency (Hz)	Limits (Low ; High) (Hz)
80	Steel	0.290	0.285	0.245 ; 0.544
	Concrete	0.458	0.432	
	Hybrid	0.44	0.407	
100	Steel	0.232	0.251	0.245 ; 0.544
	Concrete	0.315	0.333	
	Hybrid	0.346	0.338	
120	Steel	0.212	0.238	0.245 ; 0.544
	Concrete	0.294	0.261	
	Hybrid	0.321	0.297	

9.2.2 Buckling Analysis

The buckling analyses was done for all of the towers to check that the towers are, in fact, safely designed with regard to buckling. It should be noted that the buckling analyses only show "safety factors" with regard to buckling of the towers and not to overall stability. The buckling analysis result for the 80m steel tower is shown in Figure 9.9, with a large deformation scale factor for ease of visualization.

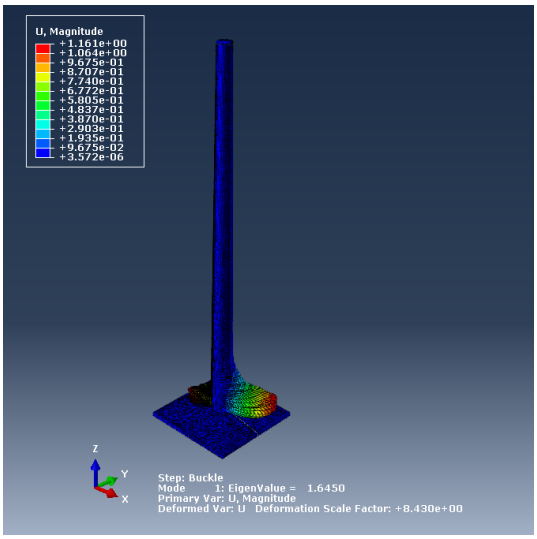

Figure 9.9: Results of the Abaqus buckling analysis for the 80m steel tower.

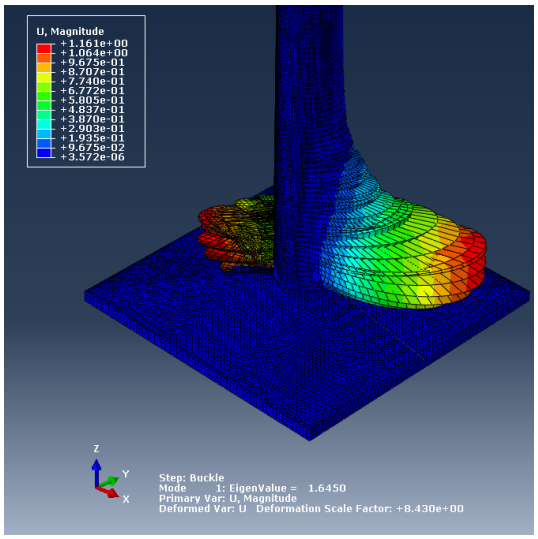

Figure 9.10: In depth view of buckling mode.

All the buckling failure modes of the tower are similar to that shown in Figures 9.9 and 9.10, with the section at the base of the tower failing in a pinching and bursting type manner. The buckling analysis was run on all nine of the towers, the results of which are shown in Table 9.7.

Table 9.7: Results from Abaqus buckling analyses on wind turbine towers.

Height (m)	Tower Type	Eigenvalue
80	Steel	1.645
	Concrete	10.1
	Hybrid	2.25
100	Steel	2.84
	Concrete	4.65
	Hybrid	2.25
120	Steel	3.48
	Concrete	2.38
	Hybrid	2.27

As can be seen in Table 9.7, the concrete towers are not susceptible to buckling failure at lower hub heights, due to the thick cross sections. As mentioned previously in section 8.3, the loading pattern was adjusted for the concrete towers. The buckling analyses done for the concrete towers showed that the buckling resistance decreases considerably with increasing hub height. The trend shows that buckling may be a governing design factor to consider in the design of concrete towers taller than 120m.

The buckling resistance of the hybrid towers is governed by the steel portion on top. The buckling strength of the steel towers can be seen to, counter-intuitively, increase with increasing tower height. This is due to the need for the increased shell thickness to comply with the frequency-stiffness requirements, as described in section 9.2.1. Thus, it is confirmed that the stiffness requirements govern the taller steel tower design and not buckling failure.

It should be noted here there was some concern that the conservative loading approximation, made with regard to the wind loading on the tower, may not reflect the true buckling shape of the steel towers. A verifying static and buckling analysis was done on one of the towers using a more accurate, though time consuming, approximation of the wind loading. This analysis revealed that the tower deformed with more of an oval-like shape in the static analysis. The results from the verifying buckling analysis confirmed that the original approximation was in fact conservative with regard to the buckling strength of the steel towers.

9.2.3 Static Load Analysis - Tower Deflections

Firstly, the static load analysis aimed to investigate tower deflections. There are no limits set by wind turbine tower design standards with regard to tower top deflections. Wind turbine manufacturers however, do occasionally specify a maximum tower top deflection for towers. This is to limit excessive fatigue damage to the tower, as well as to ensure that the contents of the turbine do not sustain damage caused by the back-and-forth motion of the tower. As such, the steel towers may need to have even thicker shell sections in order to comply with the stiffness requirements imposed by these deflection limits. The result of the static load analysis, with regard to tower top deflection, for the 120m towers is shown in Figure 9.11.

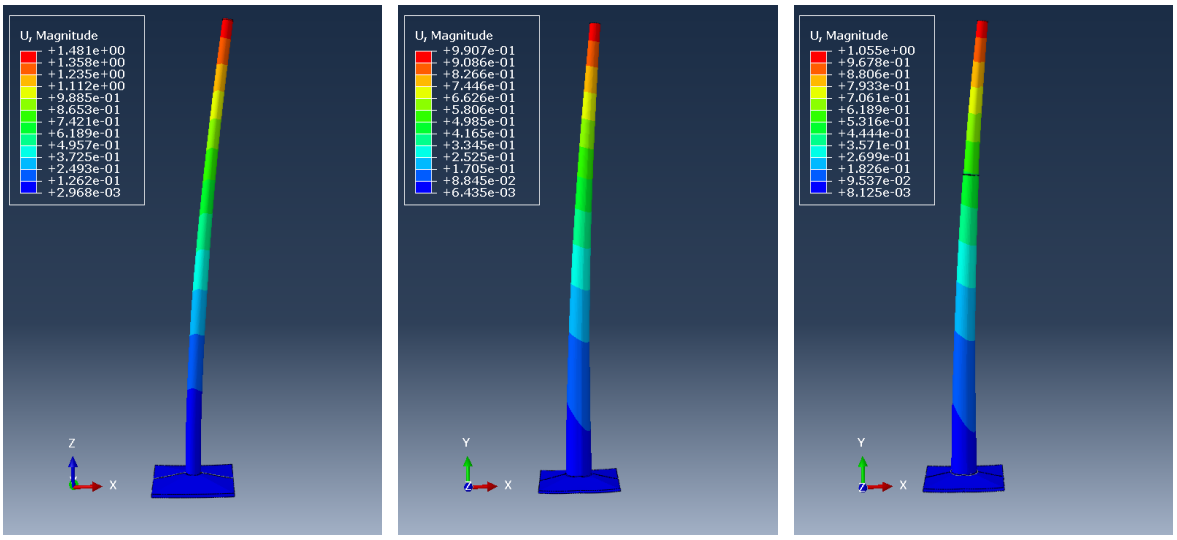

Figure 9.11: Maximum tower deflections for the 120m steel, concrete and hybrid towers. Deflections are portrayed in meters.

The results for the maximum deflections of the towers as obtained from the Abaqus analyses are shown in Table 9.8.

Table 9.8: Abaqus tower-top deflection results.

Height (m)	**Tower Type**	**Tower Top Deflection (m)**	**Deflection as % of Tower Height**
80	Steel	0.92	1.15
	Concrete	0.371	0.46
	Hybrid	0.519	0.65
100	Steel	1.35	1.35
	Concrete	0.600	0.600
	Hybrid	0.796	0.796
120	Steel	1.481	1.24
	Concrete	0.99	0.825
	Hybrid	1.055	0.88

As can be seen from Table 9.8, the concrete and concrete-steel hybrid towers do not have problems related to excessive deflections. Due to the thick concrete cross sections, the concrete portions of the tower are extremely stiff and so the tower deflections are much lower than for the steel towers.

The steel towers, particularly the 100m tower, deflect much more than the concrete-based towers due to their relatively thin sections. The 120m steel tower would also have had problems with excessive deflections, had the cross section not already been enlarged to comply with the natural frequency requirements.

It is a possibility that the 100m steel tower would need to have thicker sections to limit deflections to comply with turbine manufacturer deflection limits. In this study, it will be kept as it is. It should be noted that due to the conservative assumptions made with regard to the wind loading, the actual

deflections will likely be lower than those shown in Table 9.8.

9.2.4 Static Load Analysis - Tower Stress Calculation Verification

As the tower is not as simple a structure to model as it seems, it was expected that the hand calculations and the FEM analyses would bear slightly different results, with respect to the stresses in the tower. The main concern that arose from the comparison between the hand calculations and the FEM output is that the maximum and minimum stresses did not occur at the same places in the FEM analysis and the hand calculations.

For the hand calculations for the concrete towers, the maximum tensile stresses occurred around two-fifths of the way up the tower in all three of the towers. The maximum tensile stress for the 80 and 100m steel towers was present between half way and three-fifths of the way up the tower. The 120m steel tower differs from the norm due to the alterations made to the tower geometry to adjust the natural frequency and so the maximum tensile stress was found three-quarters of the way up the tower.

The hand calculations for the hybrid towers showed that in all cases, the maximum tensile stress in the steel was just above the interface to the concrete portion. The maximum tensile stress in the concrete part of the hybrid towers always seemed to be between 40 and 45m of tower height.

The concern is that in the FEM analyses, all of the maximum tensile and compression stresses are at the bottom of the respective sections for both concrete and steel sections. The maximum and minimum stresses from the FEM analysis conform to the maxima and minima from the hand calculations, but the positions at which they occur do not. Initially it was thought that only having one element over the tower thickness could be affecting the results. This theory proved to be flawed however, as a model of the 80m concrete tower was created, with 4 elements over the tower thickness, that yielded almost identical values and maxima and minima positions.

The important aspect, and the main reason for the accompanying FEM analysis, was to check that none of the crucial design stresses (compression, tension and yielding) were exceeded. Even though the results from the FEM analyses differ from the hand calculations, none of the critical values were exceeded, indicating that the designs are sound, with regard to material strength. The differences are shown in Figure 9.12 and 9.13, for the concrete towers. The hand calculations can be seen in Appendix B. It should be noted that the following graphs consider compression stresses as positive and tension stresses, negative.

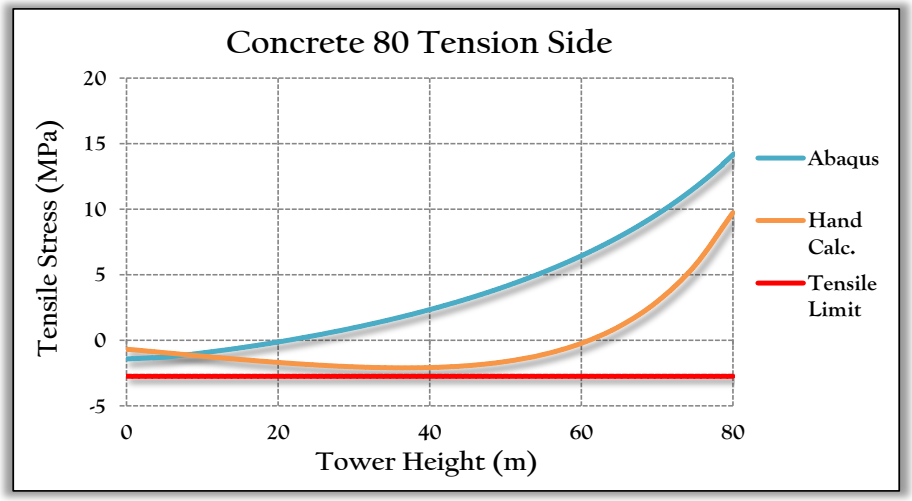

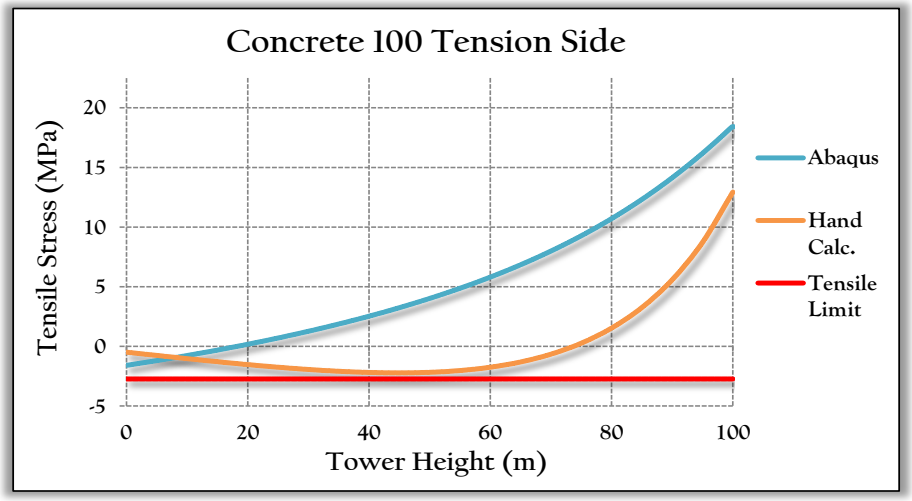

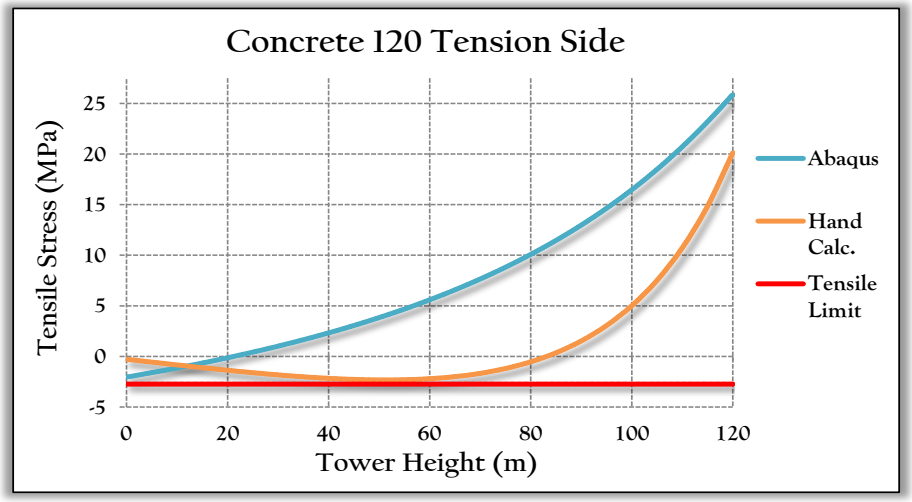

Figure 9.12: Tension-side stress comparisons between Abaqus FEM analyses and hand calculations for concrete towers with heights of 80, 100 and 120m.

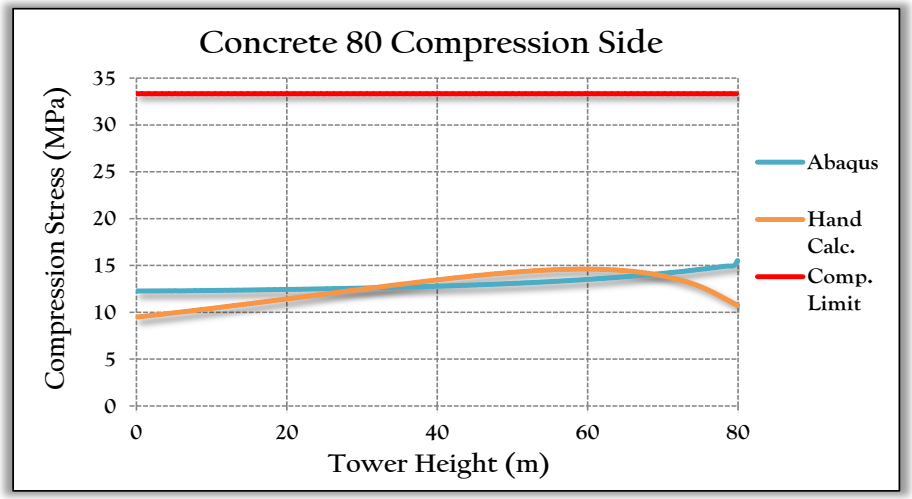

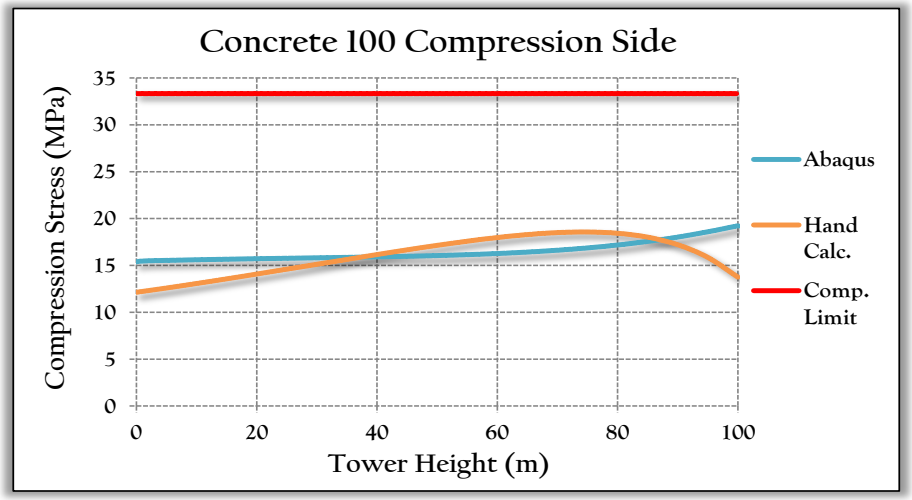

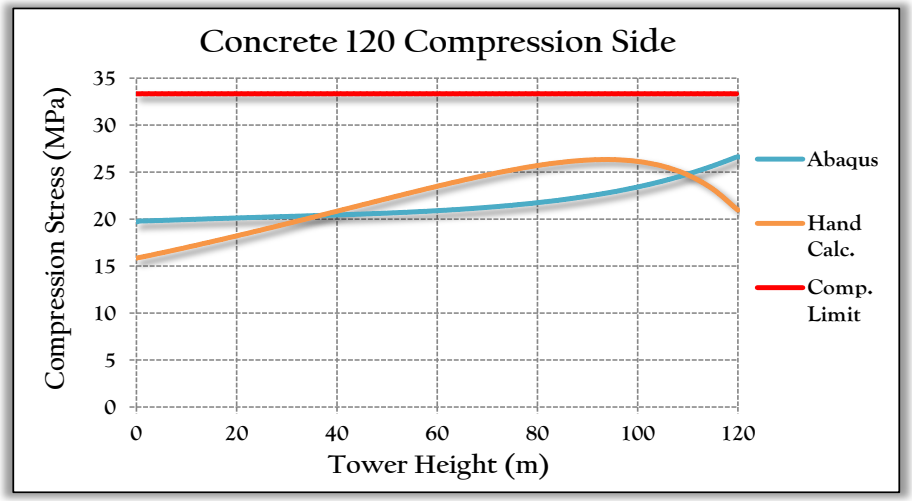

Figure 9.13: Compression-side stress comparisons between Abaqus FEM analyses and hand calculations for concrete towers with heights of 80, 100 and 120m.

As can be seen from Figure 9.12, the hand calculations are somewhat conservative with respect to the tensile stresses. The tensile stresses are the critical stresses in the concrete sections which, if exceeded, will cause the concrete to crack, thereby significantly lowering the stiffness, natural frequency and fatigue performance, as well as increasing the deflection of the towers considerably. As can be seen in Figure 9.13, the prestressing force has not yet reached the point at which crushing of the concrete becomes a problem (closer to the compression limit).

9.3 Prestressing Requirements Results

Table 9.9: Pre-stressing in the design of the towers.

		Per Tendon - 15.2mm EHT Strands					
Tower	**System Designation**	**Nr. Strands**	**MBL Force (kN)**	**Initial PS Force (kN)**	**Design PS Force (kN)**	**Losses**	**Total PS Force in Tower (kN)**
Conc 80	1206	10	2 610	2 088	1 493	17.8%	23 888
Hyb 80	1906	13	3 393	2 714	2 076	12%	33 216
Conc 100	1906	17	4 437	3 550	2 455	20.5%	39 280
Hyb 100	2206	20	5 220	4 176	3 091	14.9	49 456
Conc 120	3106	27	7 047	5 638	3 769	23.1%	60 304
Hyb 120	3106	27	7 047	5 638	4036	17.7%	62 944

It should be noted that PS and MBL refer to Pre-Stressing and the Mimimum Breaking Load of the strand. As can be seen from Table 9.9, the losses in prestressing force in the concrete towers are considerably higher than in the hybrid towers. As mentioned in Section 7.3, this is due to the losses associated with wobble friction acting along the longer lengths of prestressing cable required to span the entire tower height.

The hybrid towers are shown to require more initial prestressing force than the concrete towers, with the exception of the 120m tower, which requires the same. The hybrid towers do however, have fewer losses than the concrete towers, so the prestressing in the hybrid tower is more “effective”. Even so, the hybrid towers will be more expensive with regard to prestressing force, with the exception of the 120m tower. A designer can further optimize the hybrid towers by introducing larger concrete sections. This will reduce the prestressing requirements of the tower at the expense of the extra volume of concrete required to increase the tower sections.

This is rather counter-intuitive, as one would expect the concrete towers to be much more demanding in terms of prestressing force, due to the considerably longer spans. For all the towers the concrete parts of the concrete towers are 40m longer than the concrete parts of the hybrid towers. This is due

to the quicker tapering of the concrete section of the hybrid towers.

Considering the 80m tower for example, the concrete tower diameter tapers from 7.5m to 3m over a length of 80m, whereas the concrete part of the hybrid tower tapers from 7.5m to 4.6m over a distance of 40m. This corresponds to a gradient of 0.056(m/m) vs 0.073(m/m) for the concrete and hybrid towers, respectively. The significance of this is that the concrete tower sections have a greater section diameter and wall thickness than the hybrid towers at an equivalent height.

As has been shown in this section, a FEM analysis can provide essential tools to aid in the design. It is up to the designer to decide to what extent to use the FEM results or the hand calculations or a combination of the two, in order to dimension the tower and foundation. The natural frequency of the system, however, must be verified through the use of a suitable FEM model.

9.4 Cost Comparison Results

The costs used in the comparison were obtained from South African manufacturers and suppliers and are exclusive of labour, professional design and construction fees, due to the material cost comparison nature of this project. The costs used are an average of the 2014 prices obtained from various suppliers/manufacturers and can be seen in Table 9.10.

Table 9.10: Material prices used in the tower cost comparison.

Constituent/Material	**Unit**	**Cost (R)**
Reinforcing Steel Cost	R/ton	15 251
Steel Tower Cost	R/ton	18 912
Tower Concrete Cost	R/m^3	2 007
Foundation Concrete Cost	R/m^3	1 400
Prestressing - Anchors + Couplers	R/tower	33 440
Prestressing - Tendons & Support Clips	R/MN/m	120

The volume or mass of the tower and foundation constituents and their associated costs are shown in the following tables:

Table 9.11: Foundations - Material use and cost.

		Concrete (m^3)	Steel Reinforcing (ton)	Material Cost
Steel	80	606	53.11	R 1 658 717
	100	707	62.85	R 1 948 728
	120	921	82.46	R 2 547 662
Concrete	80	459	38.26	R 1 226 405
	100	622	47.04	R 1 588 619
	120	774	72.81	R 2 194 576
Hybrid	80	598	43.98	R 1 508 259
	100	721	62.89	R 1 968 963
	120	832	71.65	R 2 258 035

Table 9.12: Tower - Material use and cost.

		Tower Steel (ton)	Tower Concrete (m^3)	Pre-stressing (MN)	Length (m)	Pre-stressing Cost	Tower Cost
Steel	80	183.6	-	-	-	-	R 3 471 608
	100	330.6	-	-	-	-	R 6 252 465
	120	685.7	-	-	-	-	R 12 968 527
Concrete	80	-	306	33.41	80	R 354 157	R 968 705
	100	-	457	56.79	100	R 714 963	R 1 632 051
	120	-	608	90.20	120	R 1 332 343	R 2 552 493
Hybrid	80	72.2	147	43.43	80	R 450 372	R 1 661 436
	100	72.2	221	66.82	100	R 835 232	R 1 808 977
	120	72.2	434	90.20	120	R 1 332 343	R 2 236 468

Table 9.13: Total tower and foundation material costs.

		Foundation Cost	Tower Cost	Total Material Cost for Tower and Foundation
Steel	80	R 1 658 717	R 3 471 608	R5 130 326
	100	R 1 948 728	R 6 252 465	R 8 201 193
	120	R 2 547 662	R 12 968 527	R 15 516 189
Concrete	80	R 1 226 405	R 968 705	R 2 195 111
	100	R 1 588 619	R 1 632 051	R 3 220 670
	120	R 2 194 576	R 2 552 493	R 4 747 069
Hybrid	80	R 1 508 259	R 1 661 436	R 3 169 695
	100	R 1 968 963	R 1 808 977	R 3 777 940
	120	R 2 258 035	R 2 236 468	R 4 494 503

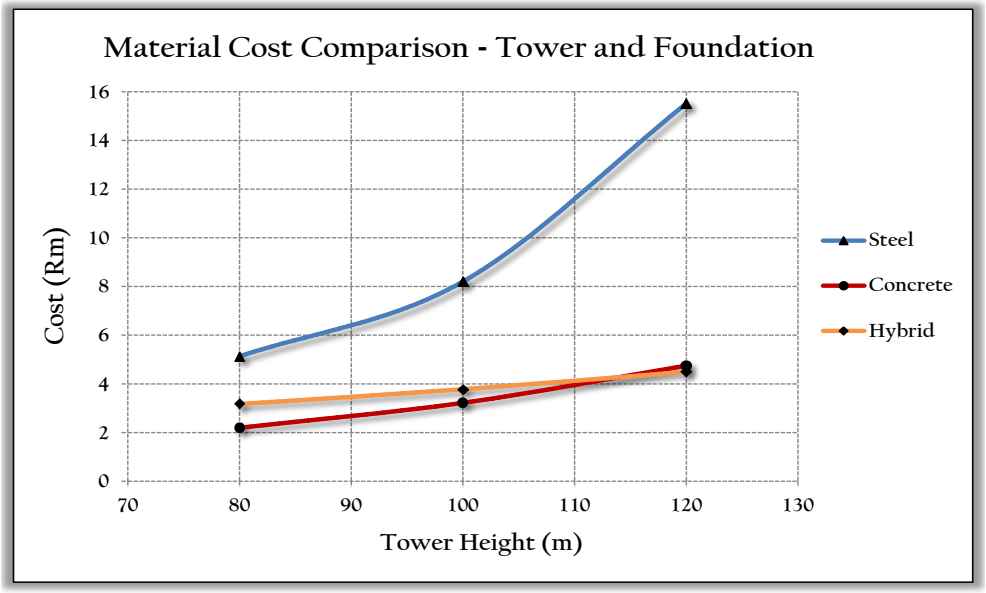

Figure 9.14: Tower material cost comparison for the 9 wind turbine towers and foundations.

As can be seen from Tables 9.10 through 9.13 and Figure 9.14, the concrete and hybrid towers are less material cost-intensive than the steel towers, particularly for the 100 and 120m towers. The trend seems to show that the hybrid towers will become more cost effective than the concrete towers at hub heights greater than 110-115m. The steel towers are shown to be disproportionately material cost intensive at hub heights greater than 100m.

Material costs are not the only costs associated with the production and erection of the tower and foundation. Other costs associated with transport, labour and lifting costs, amongst others, also play a role in determining the cost of a finished product. From the trends in industry since 80m hub heights became the norm, it is clear that the steel towers are more cost-effective at 80m hub heights, as more than 90 percent of the world's 80m turbines rest on steel towers. The other costs must therefore outweigh the material savings seen in Figure 9.14.

Ideally, these costs would have been obtained and a full cost comparison been done, to present the findings similar to those in Figure 9.14. As time and resources have allowed, coupled with the secrecy of the maturing South African wind industry, however, the study had to be limited to a material cost comparison. The material costs presented here are indicative of the concrete and hybrid towers becoming competitive at hub heights of 100m and above.

In light of the material cost comparison, a graph comparing the likely cost of the various towers and foundations was deduced. Note that this graph (Figure 9.15) is a deduction, based on the calculated material costs and serves as more of an illustration of how the costs of concrete and hybrid become more competitive for taller towers. The intersections of the various towers are therefore, not fully accurate and it may be that the steel towers are still more cost-effective for a 100m hub height.

The graph reflects the fact that the unconsidered costs will increase linearly, as a function of the hub height. Particularly, the graph accounts for the fact that the unconsidered costs for the steel towers

increase linearly, not following the exponential curve as shown in Figure 9.14.

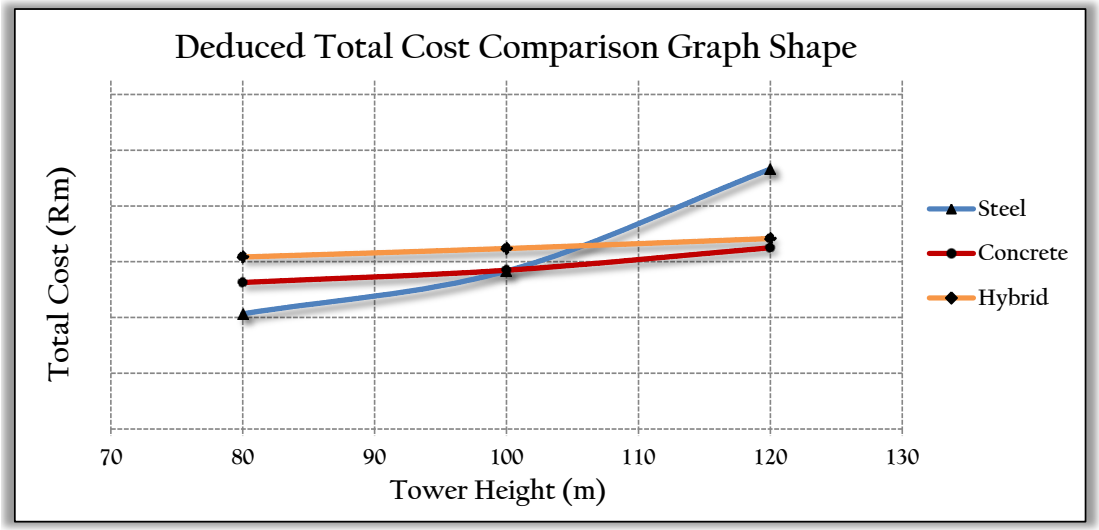

Figure 9.15: Cost comparison deduction for the three designs of wind turbine towers and foundations.

It follows from the material cost comparison that unless the steel tower designs begin to incorporate methods that can overcome the 4.5m base diameter transport limitation, it is likely that the global trend of using steel towers as the default tower in wind turbine support structures will change rapidly. Concrete and hybrid towers have shown to be less material cost-intensive (and therefore leading to reduced total cost) than their steel counterparts at greater hub heights. For wind sites that require hub heights of between 80 and 100m, steel towers will, more than likely, still be the tower of choice, even though the material costs are still higher than for the concrete or hybrid towers.

9.5 Revenue Generation Results

As discussed in sections 2.4 and 4.2, the increase in hub height from 80 to 100 and 120m will result in increased revenue generation. The following is an example of how the revenue would be increased, as a consequence of using taller towers. The data used here is from the Napier WASA mast. This specific site has a mediocre increase-in-wind-speed versus height for South Africa and serves as a good example of how an increased hub height can be beneficial to both investor and power utility. The increased revenue generation of the wind turbines for the tower heights greater than 80m are shown in Tables 9.14 and 9.15, for a Vestas V112 3MW turbine. The wind speed increase is given with reference to the 80m hub height.

Table 9.14: Revenue per tower height and calendar year.

			Hub Height		
			80	**100**	**120**
2011	Average Wind Speed	v (m/s)	8.71	8.97	9.19
	Wind Speed Increase	%	0.00	2.91	5.42
	Energy Generated	MWh	12 865	13 312	13 679
	Capacity Factor		0.500	0.517	0.531
2012	Average Wind Speed	v (m/s)	8.27	8.53	8.74
	Wind Speed Increase	%	0.00	3.18	5.77
	Energy Generated	MWh	12 927	13 384	13 735
	Capacity Factor		0.49	0.507	0.521
2013	Average Wind Speed	v (m/s)	8.91	9.20	9.43
	Wind Speed Increase	%	0.00	3.21	5.84
	Energy Generated	MWh	13 643	14 125	14 496
	Capacity Factor		0.506	0.524	0.538

Table 9.15: Increase in revenue generated due to taller towers.

		Hub Height		
		80	**100**	**120**
2011	Revenue Generated	R 9 520 346	R 9 851 232	R 10 122 336
2012	Revenue Generated	R 9 565 679	R 9 904 123	R 10 164 264
2013	Revenue Generated	R 10 095 688	R 10 452 212	R 10 727 068
Averaged 20 Year Revenue		R 194 544 762	R 201 383 789	R 206 757 795
Percent Revenue Increase		0.00	3.52	6.28

A price per kWh generated of 74c, the current price paid by ESKOM, was used in the revenue generation comparison. The last row uses the averaged 20 year revenue of the 80m towers as a reference. From Tables 9.14 and 9.15, one can see the variation in annual average wind speed over the three years, which further emphasizes the point made in Section 4.2: that there can be substantial average wind speed variation from year to year.

The increase in revenue generated follows the wind speed increase more or less linearly, although it will change depending on how far along the power curve of the wind turbine the annual average wind speed is (see Figure 4.3). The increased revenue means that a cost-increase, in increasing the tower hub height, must remain lower than 3.52 and 6.28 percent of the total project cost for hub heights of 100 and 120m respectively, in order for the height increase to be viable.

The total cost of a tower will tend to follow the material cost of the tower and therefore as the cost of the materials increase, the cost of the tower must also increase. There are other factors that come in to play, such as the transport of the materials and the labour associated with the erection of the

tower, but it is assumed that the non-material costs of the tower will increase at a less significant rate than the cost of materials, for an increase in tower height.

References

Breccolotti M. Ubertini, F. and I. Venanzi (2009). *Natural frequencies of prestressed concrete beams: theoretical prediction and numerical validation*. Tech. rep. Department of Civil and Environmental Engineering, University of Perugia, Italy.

Chapter 10

Conclusion and Recommendations

10.1 Summary

This project conducted literature studies on the global and South African wind power generation industries to gain insight as to the current trends in and to assess the state of, the global and local wind industries. An analysis was done on the local wind resource to determine the potential for the use of taller wind turbine towers in South Africa. Nine towers and foundations, three of each tower type (steel, concrete and concrete-steel hybrid) were designed according to current design methods. Each tower was designed for hub heights of 80, 100 and 120m.

The designs were verified using the *Abaqus* finite element modeling software, with respect to the natural frequency, stresses, deflections and buckling resistance of the towers and foundations. The material costs of the designs were then compared in order to determine the viability of each tower design with respect to the others. The increased revenue, as a consequence of the increase in hub height, was also calculated for each of the 80, 100 and 120m hub heights. This serves as an illustration of how increases in hub height increase the energy generated and consequently, the revenue generated by taller wind turbines. Guidelines to the use of taller wind turbine towers of the three tower designs are proposed to the reader.

10.2 Conclusions

The designs of the wind turbine foundations were highly dependent on the choice of underlying soil parameters. Given the favourable soil conditions used in this project, the design of the foundation for the steel and hybrid towers was governed by the weight of the foundation needed to stabilize the structure against overturning for the case of water table at ground-surface level. The foundation designs of the concrete towers were governed by a combination of bearing capacity and foundation weight required to stabilize against overturning, also for the case of water table at ground-surface level.

The design of the reinforcing in the foundation was always far below the minimum required amount for the section, as stipulated in Eurocode 2. The amount of reinforcing steel in the foundation was determined by this minimum requirement, although this may not be the case when designing for IEC wind class II or I. None of the foundations are subject to punching shear failure, even without punching shear reinforcement, although the concrete towers were just under the limit of requiring punching shear reinforcement. Foundations for concrete towers taller than 120m will not be able to provide sufficient shear resistance without shear reinforcing, while the steel and hybrid tower foundations may still have adequate shear resistance.

The amount of prestressing present in the concrete sections of the towers had an effect on the size of the foundations. Reduced prestressing force in the concrete and hybrid towers meant that thicker tower shells were required. Thicker tower shells result in heavier towers which stabilize the support system against overturning moments. Less foundation weight is therefore required for stabilization purposes, which results in less concrete use in the foundations. It should be noted that this increase in weight may cause bearing capacity failure in weaker soils.

Considering the tower designs, the steel tower design was governed by the natural-frequency stiffness requirements of the tower, primarily, to ensure that the natural frequency lies within the acceptable limits as determined by the choice of turbine, but also to limit deflections. However, it may be that the fatigue life of the steel could govern the 80 and 100m towers. The design of both the concrete and hybrid towers was made difficult by the lack of tensile resistance of the concrete. Both designs, therefore, employed prestressing as a means of bypassing this problem.

The tensile stresses in the sections thus governed the design of the concrete sections, although buckling may become an important design factor when designing towers taller than 120m. There is potential for the optimization of the towers by increasing the concrete section thickness to decrease the prestressing requirements, as the prestressing costs represent a large proportion (between 35 and 50 percent and 25 and 60 percent for the concrete and hybrid towers, respectively) of the material costs.

According to the results from this project, it can be seen that the material requirements associated with the foundation of concrete and hybrid wind turbine towers are lower than those of the steel towers for the given design assumptions. Consequently and additionally, the material cost of the studied steel towers and foundations in a South African context, are higher than their concrete and hybrid counterparts, particularly for hub heights in excess of 100m. The increased revenue, due to increases in hub height from 80 to 100 and 120m for a Vestas V112-3MW turbine, was shown to be in the vicinity of 3.52 and 6.28 percent respectively, with an average capacity factor increase of the same magnitudes. This indicated that there is potential financial and power-generation reward in using taller towers in South Africa.

10.3 Recommendations

The fatigue design of the steel towers for load repetitions of the order of 10^6, may be one of the governing factors in determining the tower shell thickness. The shell thickness of the towers plays a significant role in the cost of the steel towers. Due to the dominance of case-specific wind turbine loads, which are difficult to obtain for particular turbines due to commercial secrecy, accurate consideration without actual fatigue data is complicated. This is therefore an important topic that needs to be investigated.

The wall thickness of the concrete tower and tower sections can be optimized by using higher grades of concrete. The trade-off between the increased concrete cost and the reduction in prestressing cost would be of interest to investigate.

A full cost analysis of increases in hub height may also be of particular interest, in conjunction with the work done in this project, to determine a threshold for which each tower becomes viable and subsequently not viable. In addition to this, further investigations into the sensitivity of the following aspects on cost would be beneficial:

- Soil type and associated parameters;
- Further geometric and material optimization;
- Turbine type and associated weight, rotation speed and nameplate capacity;
- Tower dimension and shell thicknesses optimization for reduced prestressing requirements;
- Different IEC wind classes.

Most importantly, the fact that the steel towers are subject to the 4.5m diameter transport limit severely limits the use of steel in taller towers. A change in the manufacture and/or design and erection of the tower that can alleviate this problem would significantly reduce the cost of the steel towers and therefore the levelized cost of energy for wind energy generation.

An aspect of wind farms that has been prevalent in the news of late is the consideration of the costs of operation and maintenance plans throughout the lifetime of a wind energy project. An investigation into the effect of different options and periods of operation and maintenance plans on the availability and capacity factors of wind farms would help potential wind farm developers to more accurately predict said factors. This would reduce the risk on investors and help power utilities to better plan future power procurement projects.

A mention of the sustainability of the wind energy industry in South Africa was made in this project. This is an important matter, particularly with the current low price of wind energy in South Africa. The degree of localization of the constituents of the wind turbines and support structures will have a considerable effect on whether the wind energy industry becomes sustainable in South Africa. Research should therefore be carried out with regard to the sustainability of the wind energy industry in South Africa and to assess whether the local content requirements set out in the REIPPP are effective in promoting this sustainability in South Africa

Appendices

Appendix A

General Data

A.1 Wind Turbine Material Information

This section deals with the data that was used in the design of the various towers and supporting structures. The information is shown in the following tables:

Material Information - Steel			
Tower Steel - S355JR			
Description	**Symbol**	**Value**	**Unit**
Design Young's Modulus	E_d	200	GPa
Design Yield Strength	σ_{yd}	301.5	MPa
Poisson's Ratio	ν	0.3	
Density	ρ_s	7800	$\frac{kg}{m^3}$
Reinforcing Steel - Deformed High Yield Steel Bars			
Description	**Symbol**	**Value**	**Unit**
Design Young's Modulus	E_d	200	GPa
Yield Strength	σ_y	450	MPa
Poisson's Ratio	ν	0.3	
Density	ρ_s	7800	$\frac{kg}{m^3}$

Material Information - Concrete			
Concrete in Towers - C50/60			
Description	**Symbol**	**Value**	**Unit**
Design Young's Modulus	E_d	30.83	GPa
Design Compression Strength	σ_{yd}	40	MPa
Design Mean Tensile Strength	σ_{yd}	2.73	MPa
Poisson's Ratio	ν	0.2	
Density	ρ_s	2400	$\frac{kg}{m^3}$
Unit Weight	$\gamma_{concrete}$	23.5	$\frac{kN}{m^3}$
Concrete in Foundations - C30/37			
Description	**Symbol**	**Value**	**Unit**
Design Young's Modulus	E_d	26.67	GPa
Design Compression Strength	σ_{yd}	24.67	MPa
Design Mean Tensile Strength	σ_{yd}	1.93	MPa
Poisson's Ratio	ν	0.2	
Density	ρ_s	2400	$\frac{kg}{m^3}$
Unit Weight	$\gamma_{concrete}$	23.5	$\frac{kN}{m^3}$

The properties of the concrete used in this project were obtained from a publication by The Concrete Centre in the UK, "Properties of Concrete for use in Eurocode 2" (The Concrete Centre, 2008).

Appendix B

Tower Forces and Moments

B.1 Wind Loads on Blades and Nacelle

Wind Force per Feathered Blade				
Distance Along Blade	**Blade Thickness**	**Blade Chord Length**	**Force Combination Resultant x**	**Force Combination Resultant y**
(m)	**(m)**	**(m)**	**F_x;(kN)**	**F_y;(kN)**
0	2.55	2.42		
1	1.80	2.48	2.54	0.42
1	1.50	2.54	2.04	0.43
2	1.35	2.62	1.83	0.44
3	1.10	2.87	4.99	1.41
4	1.00	3.04	3.06	1.01
5	0.90	3.21	2.92	1.07
6	0.80	3.37	2.78	1.13
7	0.70	3.51	2.64	1.18
8	0.60	3.63	2.49	1.23
9	0.55	3.73	2.38	1.26
10	0.50	3.79	2.31	1.29
12	0.43	3.85	4.43	2.62
14	0.38	3.79	4.19	2.62
16	0.35	3.65	3.96	2.55
18	0.32	3.43	3.73	2.43
20	0.30	3.16	3.46	2.26
25	0.25	2.46	7.46	4.82
30	0.20	1.92	5.94	3.75
35	0.17	1.66	4.89	3.07
40	0.14	1.59	4.29	2.79
45	0.11	1.41	3.79	2.57
50	0.09	0.87	2.93	1.95
55	0.07	0.00	1.50	0.75
		Total per Blade	**80.54**	**43.08**

Nacelle and Blades Wind Load								
	Force on Blades		Force on Nacelle		Total		Foundation Moments	
Tower Height	F_x	F_y	F_x	F_y	F_x	F_y	M_x	M_y
(m)	(kN)	(kN)	(kN)	(kN)	(kN)	(kN)	(kNm)	(kNm)
80	241.6	64.6	30.0	9.5	271.6	74.1	22 270	6 079
100	241.6	64.6	30.0	9.5	271.6	74.1	27 702	7 562
120	241.6	64.6	30.0	9.5	271.6	74.1	33 134	9 045

The wind force per blade was calculated using the hub-height wind pressure, $q_p(z)$, of 2.29 kPa. The IEC 61400 prescribes a yaw misalignment of 15 degrees on wind direction for the ultimate limit state. The force combination resultants in the x and y direction were calculated as follows, where $A_{blade,x}$ and $A_{blade,y}$ are the cross-sectional areas, with reference parallel to the x and y directions, respectively:

$$F_x = 0.85 \cdot q_p(z) A_{blade,x} + 0.15 \cdot q_p(z) A_{blade,y} \tag{B.1}$$

$$F_y = 0.15 \cdot q_p(z) A_{blade,y} \tag{B.2}$$

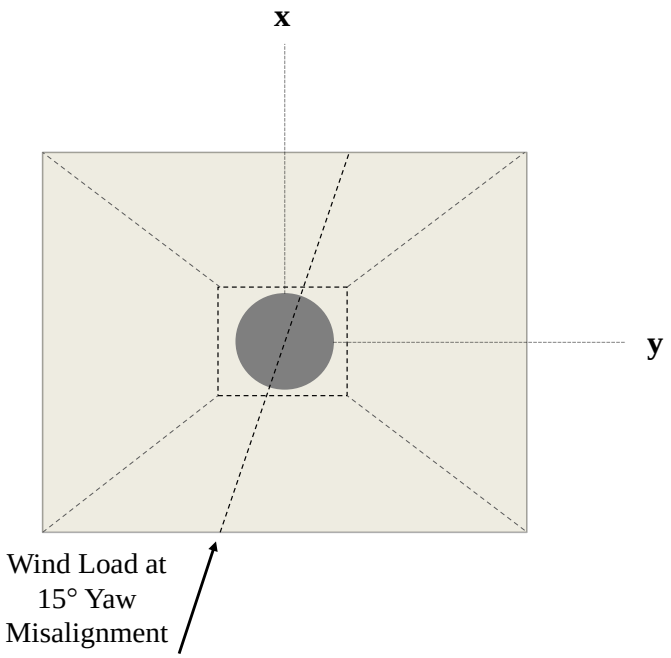

The "Blades" column in the table above contains the total wind force from the previous table, multiplied by the respective number of blades exposed to the wind force, i.e. 3 for the x direction and only 1.5 for the y direction. The moments are simply the forces multiplied by the tower height, plus half of the nacelle height. The notations M_x and M_y denote bending causing stress in the x and y direction, respectively.

B.2 Wind Loads on Towers

Steel 80m Tower Wind Loads							
Tower Height H	**Tower Diameter** D_{tower}	**Wind Pressure** $q_p(z)$	**Height of Action** H_i	**Σ Force** F_{xi}	**Σ Force** F_{yi}	**Moments** M_{xi}	**Moments** M_{yi}
(m)	**(m)**	**(kPa)**	**(m)**	**(kN)**	**(kN)**	**(kNm)**	**(kNm)**
80	3.00	2.29					
75	3.09	2.26	77.5	25.9	31.11	2 010.73	2 410.93
70	3.19	2.22	72.5	26.4	31.60	1 910.62	2 290.89
65	3.28	2.19	67.5	26.7	32.03	1 803.35	2 162.27
60	3.38	2.15	62.5	27.0	32.41	1 689.29	2 025.51
55	3.47	2.11	57.5	27.3	32.71	1 568.84	1 881.08
50	3.56	2.06	52.5	27.5	32.94	1 442.45	1 729.55
45	3.66	2.02	47.5	27.6	33.08	1 310.64	1 571.50
40	3.75	1.96	42.5	27.6	33.12	1 173.99	1 407.65
35	3.84	1.91	37.5	27.6	33.03	1 033.16	1 238.79
30	3.94	1.84	32.5	27.4	32.80	888.97	1 065.90
25	4.03	1.77	27.5	27.0	32.37	742.38	890.14
20	4.13	1.69	22.5	26.4	31.69	594.63	712.99
15	4.22	1.58	17.5	25.6	30.65	447.36	536.40
10	4.31	1.45	12.5	24.2	29.05	302.89	363.17
5	4.41	1.24	7.5	22.0	26.36	164.90	197.72
0	4.50	1.24	2.5	20.8	24.88	51.88	62.20
			Total	**416.9**	**499.85**	**17 136.08**	**20 246.69**

Concrete 80m Tower Wind Loads							
Tower Height H	**Tower Diameter** D_{tower}	**Wind Pressure** $q_p(z)$	**Height of Action** H_i	**Σ Force** F_{xi}	**Σ Force** F_{yi}	**Moments** M_{xi}	**Moments** M_{yi}
(m)	**(m)**	**(kPa)**	**(m)**	**(kN)**	**(kN)**	**(kNm)**	**(kNm)**
80	3.00	2.29					
75	3.28	2.26	77.5	26.7	32.07	2 072.60	2 485.11
70	3.56	2.22	72.5	28.7	34.43	2 081.72	2 496.04
65	3.84	2.19	67.5	30.6	36.68	2 064.70	2 475.64
60	4.13	2.15	62.5	32.4	38.80	2 022.39	2 424.90
55	4.41	2.11	57.5	34.0	40.78	1 955.67	2 344.91
50	4.69	2.06	52.5	35.5	42.61	1 865.57	2 236.88
45	4.97	2.02	47.5	36.9	44.26	1 753.20	2 102.14
40	5.25	1.96	42.5	38.1	45.70	1 619.81	1 942.20
35	5.53	1.91	37.5	39.1	46.90	1 466.83	1 758.78
30	5.81	1.84	32.5	39.9	47.81	1 295.96	1 553.90
25	6.09	1.77	27.5	40.3	48.36	1 109.20	1 329.97
20	6.38	1.69	22.5	40.4	48.44	909.04	1 089.97
15	6.66	1.58	17.5	39.9	47.87	698.69	837.75
10	6.94	1.45	12.5	38.6	46.29	482.63	578.68
5	7.22	1.24	7.5	35.7	42.80	267.74	321.03
0	7.50	1.24	2.5	34.3	41.12	85.73	102.80
			Total	**571.2**	**684.92**	**21 751.49**	**26 080.70**

Hybrid 80m Tower Wind Loads							
Tower Height H	**Tower Diameter** D_{tower}	**Wind Pressure** $q_p(z)$	**Height of Action** H_i	**Σ Force** F_{xi}	**Σ Force** F_{yi}	**Moments** M_{xi}	**Moments** M_{yi}
(m)	**(m)**	**(kPa)**	**(m)**	**(kN)**	**(kN)**	**(kNm)**	**(kNm)**
80	3.00	2.29					
75	3.16	2.26	77.5	26.2	31.46	2 033.41	2 438.13
70	3.33	2.22	72.5	27.2	32.64	1 973.35	2 366.11
65	3.49	2.19	67.5	28.1	33.74	1 899.18	2 277.17
60	3.65	2.15	62.5	29.0	34.75	1 811.42	2 171.95
55	3.81	2.11	57.5	29.8	35.67	1 710.68	2 051.16
50	3.98	2.06	52.5	30.4	36.49	1 597.60	1 915.57
45	4.14	2.02	47.5	31.0	37.18	1 472.91	1 766.07
40	4.60	1.96	42.5	31.5	37.73	1 337.45	1 603.65
35	4.96	1.91	37.5	34.7	41.60	1 301.02	1 559.96
30	5.33	1.84	32.5	36.2	43.36	1 175.29	1 409.21
25	5.69	1.77	27.5	37.3	44.73	1 025.94	1 230.13
20	6.05	1.69	22.5	38.0	45.60	855.73	1 026.04
15	6.41	1.58	17.5	38.2	45.78	668.20	801.19
10	6.78	1.45	12.5	37.5	44.91	468.20	561.39
5	7.14	1.24	7.5	35.1	42.07	263.13	315.50
0	7.50	1.24	2.5	34.1	40.89	85.26	102.23
			Total	**524.3**	**628.60**	**19 678.78**	**23 595.46**

.

Steel 100m Tower Wind Loads							
Tower Height H	**Tower Diameter** D_{tower}	**Wind Pressure** $q_p(z)$	**Height of Action** H_i	**Σ Force** F_{xi}	**Σ Force** F_{yi}	**Moments** M_{xi}	**Moments** M_{yi}
(m)	**(m)**	**(kPa)**	**(m)**	**(kN)**	**(kN)**	**(kNm)**	**(kNm)**
100	3.00	2.29					
95	3.08	2.26	97.5	25.9	31.1	2 525.50	3 028.15
90	3.15	2.24	92.5	26.2	31.5	2 426.86	2 909.88
85	3.23	2.21	87.5	26.5	31.8	2 322.41	2 784.64
80	3.30	2.18	82.5	26.8	32.2	2 212.38	2 652.71
75	3.38	2.15	77.5	27.1	32.4	2 097.01	2 514.38
70	3.45	2.12	72.5	27.3	32.7	1 976.56	2 369.96
65	3.53	2.08	67.5	27.4	32.9	1 851.33	2 219.80
60	3.60	2.05	62.5	27.5	33.0	1 721.62	2 064.28
55	3.68	2.01	57.5	27.6	33.1	1 587.80	1 903.83
50	3.75	1.96	52.5	27.6	33.1	1 450.26	1 738.91
45	3.83	1.92	47.5	27.6	33.1	1 309.44	1 570.06
40	3.90	1.87	42.5	27.4	32.9	1 165.85	1 397.89
35	3.98	1.82	37.5	27.2	32.6	1 020.10	1 223.13
30	4.05	1.76	32.5	26.9	32.2	872.89	1 046.63
25	4.13	1.69	27.5	26.4	31.6	725.11	869.43
20	4.20	1.61	22.5	25.7	30.8	577.86	692.87
15	4.28	1.51	17.5	24.7	29.6	432.63	518.74
10	4.35	1.38	12.5	23.3	28.0	291.55	349.58
5	4.43	1.18	7.5	21.1	25.3	158.01	189.46
0	4.50	1.18	2.5	19.8	23.7	49.49	59.35
			Total	**520.1**	**623.6**	**26 774.7**	**32 103.7**

.

Concrete 100m Tower Wind Loads							
Tower Height H	**Tower Diameter** D_{tower}	**Wind Pressure** $q_p(z)$	**Height of Action** H_i	**Σ Force** F_{xi}	**Σ Force** F_{yi}	**Moments** M_{xi}	**Moments** M_{yi}
(m)	**(m)**	**(kPa)**	**(m)**	**(kN)**	**(kN)**	**(kNm)**	**(kNm)**
100	3.00	2.29					
95	3.23	2.26	97.5	26.5	31.8	2 587.86	3 102.92
90	3.45	2.24	92.5	28.1	33.7	2 602.29	3 120.23
85	3.68	2.21	87.5	29.7	35.6	2 595.64	3 112.25
80	3.90	2.18	82.5	31.1	37.3	2 568.39	3 079.58
75	4.13	2.15	77.5	32.5	39.0	2 521.12	3 022.90
70	4.35	2.12	72.5	33.9	40.6	2 454.41	2 942.91
65	4.58	2.08	67.5	35.1	42.1	2 368.90	2 840.39
60	4.80	2.05	62.5	36.2	43.5	2 265.29	2 716.16
55	5.03	2.01	57.5	37.3	44.7	2 144.35	2 571.15
50	5.25	1.96	52.5	38.2	45.8	2 006.92	2 406.36
45	5.48	1.92	47.5	39.0	46.8	1 853.96	2 222.95
40	5.70	1.87	42.5	39.7	47.6	1 686.52	2 022.19
35	5.93	1.82	37.5	40.2	48.1	1 505.86	1 805.57
30	6.15	1.76	32.5	40.4	48.5	1 313.42	1 574.83
25	6.38	1.69	27.5	40.4	48.4	1 110.95	1 332.06
20	6.60	1.61	22.5	40.0	48.0	900.63	1 079.88
15	6.83	1.51	17.5	39.2	47.0	685.32	821.72
10	7.05	1.38	12.5	37.5	45.0	469.01	562.36
5	7.28	1.18	7.5	34.4	41.2	257.95	309.30
0	7.50	1.18	2.5	32.8	39.3	81.94	98.25
			Total	**712.3**	**854.0**	**33 980.75**	**40 743.96**

.

Hybrid 100m Tower Wind Loads							
Tower Height H	**Tower Diameter** D_{tower}	**Wind Pressure** $q_p(z)$	**Height of Action** H_i	**Σ Force** F_{xi}	**Σ Force** F_{yi}	**Moments** M_{xi}	**Moments** M_{yi}
(m)	**(m)**	**(kPa)**	**(m)**	**(kN)**	**(kN)**	**(kNm)**	**(kNm)**
100	3.00	2.29					
95	3.16	2.26	97.5	26.3	31.5	2 561.87	3 071.76
90	3.33	2.24	92.5	27.3	32.8	2 529.20	3 032.58
85	3.49	2.21	87.5	28.4	34.0	2 481.79	2 975.74
80	3.65	2.18	82.5	29.3	35.2	2 420.05	2 901.72
75	3.81	2.15	77.5	30.3	36.3	2 344.41	2 811.02
70	3.98	2.12	72.5	31.1	37.3	2 255.31	2 704.18
65	4.14	2.08	67.5	31.9	38.2	2 153.25	2 581.81
60	4.60	2.05	62.5	32.6	39.1	2 038.77	2 444.54
55	4.84	2.01	57.5	35.8	43.0	2 060.69	2 470.83
50	5.08	1.96	52.5	36.9	44.3	1 938.56	2 324.40
45	5.33	1.92	47.5	37.9	45.4	1 799.22	2 157.32
40	5.57	1.87	42.5	38.7	46.4	1 643.76	1 970.92
35	5.81	1.82	37.5	39.3	47.1	1 473.48	1 766.74
30	6.05	1.76	32.5	39.7	47.6	1 289.85	1 546.57
25	6.29	1.69	27.5	39.8	47.7	1 094.69	1 312.56
20	6.53	1.61	22.5	39.6	47.4	890.22	1 067.40
15	6.78	1.51	17.5	38.8	46.5	679.36	814.58
10	7.02	1.38	12.5	37.3	44.7	466.20	558.98
5	7.26	1.18	7.5	34.3	41.1	257.05	308.22
0	7.50	1.18	2.5	32.7	39.3	81.84	98.13
			Total	**688.0**	**824.9**	**32 459.57**	**38 920.01**

.

Steel 120m Tower Wind Loads							
Tower Height H	**Tower Diameter** D_{tower}	**Wind Pressure** $q_p(z)$	**Height of Action** H_i	**Σ Force** F_{xi}	**Σ Force** F_{yi}	**Moments** M_{xi}	**Moments** M_{yi}
(m)	**(m)**	**(kPa)**	**(m)**	**(kN)**	**(kN)**	**(kNm)**	**(kNm)**
120	3	2.29					
115	3.1	2.27	117.5	26.0	31.2	3 059.00	3 667.83
110	3.2	2.24	112.5	26.6	31.9	2 996.04	3 592.35
105	3.3	2.22	107.5	27.2	32.6	2 924.36	3 506.40
100	3.4	2.20	102.5	27.7	33.3	2 844.17	3 410.25
95	3.5	2.17	97.5	28.3	33.9	2 755.69	3 304.15
90	3.6	2.15	92.5	28.7	34.5	2 659.16	3 188.41
85	3.7	2.12	87.5	29.2	35.0	2 554.83	3 063.32
80	3.8	2.09	82.5	29.6	35.5	2 442.98	2 929.21
75	3.9	2.06	77.5	30.0	36.0	2 323.91	2 786.44
70	4	2.03	72.5	30.3	36.4	2 197.93	2 635.39
65	4.1	2.00	67.5	30.6	36.7	2 065.40	2 476.48
60	4.2	1.96	62.5	30.8	37.0	1 926.69	2 310.16
55	4.3	1.93	57.5	31.0	37.2	1 782.23	2 136.94
50	4.4	1.89	52.5	31.1	37.3	1 632.48	1 957.40
45	4.5	1.84	47.5	31.1	37.3	1 477.99	1 772.16
40	4.5	1.80	42.5	30.7	36.8	1 304.87	1 564.58
35	4.5	1.75	37.5	29.9	35.8	1 119.99	1 342.90
30	4.5	1.69	32.5	28.9	34.7	940.46	1 127.64
25	4.5	1.62	27.5	27.9	33.4	766.90	919.54
20	4.5	1.54	22.5	26.7	32.0	600.15	719.60
15	4.5	1.45	17.5	25.2	30.2	441.37	529.21
10	4.5	1.32	12.5	23.4	28.0	292.26	350.43
5	4.5	1.14	7.5	20.8	24.9	155.69	186.68
0	4.5	1.14	2.5	19.2	23.0	47.95	57.49
			Total	**671.0**	**804.5**	**41 312.51**	**49 534.96**

.

Concrete 120m Tower Wind Loads							
Tower Height H	**Tower Diameter** D_{tower}	**Wind Pressure** $q_p(z)$	**Height of Action** H_i	**Σ Force** F_{xi}	**Σ Force** F_{yi}	**Moments** M_{xi}	**Moments** M_{yi}
(m)	**(m)**	**(kPa)**	**(m)**	**(kN)**	**(kN)**	**(kNm)**	**(kNm)**
120	3.00	2.29					
115	3.19	2.27	117.5	26.4	31.7	3 102.87	3 720.44
110	3.38	2.24	112.5	27.7	33.3	3 120.88	3 742.03
105	3.56	2.22	107.5	29.0	34.8	3 121.19	3 742.41
100	3.75	2.20	102.5	30.3	36.3	3 104.18	3 722.00
95	3.94	2.17	97.5	31.5	37.8	3 070.19	3 681.26
90	4.13	2.15	92.5	32.6	39.1	3 019.64	3 620.64
85	4.31	2.12	87.5	33.7	40.5	2 952.93	3 540.65
80	4.50	2.09	82.5	34.8	41.7	2 870.51	3 441.82
75	4.69	2.06	77.5	35.8	42.9	2 772.85	3 324.73
70	4.88	2.03	72.5	36.7	44.0	2 660.47	3 189.99
65	5.06	2.00	67.5	37.5	45.0	2 533.94	3 038.27
60	5.25	1.96	62.5	38.3	45.9	2 393.85	2 870.30
55	5.44	1.93	57.5	39.0	46.7	2 240.89	2 686.89
50	5.63	1.89	52.5	39.5	47.4	2 075.79	2 488.93
45	5.81	1.84	47.5	40.0	47.9	1 899.39	2 277.42
40	6.00	1.80	42.5	40.3	48.3	1 712.64	2 053.51
35	6.19	1.75	37.5	40.4	48.5	1 516.65	1 818.51
30	6.38	1.69	32.5	40.4	48.4	1 312.72	1 573.99
25	6.56	1.62	27.5	40.1	48.1	1 102.42	1 321.83
20	6.75	1.54	22.5	39.5	47.3	887.73	1 064.41
15	6.94	1.45	17.5	38.4	46.0	671.25	804.85
10	7.13	1.32	12.5	36.5	43.8	456.66	547.55
5	7.31	1.14	7.5	33.3	39.9	249.76	299.47
0	7.50	1.14	2.5	31.6	37.8	78.92	94.62
			Total	**853.4**	**1023.2**	**48 928.31**	**58 666.55**

.

Hybrid 120m Tower Wind Loads							
Tower Height H	**Tower Diameter** D_{tower}	**Wind Pressure** $q_p(z)$	**Height of Action** H_i	**Σ Force** F_{xi}	**Σ Force** F_{yi}	**Moments** M_{xi}	**Moments** M_{yi}
(m)	**(m)**	**(kPa)**	**(m)**	**(kN)**	**(kN)**	**(kNm)**	**(kNm)**
120	3.00	2.29					
115	3.16	2.27	117.5	26.3	31.5	3 090.34	3 705.41
110	3.33	2.24	112.5	27.4	32.9	3 085.21	3 699.26
105	3.49	2.22	107.5	28.5	34.2	3 064.96	3 674.98
100	3.65	2.20	102.5	29.6	35.4	3 029.89	3 632.93
95	3.81	2.17	97.5	30.6	36.7	2 980.34	3 573.51
90	3.98	2.15	92.5	31.5	37.8	2 916.64	3 497.15
85	4.14	2.12	87.5	32.4	38.9	2 839.19	3 404.27
80	4.60	2.09	82.5	33.3	39.9	2 748.36	3 295.36
75	4.78	2.06	77.5	36.5	43.8	2 831.32	3 394.84
70	4.96	2.03	72.5	37.4	44.8	2 710.90	3 250.45
65	5.14	2.00	67.5	38.2	45.8	2 576.97	3 089.86
60	5.33	1.96	62.5	38.9	46.6	2 430.12	2 913.79
55	5.51	1.93	57.5	39.5	47.4	2 271.03	2 723.03
50	5.69	1.89	52.5	40.0	48.0	2 100.41	2 518.46
45	5.87	1.84	47.5	40.4	48.4	1 919.11	2 301.07
40	6.05	1.80	42.5	40.7	48.8	1 728.05	2 071.98
35	6.23	1.75	37.5	40.8	48.9	1 528.32	1 832.50
30	6.41	1.69	32.5	40.7	48.7	1 321.21	1 584.17
25	6.59	1.62	27.5	40.3	48.3	1 108.28	1 328.86
20	6.78	1.54	22.5	39.6	47.5	891.48	1 068.91
15	6.96	1.45	17.5	38.5	46.1	673.39	807.42
10	7.14	1.32	12.5	36.6	43.9	457.68	548.77
5	7.32	1.14	7.5	33.3	40.0	250.08	299.86
0	7.50	1.14	2.5	31.6	37.9	78.95	94.66
			Total	**852.6**	**1022.2**	**48 632.22**	**58 311.52**

B.3 Total Forces

The total forces acting on the tower are shown in the following tables. These values include the secondary moments caused by the tower eccentricity ($P - \Delta$ effect), as well as partial load factors.

Steel 80m Final Tower Force and Stress Summary

Height (m)	Tower Diameter (m)	Shell Thickness (m)	Section Area (m^2)	Moment of Inertia (m^4)	Combined Moment (kNm)	Own Weight Stress (MPa)	Bending Stress (MPa)	Stress (T Side) (MPa)	Stress (C Side) (MPa)
80	3.00	0.015	0.14	0.157	563	14.88	5.39	9.48	20.27
75	3.09	0.016	0.16	0.185	4 993	13.86	41.68	-27.82	55.54
70	3.19	0.017	0.17	0.217	9 312	13.03	68.27	-55.25	81.30
65	3.28	0.019	0.19	0.253	13 469	12.34	87.28	-74.94	99.62
60	3.38	0.020	0.21	0.293	17 451	11.77	100.52	-88.75	112.29
55	3.47	0.021	0.23	0.337	21 250	11.30	109.36	-98.06	120.66
50	3.56	0.022	0.25	0.386	24 855	10.91	114.82	-103.91	125.74
45	3.66	0.023	0.27	0.439	28 260	10.59	117.69	-107.10	128.28
40	3.75	0.025	0.29	0.498	31 457	10.32	118.56	-108.23	128.88
35	3.84	0.026	0.31	0.561	34 440	10.11	117.89	-107.78	127.99
30	3.94	0.027	0.33	0.631	37 205	9.93	116.05	-106.11	125.98
25	4.03	0.028	0.35	0.707	39 749	9.79	113.32	-103.53	123.11
20	4.13	0.029	0.38	0.789	42 071	9.68	109.94	-100.26	119.62
15	4.22	0.030	0.40	0.878	44 171	9.60	106.09	-96.49	115.69
10	4.31	0.032	0.43	0.974	46 057	9.54	101.92	-92.38	111.46
5	4.41	0.033	0.45	1.078	47 737	9.50	97.57	-88.06	107.07
0	4.50	0.034	0.48	1.189	49 251	9.48	93.17	-83.69	102.65

.

.

Concrete 80m Final Tower Force and Stress Summary

Height (m)	Tower Diameter (m)	Shell Thickness (m)	Section Area (m^2)	Moment of Inertia (m^4)	Combined Moment (kNm)	Own Weight Stress (MPa)	Bending Stress (MPa)	Pre-stressing Stress (MPa)	Stress (T Side) (MPa)	Stress (C Side) (MPa)
80	3.00	0.200	1.76	1.733	563	1.189	0.487	9.04	9.744	10.72
75	3.28	0.205	1.98	2.351	5 024	1.208	3.506	8.03	5.728	12.74
70	3.56	0.209	2.21	3.112	9 541	1.234	5.461	7.19	2.960	13.88
65	3.84	0.214	2.44	4.034	14 034	1.266	6.687	6.49	1.065	14.44
60	4.13	0.219	2.68	5.136	18 463	1.303	7.414	5.89	-0.221	14.61
55	4.41	0.223	2.94	6.440	22 790	1.344	7.797	5.38	-1.074	14.52
50	4.69	0.228	3.20	7.965	26 978	1.387	7.938	4.94	-1.614	14.26
45	4.97	0.233	3.46	9.735	30 995	1.432	7.910	4.55	-1.926	13.89
40	5.25	0.238	3.74	11.772	34 807	1.480	7.761	4.21	-2.069	13.45
35	5.53	0.242	4.02	14.101	38 385	1.528	7.528	3.91	-2.088	12.97
30	5.81	0.247	4.32	16.747	41 702	1.578	7.237	3.64	-2.014	12.46
25	6.09	0.252	4.62	19.735	44 735	1.629	6.907	3.41	-1.872	11.94
20	6.38	0.256	4.93	23.093	47 463	1.681	6.551	3.19	-1.680	11.42
15	6.66	0.261	5.24	26.848	49 871	1.734	6.182	3.00	-1.452	10.91
10	6.94	0.266	5.57	31.028	51 953	1.787	5.808	2.82	-1.201	10.41
5	7.22	0.270	5.90	35.665	53 711	1.840	5.436	2.66	-0.936	9.94
0	7.50	0.275	6.24	40.788	55 196	1.894	5.075	2.51	-0.667	9.48

Hybrid 80m Final Tower Force and Stress Summary

	Height (m)	Tower Diameter (m)	Shell Thickness (m)	Section Area (m^2)	Moment of Inertia (m^4)	Combined Moment (kNm)	Own Weight Stress (MPa)	Bending Stress (MPa)	Pre-stressing Stress (MPa)	Stress (T Side) (MPa)	Stress (C Side) (MPa)
Steel	80	3	0.015	0.14	0.157	563	14.88	5.39	0	9.48	20.27
	75	3.1625	0.016	0.16	0.199	4 985	13.51	39.66	0	-26.15	53.17
	70	3.325	0.018	0.18	0.249	9 357	12.42	62.56	0	-50.14	74.98
	65	3.4875	0.019	0.20	0.307	13 617	11.54	77.26	0	-65.72	88.80
	60	3.65	0.020	0.23	0.376	17 743	10.83	86.19	0	-75.36	97.02
	55	3.8125	0.021	0.25	0.455	21 715	10.25	91.02	0	-80.77	101.28
	50	3.975	0.023	0.28	0.546	25 514	9.78	92.94	0	-83.16	102.72
	45	4.1375	0.024	0.31	0.649	29 123	9.39	92.79	0	-83.39	102.18
	40	4.30	0.025	0.34	0.767	32 525	9.08	91.17	0	-82.08	100.25
Concrete	40	4.60	0.20	2.76	6.704	32 525	1.10	11.16	7.79	-2.26	20.06
	35	4.96	0.20	2.99	8.499	35 872	1.17	10.47	7.18	-2.12	18.83
	30	5.33	0.20	3.22	10.588	39 028	1.24	9.81	6.66	-1.91	17.72
	25	5.69	0.20	3.45	12.995	41 957	1.31	9.18	6.21	-1.65	16.71
	20	6.05	0.20	3.68	15.742	44 628	1.39	8.58	5.82	-1.37	15.78
	15	6.41	0.20	3.90	18.851	47 015	1.46	8.00	5.47	-1.06	14.93
	10	6.78	0.20	4.13	22.345	49 100	1.53	7.44	5.16	-0.74	14.14
	5	7.14	0.20	4.36	26.246	50 878	1.61	6.92	4.89	-0.42	13.42
	0	7.50	0.20	4.59	30.576	52 390	1.68	6.43	4.64	-0.10	12.75

Steel 100m Final Tower Force and Stress Summary

Height (m)	Tower Diameter (m)	Shell Thickness (m)	Section Area (m^2)	Moment of Inertia (m^4)	Combined Moment (kNm)	Own Weight Stress (MPa)	Bending Stress (MPa)	Stress (T Side) (MPa)	Stress (C Side) (MPa)
100	3.00	0.015	0.14	0.157	543	14.88	5.20	9.68	20.08
95	3.08	0.017	0.16	0.191	5 493	13.29	44.24	-30.94	57.53
90	3.15	0.019	0.19	0.229	10 393	12.10	71.47	-59.37	83.57
85	3.23	0.021	0.21	0.271	15 137	11.18	89.98	-78.80	101.17
80	3.30	0.023	0.24	0.318	19 714	10.47	102.33	-91.86	112.81
75	3.38	0.025	0.26	0.369	24 117	9.92	110.26	-100.34	120.17
70	3.45	0.027	0.29	0.425	28 337	9.48	114.94	-105.46	124.42
65	3.53	0.029	0.32	0.487	32 367	9.13	117.23	-108.09	126.36
60	3.60	0.031	0.35	0.553	36 202	8.86	117.74	-108.87	126.60
55	3.68	0.033	0.38	0.626	39 835	8.66	116.91	-108.26	125.57
50	3.75	0.035	0.41	0.705	43 261	8.50	115.09	-106.60	123.59
45	3.83	0.037	0.44	0.790	46 476	8.38	112.54	-104.16	120.92
40	3.90	0.039	0.47	0.882	49 476	8.30	109.44	-101.14	117.74
35	3.98	0.041	0.51	0.980	52 260	8.25	105.94	-97.70	114.19
30	4.05	0.043	0.54	1.087	54 824	8.22	102.18	-93.96	110.40
25	4.13	0.045	0.58	1.200	57 171	8.22	98.23	-90.02	106.45
20	4.20	0.047	0.61	1.322	59 301	8.23	94.19	-85.96	102.42
15	4.28	0.049	0.65	1.452	61 220	8.26	90.09	-81.83	98.35
10	4.35	0.051	0.69	1.591	62 933	8.30	86.01	-77.71	94.31
5	4.43	0.053	0.73	1.740	64 455	8.36	81.98	-73.62	90.34
0	4.50	0.055	0.77	1.897	65 824	8.43	78.07	-69.64	86.49

Concrete 100m Final Tower Force and Stress Summary

Height (m)	Tower Diameter (m)	Shell Thickness (m)	Section Area (m^2)	Moment of Inertia (m^4)	Combined Moment (kNm)	Own Weight Stress (MPa)	Bending Stress (MPa)	Pre-stressing Stress (MPa)	Stress (T Side) (MPa)	Stress (C Side) (MPa)
100	3.00	0.250	2.16	2.059	563	0.969	0.410	12.38	12.935	13.76
95	3.23	0.254	2.37	2.633	5 826	1.035	3.568	11.25	8.720	15.86
90	3.45	0.258	2.58	3.312	11 160	1.102	5.813	10.29	5.583	17.21
85	3.68	0.261	2.80	4.105	16 486	1.168	7.379	9.47	3.256	18.01
80	3.90	0.265	3.03	5.025	21 771	1.235	8.449	8.75	1.533	18.43
75	4.13	0.27	3.26	6.081	26 983	1.301	9.151	8.11	0.265	18.57
70	4.35	0.27	3.49	7.287	32 092	1.367	9.579	7.56	-0.656	18.50
65	4.58	0.28	3.73	8.653	37 069	1.433	9.799	7.06	-1.307	18.29
60	4.80	0.28	3.98	10.193	41 887	1.499	9.863	6.61	-1.750	17.98
55	5.03	0.28	4.23	11.919	46 518	1.564	9.806	6.21	-2.028	17.58
50	5.25	0.29	4.48	13.844	50 938	1.629	9.659	5.85	-2.177	17.14
45	5.48	0.29	4.74	15.982	55 123	1.694	9.442	5.53	-2.223	16.66
40	5.70	0.30	5.01	18.347	59 050	1.759	9.173	5.23	-2.188	16.16
35	5.93	0.30	5.28	20.953	62 700	1.823	8.865	4.95	-2.089	15.64
30	6.15	0.30	5.56	23.815	66 055	1.887	8.529	4.70	-1.939	15.12
25	6.38	0.31	5.84	26.949	69 100	1.951	8.173	4.47	-1.750	14.60
20	6.60	0.31	6.13	30.369	71 823	2.015	7.805	4.26	-1.530	14.08
15	6.83	0.31	6.42	34.091	74 217	2.079	7.429	4.06	-1.288	13.57
10	7.05	0.32	6.72	38.133	76 283	2.142	7.052	3.88	-1.029	13.07
5	7.28	0.32	7.02	42.510	78 027	2.205	6.677	3.71	-0.761	12.59
0	7.50	0.33	7.33	47.239	79 506	2.268	6.312	3.55	-0.491	12.13

Hybrid 100m Final Tower Force and Stress Summary

	Height (m)	Tower Diameter (m)	Shell Thickness (m)	Section Area (m^2)	Moment of Inertia (m^4)	Combined Moment (kNm)	Own Weight Stress (MPa)	Bending Stress (MPa)	Pre-stressing Stress (MPa)	Stress (T Side) (MPa)	Stress (C Side) (MPa)
Steel	100	3	0.015	0.14	0.157	563	14.88	5.39	0	9.48	20.27
	95	3.1625	0.016	0.16	0.199	5 805	13.51	46.19	0	-32.67	59.70
	90	3.325	0.018	0.18	0.249	11 046	12.42	73.85	0	-61.43	86.27
	85	3.4875	0.019	0.20	0.307	16 216	11.54	92.01	0	-80.47	103.55
	80	3.65	0.020	0.23	0.376	21 290	10.83	103.42	0	-92.59	114.26
	75	3.8125	0.021	0.25	0.455	26 249	10.25	110.03	0	-99.78	120.28
	70	3.975	0.023	0.28	0.546	31 070	9.78	113.18	0	-103.40	122.96
	65	4.1375	0.024	0.31	0.649	35 735	9.39	113.85	0	-104.46	123.25
	60	4.30	0.025	0.34	0.767	40 223	9.08	112.74	0	-103.66	121.82
Concrete	60	4.60	0.20	2.76	6.704	40 223	1.10	13.80	11.58	-1.12	26.48
	55	4.84	0.20	2.92	7.869	44 745	1.20	13.77	10.96	-1.61	25.93
	50	5.08	0.20	3.07	9.162	49 079	1.30	13.62	10.40	-1.92	25.32
	45	5.33	0.20	3.22	10.588	53 199	1.39	13.38	9.90	-2.08	24.67
	40	5.57	0.20	3.37	12.156	57 081	1.48	13.07	9.45	-2.14	24.00
	35	5.81	0.20	3.52	13.872	60 701	1.57	12.71	9.03	-2.10	23.31
	30	6.05	0.20	3.68	15.742	64 040	1.66	12.31	8.65	-1.99	22.62
	25	6.29	0.20	3.83	17.773	67 081	1.75	11.87	8.30	-1.82	21.93
	20	6.53	0.20	3.98	19.972	69 809	1.84	11.42	7.98	-1.60	21.24
	15	6.78	0.20	4.13	22.345	72 215	1.93	10.95	7.68	-1.34	20.56
	10	7.02	0.20	4.28	24.899	74 298	2.02	10.47	7.40	-1.05	19.89
	5	7.26	0.20	4.43	27.640	76 063	2.11	9.99	7.14	-0.74	19.24
	0	7.50	0.20	4.59	30.576	77 564	2.19	9.51	6.90	-0.42	18.61

Steel 120m Final Tower Force and Stress Summary

Height (m)	Tower Diameter (m)	Shell Thickness (m)	Section Area (m^2)	Moment of Inertia (m^4)	Combined Moment (kNm)	Own Weight Stress (MPa)	Bending Stress (MPa)	Stress (T Side) (MPa)	Stress (C Side) (MPa)
120	3.00	0.015	0.14	0.157	563	14.88	5.391	9.48	20.27
115	3.10	0.019	0.18	0.218	6 607	11.83	46.926	-35.09	58.76
110	3.20	0.023	0.23	0.290	12 608	9.95	69.647	-59.70	79.59
105	3.30	0.027	0.28	0.372	18 500	8.70	82.103	-73.41	90.80
100	3.40	0.031	0.33	0.466	24 268	7.83	88.618	-80.78	96.45
95	3.50	0.035	0.38	0.572	29 900	7.23	91.501	-84.27	98.73
90	3.60	0.039	0.44	0.692	35 383	6.80	92.081	-85.29	98.88
85	3.70	0.043	0.49	0.826	40 704	6.49	91.169	-84.68	97.66
80	3.80	0.047	0.55	0.976	45 853	6.27	89.282	-83.01	95.55
75	3.90	0.051	0.62	1.142	50 819	6.13	86.758	-80.63	92.88
70	4.00	0.055	0.68	1.326	55 590	6.03	83.826	-77.79	89.86
65	4.10	0.059	0.75	1.529	60 157	5.98	80.643	-74.66	86.63
60	4.20	0.063	0.82	1.752	64 510	5.97	77.319	-71.35	83.29
55	4.30	0.067	0.89	1.996	68 641	5.98	73.932	-67.95	79.91
50	4.40	0.071	0.97	2.263	72 541	6.02	70.536	-64.52	76.55
45	4.50	0.075	1.04	2.553	76 205	6.07	67.171	-61.10	73.24
40	4.50	0.075	1.04	2.553	79 602	6.59	70.165	-63.58	76.75
35	4.50	0.075	1.04	2.553	82 716	7.10	72.910	-65.81	80.01
30	4.50	0.075	1.04	2.553	85 556	7.62	75.413	-67.79	83.03
25	4.50	0.075	1.04	2.553	88 130	8.13	77.682	-69.55	85.82
20	4.50	0.075	1.04	2.553	90 449	8.65	79.726	-71.08	88.38
15	4.50	0.075	1.04	2.553	92 528	9.17	81.558	-72.39	90.73
10	4.50	0.075	1.04	2.553	94 380	9.68	83.191	-73.51	92.88
5	4.50	0.075	1.04	2.553	96 026	10.20	84.642	-74.44	94.84

Concrete 120m Final Tower Force and Stress Summary

Height (m)	Tower Diameter (m)	Shell Thickness (m)	Section Area (m^2)	Moment of Inertia (m^4)	Combined Moment (kNm)	Own Weight Stress (MPa)	Bending Stress (MPa)	Prestressing Stress (MPa)	Stress (T Side) (MPa)	Stress (C Side) (MPa)
120	3.00	0.250	2.36	2.059	563	0.888	0.410	19.65	20.132	20.95
115	3.19	0.254	2.55	2.538	6 636	0.975	4.167	18.05	14.860	23.19
110	3.38	0.258	2.74	3.092	12 792	1.059	6.981	16.66	10.737	24.70
105	3.56	0.263	2.94	3.728	18 950	1.141	9.055	15.43	7.521	25.63
100	3.75	0.267	3.14	4.452	25 083	1.221	10.564	14.35	5.010	26.14
95	3.94	0.271	3.35	5.272	31 162	1.299	11.638	13.39	3.051	26.33
90	4.13	0.275	3.56	6.194	37 164	1.375	12.375	12.53	1.530	26.28
85	4.31	0.279	3.78	7.228	43 063	1.450	12.847	11.76	0.359	26.05
80	4.50	0.283	4.01	8.380	48 834	1.524	13.112	11.06	-0.531	25.69
75	4.69	0.29	4.23	9.658	54 455	1.596	13.214	10.42	-1.193	25.24
70	4.88	0.29	4.47	11.073	59 901	1.668	13.187	9.85	-1.671	24.70
65	5.06	0.30	4.71	12.631	65 152	1.738	13.057	9.32	-1.998	24.12
60	5.25	0.30	4.95	14.341	70 187	1.808	12.847	8.84	-2.200	23.49
55	5.44	0.30	5.20	16.214	74 986	1.877	12.573	8.39	-2.302	22.84
50	5.63	0.31	5.45	18.258	79 530	1.945	12.251	7.99	-2.320	22.18
45	5.81	0.31	5.71	20.483	83 801	2.012	11.890	7.61	-2.270	21.51
40	6.00	0.32	5.97	22.899	87 785	2.079	11.501	7.26	-2.164	20.84
35	6.19	0.32	6.24	25.516	91 468	2.146	11.090	6.93	-2.013	20.17
30	6.38	0.33	6.51	28.344	94 836	2.211	10.665	6.63	-1.825	19.51
25	6.56	0.33	6.79	31.394	97 882	2.277	10.230	6.35	-1.607	18.85
20	6.75	0.33	7.07	34.677	100 598	2.342	9.791	6.08	-1.367	18.22
15	6.94	0.34	7.36	38.203	102 982	2.406	9.351	5.84	-1.109	17.59
10	7.13	0.34	7.65	41.985	105 038	2.470	8.913	5.60	-0.838	16.99
5	7.31	0.35	7.94	46.033	106 779	2.534	8.481	5.39	-0.560	16.40
0	7.50	0.35	8.25	50.360	108 260	2.597	8.061	5.18	-0.282	15.84

Hybrid 120m Final Tower Force and Stress Summary

	Height (m)	Tower Diameter (m)	Shell Thickness (m)	Section Area (m^2)	Moment of Inertia (m^4)	Combined Moment (kNm)	Own Weight Stress (MPa)	Bending Stress (MPa)	Pre-stressing Stress (MPa)	Stress (T Side) (MPa)	Stress (C Side) (MPa)
Steel	120	3	0.015	0.14	0.157	563	14.88	5.39	0.00	6.73	17.51
	115	3.1625	0.016	0.16	0.199	6 546	13.51	52.08	0.00	-41.07	63.09
	110	3.325	0.018	0.18	0.249	12 495	12.42	83.54	0.00	-73.42	93.66
	105	3.4875	0.019	0.20	0.307	18 415	11.54	104.49	0.00	-95.08	113.89
	100	3.65	0.020	0.23	0.376	24 284	10.83	117.97	0.00	-109.14	126.79
	95	3.8125	0.021	0.25	0.455	30 079	10.25	126.08	0.00	-117.73	134.44
	90	3.975	0.023	0.28	0.546	35 778	9.78	130.33	0.00	-122.37	138.30
	85	4.1375	0.024	0.31	0.649	41 362	9.39	131.78	0.00	-124.13	139.44
	80	4.30	0.025	0.34	0.767	46 811	9.08	131.21	0.00	-123.81	138.61
Concrete	80	4.60	0.30	4.05	9.412	46 811	0.75	11.44	10.74	0.06	22.93
	75	4.78	0.30	4.22	10.649	52 383	0.88	11.76	10.28	-0.60	22.92
	70	4.96	0.30	4.39	11.990	57 776	1.00	11.96	9.86	-1.10	22.81
	65	5.14	0.30	4.57	13.440	62 968	1.12	12.05	9.47	-1.46	22.64
	60	5.33	0.30	4.74	15.001	67 942	1.23	12.06	9.11	-1.72	22.40
	55	5.51	0.30	4.91	16.680	72 678	1.35	12.00	8.77	-1.88	22.12
	50	5.69	0.30	5.08	18.479	77 160	1.46	11.87	8.46	-1.95	21.79
	45	5.87	0.30	5.25	20.404	81 371	1.57	11.70	8.17	-1.96	21.44
	40	6.05	0.30	5.42	22.458	85 299	1.67	11.49	7.90	-1.91	21.07
	35	6.23	0.30	5.59	24.645	88 929	1.78	11.24	7.65	-1.81	20.67
	30	6.41	0.30	5.76	26.970	92 252	1.88	10.97	7.41	-1.67	20.26
	25	6.59	0.30	5.93	29.437	95 258	1.99	10.67	7.19	-1.49	19.84
	20	6.78	0.30	6.10	32.050	97 943	2.09	10.35	6.98	-1.29	19.42
	15	6.96	0.30	6.27	34.814	100 306	2.19	10.02	6.78	-1.06	18.99
	10	7.14	0.30	6.44	37.732	102 350	2.29	9.68	6.59	-0.80	18.56
	5	7.32	0.30	6.62	40.809	104 088	2.38	9.33	6.41	-0.54	18.13
	0	7.50	0.30	6.79	44.049	105 575	2.48	8.99	6.25	-0.26	17.71

Appendix C

Steel Tower Sections Buckling Strength Analysis

The buckling analyses was carried out, as set out in section 7.1. The crux of the matter is that the stress check value does not exceed the critical compressive stress. The 80m steel tower buckling analysis will be carried out in full and the rest will be summarized, as presenting all of the analyses in full would take up far too many pages. The value for the design axial force and bending moments in the table are for the position under consideration (Top, middle or bottom).

The check was done for the top, middle, and bottom of each steel tower section and it was accepted that the design would suffice if the criterion were met at these points. In addition, the steel towers are generally governed by stiffness requirements. It should be noted that top, middle and bottom refer to the steel tower section of hybrid and the entire tower for the steel and that "OK" refers to various code-required checks being satisfied.

Buckling Analysis - Tower Top - Steel 80m				
Description	**Symbol**	**Value**	**Unit**	**Check**
Design Axial Force	N_d	2 092	kN	
Design Bending Moment	M_d	563	kNm	
Shell thickness	t	0.015	m	
Effective Tower Radius	R	1.49	m	
Axial Stress	σ_{ad}	14.9	MPa	
Bending Stress	σ_{ad}	5.36	MPa	
Partial Reduction Factor	ϵ_a	0.59		
Partial Reduction Factor	ϵ_b	0.67		
Reduction Factor	ϵ	0.61		
Initial Critical Compressive Stress	σ_{el}	1 217	MPa	
Relative Slenderness Ratio	λ_a	0.64		OK
Critical Compressive Stress	σ_{cr}	232.32	MPa	
Initial Buckling Force	N_{el}	12 080	kN	
Relative Slenderness Ratio for Global Stability	λ_r	1.64		
Core Radius	k	0.75		
Initial Geometric Imperfection	e_{gi}	0.53	m	
Additional Increment	Δe	0.37	m	
Final Geometric Imperfection	e_g	0.90	m	
Stress Check		42.98	MPa	OK

Buckling Analysis - Tower Mid - Steel 80m				
Description	**Symbol**	**Value**	**Unit**	**Check**
Design Axial Force	N_d	2 961	kN	
Design Bending Moment	M_d	31 457	kNm	
Shell thickness	t	0.025	m	
Effective Tower Radius	R	1.86	m	
Axial Stress	σ_{ad}	10.32	MPa	
Bending Stress	σ_{ad}	117.79	MPa	
Partial Reduction Factor	ϵ_a	0.63		
Partial Reduction Factor	ϵ_b	0.7		
Reduction Factor	ϵ	0.69		
Initial Critical Compressive Stress	σ_{el}	1 592	MPa	
Relative Slenderness Ratio	λ_a	0.52		OK
Critical Compressive Stress	σ_{cr}	253.05	MPa	
Initial Buckling Force	N_{el}	38 359	kN	
Relative Slenderness Ratio for Global Stability	λ_r	1.38		
Core Radius	k	0.93		
Initial Geometric Imperfection	e_{gi}	0.54	m	
Additional Increment	Δe	0.38	m	
Final Geometric Imperfection	e_g	0.91	m	
Stress Check		148.93	MPa	OK

Buckling Analysis - Tower Bottom - Steel 80m				
Description	**Symbol**	**Value**	**Unit**	**Check**
Design Axial Force	N_d	4 523	kN	
Design Bending Moment	M_d	49 251	kNm	
Shell thickness	t	0.034	m	
Effective Tower Radius	R	2.23	m	
Axial Stress	σ_{ad}	9.48	MPa	
Bending Stress	σ_{ad}	92.47	MPa	
Partial Reduction Factor	ϵ_a	0.64		
Partial Reduction Factor	ϵ_b	0.71		
Reduction Factor	ϵ	0.71		
Initial Critical Compressive Stress	σ_{el}	1 843	MPa	
Relative Slenderness Ratio	λ_a	0.48		OK
Critical Compressive Stress	σ_{cr}	261.24	MPa	
Initial Buckling Force	N_{el}	288 094	kN	
Relative Slenderness Ratio for Global Stability	λ_r	0.66		
Core Radius	k	1.12		
Initial Geometric Imperfection	e_{gi}	0.25	m	
Additional Increment	Δe	0.09	m	
Final Geometric Imperfection	e_g	0.34	m	
Stress Check		106.37	MPa	OK

Steel Buckling Analysis Summary								
			Steel			**Hybrid**		
Description	**Symbol**	**Units**	**80**	**100**	**120**	**80**	**100**	**120**
Tower Top								
Design Axial Force	N_d	kN	2 092	2 092	2 092	2 092	2 092	2 092
Design Bending Moment	M_d	kNm	563	563	563	563	563	563
Critical Compressive Stress	σ_{cr}	MPa	232.32	237.54	237.59	237.58	237.59	237.54
Stress Check		MPa	42.98	54.06	53.865	28.44	28.44	28.24
Tower Middle								
Design Axial Force	N_d	kN	2 960	3 331	4 889	2 470	2 470	2 471
Design Bending Moment	M_d	kNm	31 457	43 261	64 510	17 743	21 290	24 836
Critical Compressive Stress	σ_{cr}	MPa	253.05	279.38	310.50	247.92	248.03	248.104
Stress Check		MPa	148.93	146.56	100.98	102.86	120.37	137.87
Tower Bottom								
Design Axial Force	N_d	kN	4 523	6 470	11 173	3 049	3 049	3 049
Design Bending Moment	M_d	kNm	49 251	65 824	97 509	32 525	40 223	47 954
Critical Compressive Stress	σ_{cr}	MPa	261.24	292.98	310.50	251.83	251.92	236.57
Stress Check		MPa	106.37	101.62	125.73	100.71	125.54	147.36
			OK	**OK**	**OK**	**OK**	**OK**	**OK**

Appendix D

Foundation Design

The first foundation design will be done in full and the rest will be summarized. In all foundation designs, the ground level is at the height of the bottom block-part of the foundation. As mentioned previously, the foundation design of the steel and hybrid tower is governed by the case when the water table is at the ground surface; the design of the concrete tower is also governed by the water table being at ground level. The concrete 80m foundation is governed by overturn, the 100m by simultaneous overturn and bearing capacity failure and the 120m tower by bearing capacity failure.

These critical cases are shown in this appendix, however, all the tower foundations were tested for the cases of water level depth well below the foundation and at the ground surface. The tables are to be used in conjunction with Figures 9.3 and D.1.

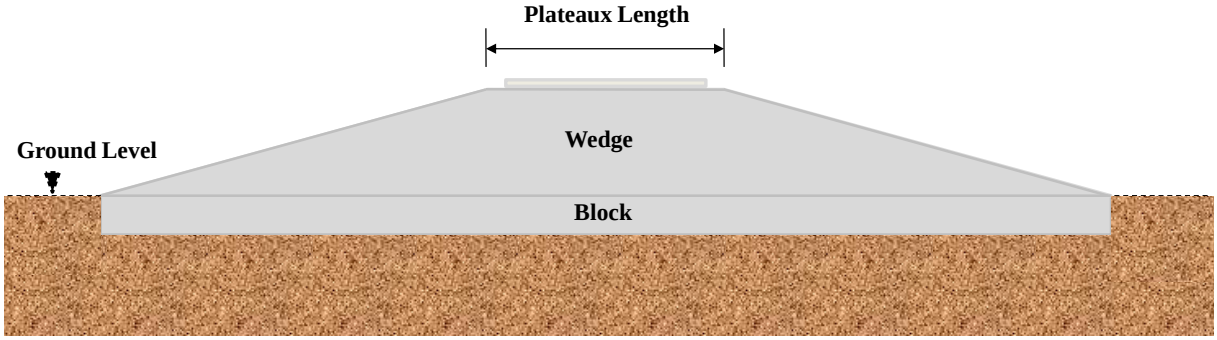

Figure D.1: Illustration of foundation dimension parameters.

D.1 Forces and Moments - Steel 80m

80m Steel Foundation - General			
Description	**Symbol**	**Value**	**Unit/Check**
Applied Shear Force XX	F_x	688	kN
Applied Shear Force YY	F_y	564	kN
Applied Moment XX	M_x	39 406	kNm
Applied Moment YY	M_y	26 626	kNm
Applied Moment ZZ	M_{zd}	2 000	kNm
Foundation Width	L	21.00	m
Foundation Depth of Block	D_b	0.75	m
Foundation Wedge Height	D_w	1.45	m
Total Foundation Height	D	2.20	m
Backfill Height	H_g	0.75	m
Groundwater Level Above Foundation Base	H_{gwl}	0.75	m
Plateuax Length;Breadth	L_p	5.00	m
Own Weight of Turbine	V_{z1}	1 705	kN
Own Weight of Tower	V_{z2}	1 980	kN
Dead Weight of Block	V_{f1}	7 773	kN
Dead Weight of Wedge	V_{f2}	6 486	kN

80m Steel Foundation - Forces and Moments Under Foundation - ULS				
Description	**Symbol**	**Equation**	**Value**	**Unit**
Applied Design Moment	M_d	$\sqrt{(M_x^2 + M_y^2)}$	49 251	kNm
Foundation Vertical Load	V_f	$V_{f1} + V_{f2}$	15 684	kN
Buoyancy Force	V_{zbd}	$10(L^2 \cdot H_{gwl})$	-3 308	kN
Total Shear at Tower Base	F_d	$\sqrt{{F_x}^2 + {F_y}^2}$	890	kN
Shear Force Eccentricity	e_q	$e_q = D$	2.20	m
Shear in X Direction	H_{dx}	$2 \cdot \frac{M_{zd}}{L'} + \sqrt{{F_d}^2 + (2 \cdot \frac{M_{zd}}{L'})^2}$	1 100	kN
Shear at 45 ° off X axis	H_{d45}	$2 \cdot \frac{M_{zd}}{L'} + \sqrt{F_d^2 + (2 \cdot \frac{M_{zd}}{L'})^2}$	1 165	kN

D.2 Bearing Capacity - Steel 80m

Bearing Capacity - 80m Steel Tower					
Parameters					
Description	**Symbol**	**Equation**	**Value**		**Units**
			Along X Axis	**45° to X axis**	
Foundation Breadth	B		21.00		m
Foundation Length	L		21.00		m
Foundation Depth	D		0.75		m
Effective Breadth	b		14.62	16.49	m
Effective Length	L'		21.00	16.49	m
Design Horizontal Force	H_d		1 100.27	1 164.66	kN
Design Vertical Force	V_d		16 061.53		kN
Unit Weight of soil	γ		18.00		
Buoyant Unit Weight	γ'		8.00		
			Drained	**Undrained**	
Angle of Shear Resistance	ϕ_i		30.00	0.00	deg.
Design Angle of shear resistance	ϕ	$\phi = Arctan\left(\frac{tan(\phi_i)}{\gamma_\phi}\right)$	24.79	0.00	deg.
		$\gamma_\phi = 1.25$	0.43	0.00	rads.
Cohesion Intercept	c_i		0.00	60.00	$\frac{kN}{m^2}$
Design Cohesion Intercept	c	$c = \frac{c_i}{\gamma_c} \quad (\gamma_c = 1.4)$	0.00	42.86	$\frac{kN}{m^2}$

Failure Mode: Rupture 1 - Drained State - 80m Steel Tower					
Parameters					
Description	**Symbol**	**Equation**	**Value**		**Units**
Design Angle of shear resistance	ϕ		0.43		rads.
Design Cohesion Intercept	c		0.00		$\frac{kN}{m^2}$
Unit Weight of soil	γ		18.00		
Buoyant Unit Weight	γ'		8.00		
			Along X Axis	**45 to X axis**	
Bearing Capacity Factors	N_q	$e^{(\pi \cdot tan(\phi))} \cdot tan(45 + \frac{\phi}{2})^2$	10.43		
	N_c	$(N_q - 1) \cdot cot(\phi)$	20.42		
	N_γ	$(\frac{1}{4}) \cdot ((N_q - 1) \cdot cos(\phi))^{(3/2)}$	2.04		
Shape Factors	S_q	$1 + 0.2 \cdot (\frac{B'}{L'})$	1.14	1.20	
	S_c	$1 + 0.2 \cdot (\frac{B'}{L'})$	1.14	1.20	
	S_γ	$1 - 0.4 \cdot (\frac{B'}{L'})$	0.72	0.60	
Inclined Loading Factors	i_q	$(1 + \frac{H_d}{(V_d + A_{eff} \cdot c \cdot cot(\phi))})^2$	0.98	0.97	
	i_c	$=i_q$	0.98	0.97	
	i_γ	$=i_q^2$	0.958	0.949	
Surcharge Pressure	q_{f2}	$\gamma \cdot D \cdot N_q \cdot s_q \cdot i_q$	139	145	kPa
Underlying Soil Weight	q_{f3}	$\gamma \cdot b \cdot N_\gamma \cdot s_\gamma \cdot i_\gamma$	146	134	kPa
Ultimate Bearing Capacity	Σq_f		285	280	kPa

Failure Mode: Rupture 1 - Undrained State ($\phi = 0$) - 80m Steel Tower					
Parameters					
Description	**Symbol**	**Equation**	**Value**		**Units**
Design Angle of shear resistance	ϕ	$\gamma_\phi = 1.25$	0.00		rads.
Design Cohesion Intercept	c	$c = \frac{c_i}{\gamma_c} \quad (\gamma_c = 1.4)$	42.86		$\frac{kN}{m^2}$
Unit Weight of soil	γ		18.00		
Buoyant Unit Weight	γ'		8.00		
			Along X Axis	45 Across X axis	
Bearing Capacity Factors	N_q	$e^{(\pi \cdot tan(\phi))} \cdot tan(45 + \frac{\phi}{2})^2$	1.00		
	N_c	$\pi + 2$	5.14		
Shape Factors	S_q	$1 + 0.2 \cdot \frac{B'}{L'}$	1.14	1.20	
	S_c	$1 + 0.2 \cdot (\frac{B'}{L'})$	1.14	1.20	
	S_γ	$1 - 0.4 \cdot (\frac{B'}{L'})$	0.72	0.60	
Inclined Loading Factors	i_q	$= i_c$	0.98	0.97	
	i_c	$0.5 + 0.5 \cdot \sqrt{\left(1 - \frac{H_d}{(A_{eff} \cdot c)}\right)}$	0.98	0.97	
	i_γ	i_{q^2}	0.96	0.95	
Shear Strength Component	q_{f1}	$c \cdot N_c \cdot s_c \cdot i_c$	245.68	257.65	kPa
Surcharge Pressure	q_{f2}	$\gamma \cdot D \cdot N_q \cdot s_q \cdot i_q$	6.69	7	kPa
Ultimate Bearing Capacity	Σq_f		252	265	kPa

Failure Mode: Extremely Eccentric Loading - Drained State - 80m Steel Tower					
Parameters					
Description	**Symbol**	**Equation**	**Value**		**Units**
Design Angle of shear resistance	ϕ		0.43		rads.
Design Cohesion Intercept	c		0.00		$\frac{kN}{m^2}$
Unit Weight of soil	γ		18.00		
Buoyant Unit Weight	γ'		8.00		
			Along X Axis	**45 to X axis**	
Bearing Capacity Factors	N_q	$e^{(\pi \cdot tan(\phi))} \cdot tan(45 + \frac{\phi}{2})^2$	10.43		
	N_c	$(N_q - 1) \cdot cot(\phi)$	20.42		
	N_γ	$(\frac{1}{4}) \cdot ((N_q - 1) \cdot cos(\phi))^{(3/2)}$	2.04		
Shape Factors	S_q	$1 + 0.2 \cdot (\frac{B'}{L'})$	1.14	1.20	
	S_c	$1 + 0.2 \cdot (\frac{B'}{L'})$	1.14	1.20	
	S_γ	$1 - 0.4 \cdot (\frac{B'}{L'})$	0.72	0.60	
Inclined Loading Factors	i_q	$(1 - \frac{H_d}{(V_d + A_{eff} \cdot c \cdot \frac{1}{tan(\phi)})})^2$	1.07	1.07	
	i_c	$=i_q$	1.07	1.07	
	i_γ	$=i_q^2$	1.142	1.15	
Underlying Soil Weight	q_{f3}	$\gamma \cdot B' \cdot N_\gamma \cdot s_\gamma \cdot i_\gamma$	442	418	kPa
Ultimate Bearing Capacity	Σq_f		442	418	kPa

Failure Mode: Extremely Eccentric Loading
Undrained State ($\phi = 0$) - 80m Steel Tower

Parameters

Description	Symbol	Equation	Value		Units
Design Angle of shear resistance	ϕ	$\gamma_\phi = 1.25$	0.00		rads.
Design Cohesion Intercept	c	$c = \frac{c_i}{\gamma_c} \quad (\gamma_c = 1.4)$	42.86		$\frac{kN}{m^2}$
Unit Weight of soil	γ		18.00		
Buoyant Unit Weight	γ'		8.00		
			Along X Axis	45 Across X axis	
Bearing Capacity Factors	N_q	$e^{(\pi \cdot tan(\phi))} \cdot tan(45 + \frac{\phi}{2})^2$	1.00		
	N_c	$\pi + 2$	5.14		
Shape Factors	S_q	$1 + 0.2 \cdot \frac{B'}{L'}$	1.14	1.20	
	S_c	$1 + 0.2 \cdot (\frac{B'}{L'})$	1.14	1.20	
	S_γ	$1 - 0.4 \cdot (\frac{B'}{L'})$	0.72	0.60	
Inclined Loading Factors	i_q	$= i_c$	0.99	0.99	
	i_c	$\sqrt{0.5 + 0.5 \cdot \sqrt{\left(1 - \frac{H_d}{(A_{eff} \cdot c)}\right)}}$	0.99	0.99	
	i_γ	$= i_{q^2}$	0.98	0.97	
Shear Strength Component	q_{f1}	$c \cdot N_c \cdot s_c \cdot i_c$	261	275	kPa
Ultimate Bearing Capacity	Σq_f		261	274	kPa
Sliding Resistance					
Resistance Against Base Sliding	R_s	Drained - $A_{eff} \cdot c + V_d \cdot tan(\phi)$	7 418.51	7 418.51	kN
		Undrained - $A_{eff} \cdot c$	13 161.13	11 655.30	kN
Resistance Against Base Sliding (Final)	R_s		7 418.51	7 418.51	kN

D.3 Summary - Steel 80m

80m Steel Foundation - Summary				
Description	**Symbol**	**Along X axis**	**45 off X axis**	**Unit ; Check**
Soil Stress	σ_s	52.30	59.06	kPa
Bearing Capacity	q_f	252	265	kPa
Factor of Safety for Bearing Capacity	$\mathbf{F_s}$	**4.83**	**4.48**	**OK**
Design Horizontal Force	H_d	1 100	1 165	kN
Sliding Resistance	R_s	7 419	7 419	kN
Factor of Safety Against Sliding	$\mathbf{F_s}$	**6.74**	**6.37**	**OK**

80m Steel Foundation - Overall Stability Check				
		Equation	**Value**	**Units**
Destabilizing	Bending	$\gamma_f \cdot \Sigma M$	49 251	kNm
	Shear	$\gamma_f \cdot e \cdot \Sigma F$	1 957	kNm
	Total	M_o	51 208	kNm
Stablizing	Tower	$\gamma_{g1} \cdot F_z \cdot \frac{B}{2}$	31 657	kNm
	Foundation	$(\gamma_{g1} \cdot F_{zf} + \gamma_{g2} \cdot V_d - \gamma_0 \cdot F_0) \cdot \frac{B}{2}$	100 012	kNm
	Total	M_r	131 669	kNm
Factor of Safety Against Overturn		$\mathbf{F_s}$	**2.57**	**OK**

Foundation Design Summary

		Soil Stress	Bearing Capacity	Fs	Sliding Force	Sliding Resistance	Fs	Overturning Moment	Stabilizing Moment	Fs
		σ_s (kPa)	q_f (kPa)		H_d (kN)	Rs (kN)		M_o (kNm)	M_r (kNm)	
Steel	**80**	59.06	264.7	4.48	1 165	7 419	6.37	51 208	131 669	2.57
	100	70.02	264.12	3.77	1 318	9 259	7.02	68 462	171 355	2.50
	120	84.80	244.07	2.88	1 529	12 849	8.41	101 054	253 746	2.51
Conc.	**80**	75.17	262.06	3.49	1 419	8457	5.96	56 880	143 996	2.53
	100	104.04	261.21	2.51	1 631	10 604	6.50	82 278	206 080	2.50
	120	104.11	260.00	2.50	1 808	14 046	7.77	112 109	310 601	2.77
Hyb.	**80**	66.21	259.44	3.92	1 342	7 769	5.79	54 247	135 574	2.50
	100	82.39	262.14	3.18	1 573	10 879	6.92	80 654	203 031	2.52
	120	99.71	262.56	2.63	1 813	13 381	7.38	111 829	281 173	2.51

Appendix E

Foundation Reinforcing Design

The first reinforcing design will be done completely and the rest will be summarized. The designs were done as described in section 6.5.

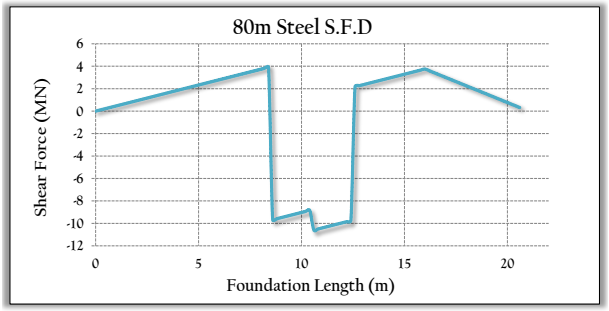

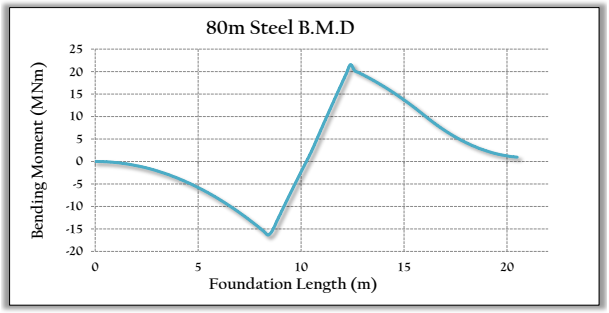

80m Steel Tensile Reinforcement Design - General			
Description	**Symbol**	**Value**	**Unit**
Total Vertical Force	F_z	4 523	kN
Own Weight of Foundation	G_d	15 684	kN
Total Applied Moment	M_d	49 251	kNm
Outer Radius of anchor ring	r_o	2.25	m
Design Horizontal Force	F_{xyd}	1 100	kN
Shear Force Eccentricity	e_q	2.2	m
Foundation Length	L	21	m
Own Weight of Foundation per meter	g_d	747	kN/m
Weight of Tower and Foundation	R_{result}	19 369	kN
Effective Breadth	b	8	m
Uniform Soil Pressure	σ_{soil}	1210.5	kN/m
Distance form Comp to Tension	d_s	4.1	m
Compression Force	F_c	13 675	kN
Tension Force	F_t	11 833	kN
Half Tower Weight	F_w	1 842	kN

80m Tensile Reinforcement Design - Top Reinforcing				
Description	**Symbol/Equation**	**Value**	**Unit**	**Check**
Max Top Moment	M_{top}	21 553	kNm	
Position		12.4	m	
Foundation Height	H	1648	mm	
Effective Height	d_2	1598	mm	
K-value	$\frac{M}{(f_{ck} \cdot b \cdot d_2^2)}$	0.0134		
K' Value		0.168		OK
Lever Arm	$z = (\frac{d}{2}) \left(1 + \sqrt{(1 - 3.53 \cdot K)}\right)$	1 518	mm	OK
Tension Steel Required	$A_s = \frac{M}{(f_{yd} \cdot z)}$	35 056	mm^2	
Minimum Steel Required	$A_{s,min} > \frac{0.26 f_{ctm} \cdot b_t \cdot d}{f_{yk}}$	79 495	mm^2	
	$A_{s,min} > 0.0013 \cdot b_t \cdot d$	43 625	mm^2	
Max Reinforcing Allowed	$0.04 \cdot A_c$	1 342 320	mm^2	OK
Final Top Steel Required	$A_{s,top}$	79 495	mm^2	
As per meter	$\frac{A_{s,top}}{L}$	3 785	$\frac{mm^2}{m}$	
Spacing	S_{top}	210	mm c/c	
Number of Bars Per Direction		100		
Steel Provided Per Direction	Y32 - 210	80 425	mm^2	
Reinforcing Ratio	ρ_2	0.0024	$\frac{mm^2}{mm^2}$	
Total Number of Bars		200		
Length of Each Bar	L_b	21.16	m	
Total Length of Steel	$NrBars \cdot BarLength$	4232.2	m	
Mass of Steel Required	$M_{steel,top}$	26718	kg	

80m Tensile Reinforcement Design - Bottom Reinforcing				
Description	**Symbol/Equation**	**Value**	**Unit**	
Max Top Moment	M_{top}	16 349	kNm	
Position		8.4	m	
Foundation Height	H	1648	mm	
Effective Height	d_2	1598	mm	
K-value	$\frac{M}{(f_{ck} \cdot b \cdot d_2^2)}$	0.0102		
K' Value		0.168		OK
Lever Arm	$z = (\frac{d}{2})\left(1 + \sqrt{(1 - 3.53 \cdot K)}\right)$	1 518	mm	OK
Tension Steel Required	$A_s = \frac{M}{(f_{yd} \cdot z)}$	26 591	mm^2	
Minimum Steel Required	$A_{s,min} > \frac{0.26 f_{ctm} \cdot b_t \cdot d}{f_{yk}}$	79 495	mm^2	
	$A_{s,min} > 0.0013 \cdot b_t \cdot d$	43 625	mm^2	
Max Reinforcing Allowed	$0.04 \cdot A_c$	1 342 320	mm^2	OK
Final Top Steel Required	$A_{s,bot}$	79 495	mm^2	
As per meter	$\frac{A_{s,bot}}{L}$	3 785	$\frac{mm^2}{m}$	
Spacing	S_{bot}	210	mm c/c	
Number of Bars Per Direction		100		
Steel Provided Per Direction	Y32 - 210	80 425	mm^2	
Reinforcing Ratio	ρ_2	0.0024	$\frac{mm^2}{mm^2}$	
Total Number of Bars		200		
Length of Each Bar	L_b	20.9	m	
Total Length of Steel	$NrBars \cdot BarLength$	4 180	m	
Mass of Steel Required	$M_{steel,top}$	26 388	kg	
Total Steel Mass in Foundation	$M_{steel,top} + M_{steel,bot}$	53 106	kg	

The bending moment and shear force diagrams and a summary of the foundation reinforcing details are shown in the following pages.

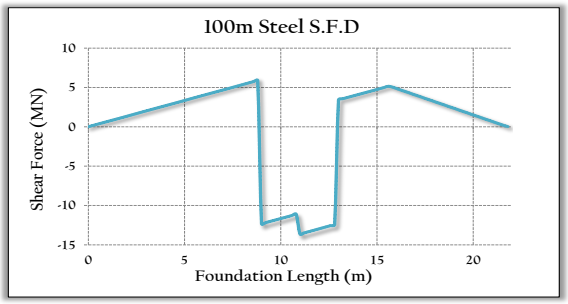

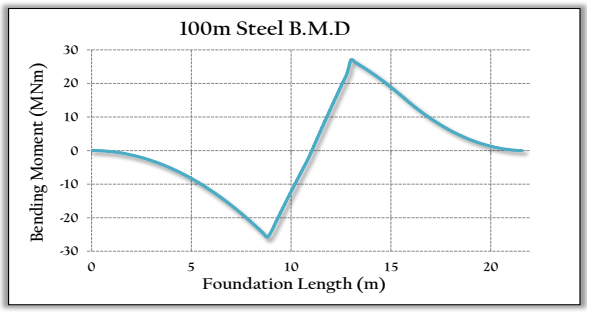

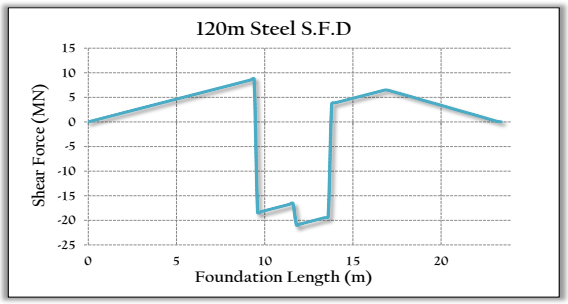

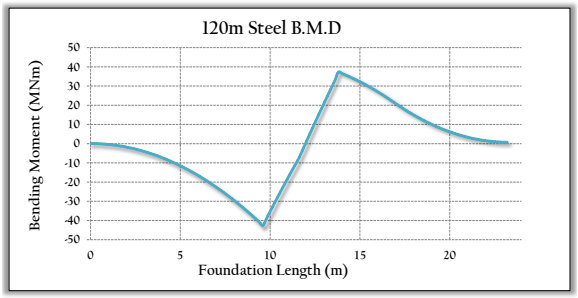

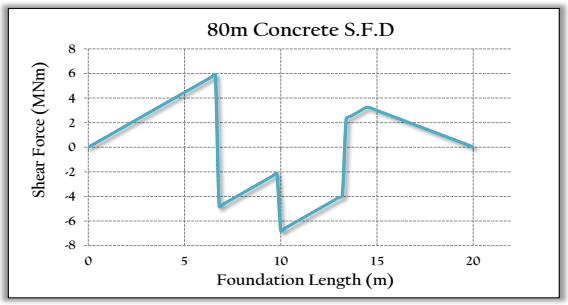

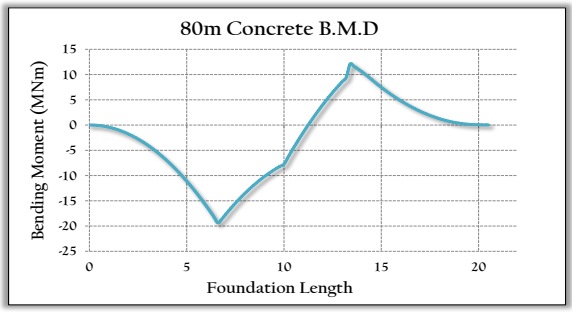

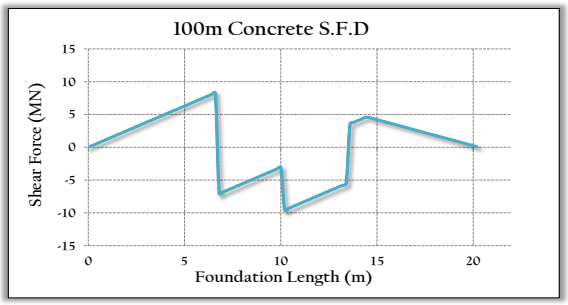

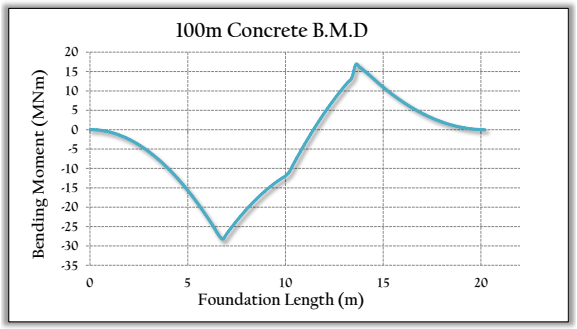

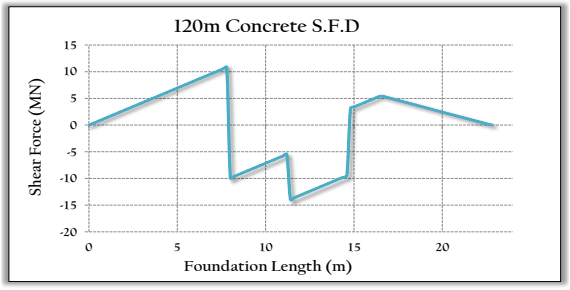

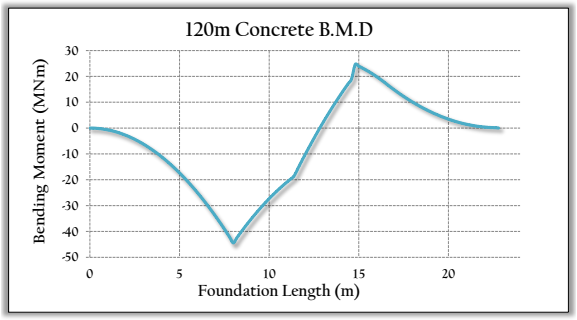

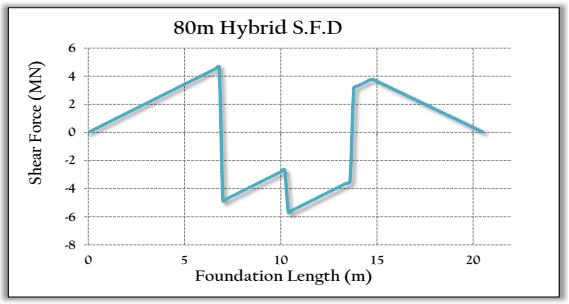

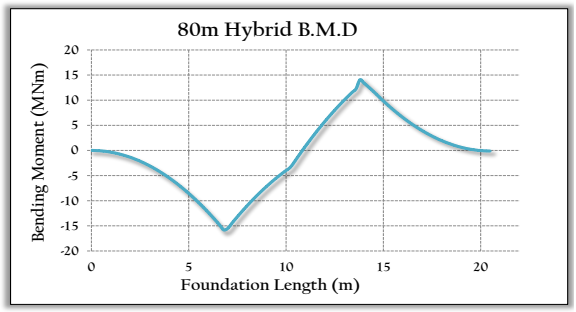

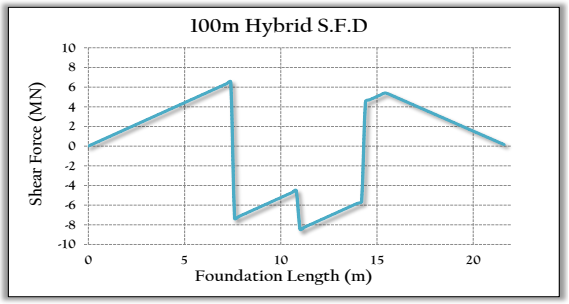

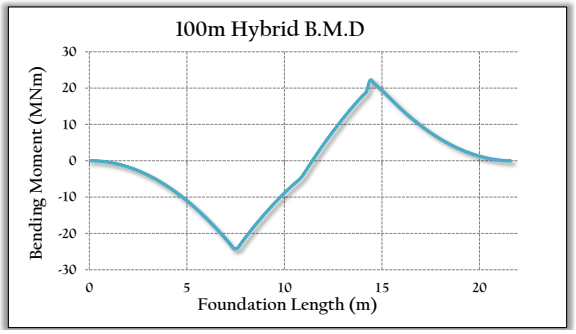

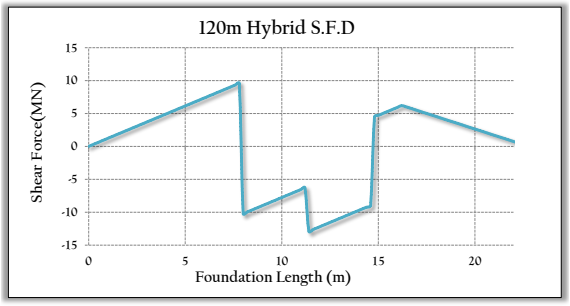

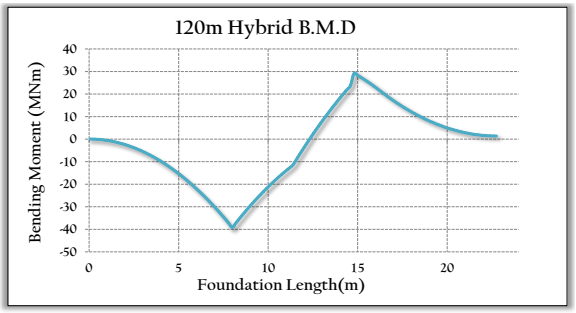

.

Foundation Flexure Reinforcing Summary

Top Reinforcing

			Tower Height									
			Steel			Concrete			Hybrid			
Description	**Symbol**	**Unit**	**80**	**100**	**120**	**80**	**100**	**120**	**80**	**100**	**120**
Ultimate Moment	$M_{d,top}$	kNm	21 553	26 989	37 233	12 083	16 827	24 599	14 074	22 168	29 147
Steel Required	$A_{s,top,req}$	mm^2	79 495	91 505	109 603	58 606	72 770	98 084	67 016	91 608	100 509
Steel Provided	$A_{s,top}$	mm^2	80 425	91 684	112 595	61 123	73 991	101 335	68 361	91 684	101 335
Mass Steel	$m_{steel,top}$	kg	26 718	31 683	41 543	19 170	23 634	36 779	22 081	31 725	36 614

Bottom Reinforcing

			Tower Height									
			Steel			Concrete			Hybrid			
Ultimate Moment	$m_{d,bot}$	kNm	16 349	25 803	42 650	19 382	28 231	44 394	15 806	24 132	39 243
Steel Required	$A_{s,bot,req}$	mm^2	79 495	91 505	109 603	58 606	72 770	98 084	67 016	91 608	100 509
Steel Provided	As, bot	mm^2	80 425	91 684	112 595	61 123	73 991	101 335	68 361	91 684	101 335
Mass Steel	$m_{steel,bot}$	kg	26 388	31 162	40 921	19 096	23 406	36 033	21 893	31 162	36 033

Total Steel Mass	M_{steel}	kg	53 106	62 846	82 464	38 266	47 040	72 813	43 975	62 887	72 647

Appendix F

Foundation Punching Shear Design

As discussed in section 6.6, the foundation will be designed so that there is no need for punching shear reinforcement.

Steel 80m Punching Shear Design - Parameters

Description	Equation	Symbol	Value	Unit
Foundation Depth at Plateau		D_p	2 200.00	mm
Foundation Depth at Corners		D_c	750.00	mm
Slope Away from Plateau	$\frac{dy}{dx}$	θ_s	-0.1813	mm/mm
Concrete Cover (Top and Bottom)		c	50.00	mm
Tower Radius		R_{tower}	2.25	m
Lower Bottom Reinforcing Ratio	$\frac{A_{s,bot}}{b_w \cdot d}$	ρ_1	0.0024	
Upper Bottom Reinforcing Ratio	$\frac{A_{s,bot}}{b_w \cdot d}$	ρ_1	0.0024	
Joint Bottom Reinforcing Ratio	$\sqrt{\rho_1 \cdot \rho_2}$	ρ_I	0.0025	
Characteristic Concrete Cylinder Strength		f_{ck}	30.00	MPa
Design Value of Concrete Compressive Strength		f_{cd}	20.00	MPa
Material Factor for Concrete		γ_c	1.50	
Vertical Design Force		V_{ED}	3 684.98	kN
Design Overturning Moment		M_{ED}	49 251.18	kNm
Eccentricity	$\frac{M_{ED}}{V_{ED}}$	e	13.37	m
Diameter of Tension Reinforcing		ϕ_{tb}	32.00	mm
Foundation Breadth		B (b_w)	21 000.00	mm
Effective Foundation Breadth		b	14 623.48	mm
Plateau Width		L_p	5 000.00	mm
Distance to Center of 1st Bottom Layer	$D - c - \frac{\phi_{tb}}{2}$	d_1	2 134.00	mm
Distance to Center of 2nd Bottom Layer	$D - c - \frac{3\phi_{tb}}{2}$	d_2	2 102.00	mm
Average Effective Depth of Reinforcing	$\frac{d_1+d_2}{2}$	d_{ave}	2 118.00	mm

Steel 80m Punching Shear Design - Check at Tower Face				
Description	**Equation**	**Symbol**	**Value**	**Unit**
	$0.6 \cdot (1 - \frac{f_{ck}}{250})$	v	0.53	
Max Allowable Punching Shear Stress	$0.4 \cdot v \cdot f_{cd}$	$v_{Rd,max}$	4.22	MPa
Beta value	$1 + 0.6 \cdot \pi \cdot \frac{e}{D_{tower}+4d_{ave}}$	β	2.94	
Max Shear Stress - Tower Face	$\beta \cdot \frac{V_{ED}}{u_0 \cdot d_{ave}}$	v_{ED}	0.36	MPa
			OK	
Steel 80m Punching Shear Design - Check at First Control Perimeter				
Control Perimeter Radius	$R_{tower} + 2d_{ave}$	x_1	5.31	m
Average Effective Depth (On slope)	$D_p + \theta_s \cdot (x_1 - \frac{L_p}{2}) - c - \phi_{tb}$	d_{ave}	1.61	m
k Value	$1 + \sqrt{\frac{200}{d_{ave}}}$	k	1.35	
Beta Value	$1 + 0.6 \cdot \pi \cdot \frac{e}{D_{tower}+4d_{ave}}$	β	3.30	
Basic Control Perimeter	$2 \cdot \pi \cdot x_1$	u_1	33.36	m
Design Punching Shear Resistance	$C_{Rd,c} \cdot k \cdot (100 \cdot \rho_1 \cdot f_{ck})^{\frac{1}{3}}$	$v_{Rd,c}$	0.32	MPa
Minimum Shear Resistance	$0.035 \cdot k^{\frac{3}{2}} \cdot f_{ck}^{\frac{1}{2}}$	v_{min}	0.30	MPa
1st Control Perimeter Area	$\pi \cdot x_1^2$	A_1	88.58	m^2
Area Where Pressure Acts		$A_{1,eff}$	78.68	m^2
Load Reduction Pressure	$V_{ED} / \left(\frac{B' \cdot B}{2}\right)$	$\sigma_{soil'}$	24.00	kPa
Pressure Slope		θ_p	1.64	$\frac{kPa}{m}$
High Pressure	LHS	σ_{LHS}	15.48	kPa
Low Pressure	RHS	σ_{RHS}	0	kPa
Average Pressure		σ_{ave}	7.74	kPa
Load Reduction	$\sigma_{ave} \cdot A_{1,eff}$	δV_{ED}	609.08	kN
Max Shear Stress - First Perimeter	$\frac{\beta \cdot V_{ED}}{u_1 \cdot d_{ave}}$	v_{ED}	0.19	MPa
			OK	

. .

Punching Shear Check - Summary

Check at Tower Face

			Steel			Concrete			Hybrid		
Description	**Symbol**	**Unit**	**80**	**100**	**120**	**80**	**100**	**120**	**80**	**100**	**120**
Max. Allow. Punching Stress	$v_{Rd,max}$	MPa	4.22	4.22	4.22	4.22	4.22	4.22	4.22	4.22	4.22
Max Stress at Tower Face	v_{ED}	MPa	0.36	0.42	0.58	0.52	0.50	0.51	0.34	0.37	0.48
			OK	**OK**	**OK**	**OK**	**OK**	**OK**	**OK**	**OK**	**OK**

Check at First Control Perimeter

			Steel			Concrete			Hybrid		
Description	**Symbol**	**Unit**	**80**	**100**	**120**	**80**	**100**	**120**	**80**	**100**	**120**
Control Perimeter Radius	x_1	m	5.31	5.55	6.03	6.11	6.59	7.09	6.33	6.71	6.93
Average Effective Depth	d_{ave}	m	1.61	1.79	1.95	1.18	1.51	1.65	1.28	1.47	1.66
Minimum Shear Resistance	v_{min}	MPa	0.30	0.30	0.29	0.33	0.31	0.3	0.32	0.31	0.3
Allow. Design Punching Shear	$v_{Rd,c}$	MPa	0.32	0.31	0.31	0.33	0.32	0.32	0.33	0.32	0.31
Max Applied Shear Stress at First Perimeter	v_{ED}	MPa	0.19	0.21	0.27	0.30	0.28	0.32	0.21	0.23	0.29
			OK	**OK**	**OK**	**OK**	**OK**	**OK**	**OK**	**OK**	**OK**

Appendix G

Prestressing Losses

The equation for the total prestressing losses, δ_{total}, is repeated here, adapted from Equation 7.22:

$$\delta_{total} = 1 - (e^{-(\mu\alpha+\kappa x)} - \delta_{anchor} - \delta_{relax})) \tag{G.1}$$

Where:

$F_{d,ps}$ = *Design prestress force per tendon* (N)

F_0 = *Initial prestress force (0.8MBL)* (N)

μ = *Curvature coefficient*

α = *Inclined angle of tower* (rad)

κ = *Wobble friction coefficient* $(\frac{rad}{m})$

x = *Strand (tower) length* (m)

δ_{anchor} = *Anchorage loss fraction*

δ_{relax} = *Steel relaxation loss fraction*

Prestressing Losses Summary

		μ	α	κ	**x**	$\delta_{\mathbf{anchor}}$	$\delta_{\mathbf{relax}}$	$\delta_{\mathbf{total}}$ (%)
Concrete	80	0.1	0.028125	0.0016	80	0.03	0.025	17.8
	100	0.1	0.0225	0.0016	100	0.03	0.025	20.5
	120	0.1	0.01875	0.0016	120	0.03	0.025	23.1
Hybrid	80	0.1	0.03625	0.0016	80	0.03	0.025	12
	100	0.1	0.024167	0.0016	100	0.03	0.025	14.9
	120	0.1	0.018125	0.0016	120	0.03	0.025	17.7

Appendix H

Foundation Stiffness

The stiffnesses of the foundations were calculated according Equations 6.22 through 6.25, in Section 6.4. The stiffnesses calculated here were used in the *Abaqus* analyses.

Foundation Stiffness Summary

			Steel			Concrete			Hybrid		
			80	**100**	**120**	**80**	**100**	**120**	**80**	**100**	**120**
Poissons Ratio	ν		0.25	0.25	0.25	0.25	0.25	0.25	0.25	0.25	0.25
Shear Modulus	G	MPa	26	26	26	26	26	26	26	26	26
Radius of Foundation	R	m	10.5	10.875	11.625	10.0	10.125	11.375	10.25	10.875	11.375
Depth to Bedrock	H	m	10	10	10	10	10	10	10	10	10
Depth of Foundation	D	m	0.75	0.75	0.95	0.8	0.95	0.65	0.7	0.7	0.8
Vertical Stiffness	k_V	GN/m	3.77	3.98	4.54	3.52	3.67	4.22	3.61	3.96	4.30
Horizontal Stiffness	k_H	GN/m	2.18	2.28	2.58	2.07	2.15	2.38	2.10	2.26	2.44
Rocking Stiffness	k_R	GNm/rad	151.25	168.21	215.12	132.11	142.05	188.56	138.97	166.29	194.96
Torsional Stiffness	k_T	GNm/rad	191.14	211.18	265.38	168.29	180.00	235.23	176.56	209.00	242.42